Precision-cut liver slices: an ex vivo model for the early onset and end-stage of liver fibrosis

Westra, Inge

Precision-cut liver slices: an *ex vivo* model for the early onset and end-stage of liver fibrosis

Inge M. Westra

Paranymphs: Dorenda Oosterhuis
Marijke Westra

This PhD project was carried out in the Division of Pharmacokinetics, Toxicology and Targeting and in the Division of Pharmaceutical Technology and Biopharmacy, Department of Pharmacy, Faculty of Mathematics and Natural Sciences, University of Groningen. The work described in this thesis was financially supported by ZonMw (project Dierproeven Begrensd II, 114000098).
Printing of this thesis was financially supported by the University of Groningen (RUG).
Cover design: Proefschriftmaken.nl || Uitgeverij BOXPress
Printed by: Proefschriftmaken.nl || Uitgeverij BOXPress
Published by: Uitgeverij BOXPress, 's-Hertogenbosch

ISBN: 978-90-8891-902-2

rijksuniversiteit groningen

Precision-cut liver slices: an *ex vivo* model for the early onset and end-stage of liver fibrosis

Proefschrift

ter verkrijging van de graad van doctor aan de
Rijksuniversiteit Groningen
op gezag van de
rector magnificus prof. dr. E. Sterken
en volgens besluit van het College voor Promoties.

De openbare verdediging zal plaatsvinden op

vrijdag 27 juni 2014 om 16.15 uur

door

Inge Marit Westra

geboren op 31 december 1982
te Heerenveen

Promotor
Prof. dr. G.M.M. Groothuis

Copromotor
Dr. P. Olinga

Beoordelingscommissie
Prof. dr. dr. D. Schuppan
Prof. dr. R.A. Bank
Prof. dr. R.J. Porte

Table of contents

Chapter 1	General introduction: Evaluation of fibrosis in precision-cut tissue slices. *Xenobiotica 2013;43(1):98-112*	**7**
Chapter 2	Scope and Outline of the thesis.	**33**
Chapter 3	Precision-cut liver slices as a model for the early onset of liver fibrosis to test antifibrotic drugs. *Toxicology and Applied Pharmacology 2014;274:328–338*	**37**
Chapter 4	The effect of antifibrotic drugs in rat precision-cut fibrotic liver slices. *PLoS One 2014;9(4):e95462*	**59**
Chapter 5	The p38-Mapk pathway is involved in fibrogenesis in rat precision-cut liver slices.	**77**
Chapter 6	Human precision-cut liver slices as an *ex vivo* model to test antifibrotic drugs in the early onset and end-stage of liver fibrosis	**97**
Chapter 7	General discussion and future perspectives	**115**
Appendices	Summary	**126**
	Nederlandse samenvatting	**129**
	Dankwoord	**132**
	Curriculum vitae	**134**

Chapter 1

Evaluation of fibrosis in precision-cut tissue slices

I.M. Westra[a], B.T. Pham[b], G.M.M Groothuis[a] and P. Olinga[b]

Xenobiotica 2013;43(1):98-112

[a]Division of Pharmacokinetics, Toxicology and Targeting, Department of Pharmacy, University of Groningen, The Netherlands
[b]Division of Pharmaceutical Technology and Biopharmacy, Department of Pharmacy, University of Groningen, The Netherlands

Abstract

1. In this review the use of precision-cut tissue slices (PCTS) of the liver, kidney, lung and intestine in fibrosis research are evaluated and future possibilities are discussed.
2. *In vivo* models or techniques that are applicable to be investigated in PCTS are discussed.
3. It is concluded that the early onset of fibrosis can be induced successfully in precision-cut tissue slices prepared from human and experimental animals.
4. Moreover, precision-cut slices of fibrotic tissue are effective in gaining new knowledge of the mechanisms of fibrosis and of the mode of action of potential antifibrotic drugs.
5. Both healthy and fibrotic human tissue slices will pave the way for the testing of novel therapeutic drugs to treat patients with fibrosis avoiding inter-species extrapolation.

Fibrosis is characterized by excessive deposition of extracellular matrix components like collagen and can result from chronic inflammation or injury (1). Fibrogenesis is a physiological phenomenon serving as part of the normal repair process after injury or inflammation, where extracellular matrix is formed by myofibroblasts to temporarily replace the injured tissue, while tissue repair is ongoing. After repair, eventually, the inflammation will be inhibited, extracellular matrix will be degraded and the myofibroblasts will undergo apoptosis. After chronic injury this repair process can be dysregulated, which leads to abnormal accumulation of the extracellular matrix and culminates into fibrosis (2). Alterations of the original tissue architecture of an organ due to high collagen levels will lead to stiffness and loss of functional cells, resulting in impaired function of the organ (1,3).
Fibrosis has been described in almost every organ and this fibrotic process shares common mechanisms in different organs (3). Inflammation and injury, being essential steps in tissue fibrosis, can trigger profibrotic signaling via activation of cytokines and differentiation of resident fibroblast, endothelial cells, epithelial cells or stellate cells into myofibroblasts, which are responsible for the deposition of extracellular matrix (ECM) (3), an indication of the typical multi-cellular character of the pathology. Transforming growth factor β (TGFβ), produced by several tissue-resident and blood-derived cells, is crucial in the development of fibrosis, through its influence on the production of extracellular matrix, matrix metalloproteinases (MMP) -enzymes that degrade ECM-, tissue inhibitor of metalloproteinases (TIMP) and on T cell function (4). Also platelet-derived growth factor (PDGF), produced by macrophages, stellate cells and mesangial cells, is an important factor in the development of organ fibrosis, it plays a vital role in proliferation, migration and survival of myofibroblasts (5,6). Hence, the levels of PDGF are increased in fibrotic tissue (5).
Many *in vitro* and animal models are available to study fibrosis. Cell culture models for fibrosis using fibroblast or myofibroblast cell lines or freshly isolated primary cells, are used to study cell behavior during exposure to fibrotic and anti-fibrotic compounds, but the interplay of the different cell types involved in organ fibrosis cannot be investigated, unless co-cultures are used (7). Furthermore, cell lines can differ from primary cells (8) and freshly isolated cells can react differently compared to cells in the tissue, because the interplay with other cells and matrix is absent (9). In experimental animal models, fibrosis can be induced by induction of chronic injury or infection, and the detailed cellular and molecular pathways of fibrosis can be studied. Recently, precision-cut tissue slices (PCTS) have shown their use in the study of fibrosis, since the multicellular process of fibrosis can be mimicked in tissue slices and they allow the study of fibrosis in human organs by using human tissue.
In this review the use of PCTS from the liver, kidney, lung and intestine in fibrosis research is evaluated and in particular, the use of PCTS in the study of the mechanisms of fibrosis and the effect of antifibrotic drugs is discussed. Most of the techniques to induce fibrosis in PCTS are based on *in vivo* models or techniques that have been used in fibrosis research to induce fibrosis. Therefore first these *in vivo* models are discussed briefly in relation to the possibilities and utilization of PCTS in fibrosis research.

Liver

In liver fibrosis, the hepatic stellate cells (HSC) are the cells that transform into the myofribroblast cells that produce the extracellular matrix. In a healthy liver, HSC are quiescent and store vitamin A.

However, after activation by chronic injury mostly caused by alcohol abuse, HCV infection, non-alcoholic steatohepatitis (NASH) or chronic drug use, HSC change into profibrogenic myofibroblast-like cells (10). Besides HSC, also portal fibroblasts and myofibroblasts derived from bone marrow are collagen-producing cells in liver fibrosis (10). During liver fibrosis, several signaling pathways are activated in HSC, among others the TGFβ/Smad signaling pathway which is activated by TGFβ, secreted by HSC, Kupffer cells, hepatocytes and platelets, the PDGF signaling pathway, activated by PDGF, secreted by HSC and infiltrating macrophages, and the mitogen-activated protein kinase (MAPK) signaling pathway (11-15).
Many types of etiologies leading to fibrosis and the end-stage of fibrosis, cirrhosis, are known. In most patients liver fibrosis or cirrhosis is induced by viral hepatitis, steatohepatitis, cholestasis, alcoholic liver disease or obesity, less common diseases like parasitic disease, autoimmune disease, neonatal liver disease, metabolic disorders, chronic inflammatory conditions and drug toxicity can also initiate fibrotic liver diseases (16).

In vivo models for liver fibrosis

Different *in vivo* animal models are available to study liver fibrosis. For detailed reviews about animal models in fibrosis, see (7,9,17-19). Both rat and mouse models are utilized for the study of fibrosis, but recently there has been a preference for mouse models, mostly because of the availability of genetically modified mice (19).
Carbon tetrachloride (CCl_4), a classic hepatotoxin, induces liver fibrosis, similar to those of acute viral hepatitis, in both rat and mouse (20). Short-term administration of CCl_4 leads to damage and necrosis of the hepatocytes, which results in inflammation and fibrosis. Intoxication up to 8 weeks will eventually lead to severe fibrosis and finally in cirrhosis (7). Therefore, the great advantage of this model is that both the early onset and established fibrosis can be studied (19). Another hepatotoxin that is capable of inducing both acute and chronic hepatic injury is thioacetamide (TAA). Chronic administration of TAA results in proliferation of bile ducts and which finally results in liver cirrhosis. The TAA model shows characteristics that are in line with a human viral hepatitis infection (21).
Another useful model of fibrosis in both rat and mouse is the bile duct ligation (BDL) model. Animals subjected to BDL develop secondary biliary cirrhosis that is characterized by accumulation of bile acids, which causes hepatocyte necrosis (22) resulting in an impaired hepatic function and cirrhosis. Similarly, biliary fibrosis is seen in mice fed with 3,5-diethoxycarbonyl-1,4-dihydrocollidine (DDC). DDC induces sclerosing cholangitis and biliary fibrosis (23).
Detailed genetically modified mouse models used in fibrosis research were used to elucidate the mechanism of fibrosis and were recently reviewed (17) and (24). An example of such a genetically modified mouse model is the $MDR2^{-/-}$ mouse, which lacks the phospholipid flippase MDR2 and spontaneously progresses to severe biliary fibrosis because of leakage of bile acids into the periductal area resulting in up-regulation of profibrogenic genes and down-regulation of collagenolytic activity (25).
Furthermore, transgenic mouse models for liver fibrosis are available. TGFβ1 transgenic mice overexpress TGFβ and develop intermediary fibrosis (26). In addition, transgenic mouse models

overexpressing PDGF-A (27), PDGF-B (28) and PDGF-C (29), were described that resulted in liver fibrosis in these mice.
The models for liver fibrosis mentioned above could be translated into the liver slices system, either to induce fibrosis in slices or to use slices of fibrotic liver to test antifibrotic drugs. Below we give an overview of research of fibrosis performed in liver slices.

Precision-cut liver slices (PCLS)

In recent years several groups have used PCLS to study various types of fibrosis, from early onset of fibrosis till the end-stage cirrhosis, in different species. The major advantage of PCLS over cell culture systems is that all cell types of the liver are present and viable and the original cell-cell and cell-matrix contacts are retained (30). A large improvement compared to *in vivo* studies is the reduction in the amount of animals needed, since up to 250 slices of 5 mm diameter and 250 µm thickness can be prepared from a normal rat liver and up to 40-45 from a normal mouse liver, while fibrotic livers are usually larger, so even more slices can be prepared from these livers. Different culturing systems for PCLS are available and have been reviewed previously (31). For the studies of liver fibrosis the dynamic organ culture system and the 6-12 wells plate incubation systems are successfully used (30,32,33). Slices of healthy liver have been used to study the mechanisms of early onset of fibrosis and the efficacy of anti-fibrotic drugs and slices from fibrotic tissue have been utilized to study the effect of anti-fibrotic drugs in fully developed fibrotic liver tissue (34).

Early onset of fibrosis and PCLS
To study the early onset of fibrosis a variety of models were applied using PCLS, both by exposure to fibrogenic compounds as well as by prolonged incubation.

Ethanol
Alcohol abuse leads to fatty liver, apoptosis, necrosis, fibrosis and cirrhosis (35). Klassen *et al.* started to investigate PCLS as an *in vitro* method to study alcoholic liver injury by exposing rat liver slices to 25mM ethanol for up to 96h (36), and observed oxidation of ethanol, acetaldehyde production, fatty liver, altered redox state and decreased secretion of albumin. All these processes could be inhibited by 4-methylpyrazole (4-MP), an inhibitor of ethanol metabolism, showing the involvement of metabolism in the ethanol-induced damage and the applicability of PCLS to study ethanol-induced liver injury (36). Schaffert *et al.* showed that ethanol treatment up to 48 hours could induce a fibrogenic response in rat PCLS, as it resulted in increased α-smooth muscle actin (αSMA) and collagen 1a1 production (37). Furthermore, IL-6, a multifunctional cytokine known to have both antifibrotic and profibrotic effects dependent on the exposure time, was increased in PCLS treated with ethanol (37). Guo *et al.* treated PCLS with acetaldehyde (350µM), the toxic metabolite of alcohol to induce HSC activation (38). Besides an increased LDH leakage, also several characteristics of onset of fibrosis were observed, such as increased αSMA staining in the space of Disse, TGFβ secretion, hydroxyproline and TIMP-1 protein content, and a decreased MMP-1 protein content (38). In addition, sodium ferulate (SF), the sodium salt of ferulic acid, inhibited HSC activation and collagen production stimulated by acetaldehyde. Furthermore, SF increased MMP-1 expression and decreased

TIMP-1 expression, showing that SF may be beneficial to treat alcoholic liver disease by suppressing the noxious effects of the metabolite of ethanol and by inhibiting activation of HSC (38). The effects induced in PCLS by ethanol and its metabolites correlate well with *in vivo* chemically induced fibrosis and therefore demonstrate the added value of this model to study the mechanism and therapeutic effects of potential anti-fibrotic drugs in alcoholic liver disease that may lead to fibrogenesis.

Bile acids

An alternative way to study biliary fibrosis is by incubating PCLS in the presence of bile acids. Clouzeau-Girard *et al.* studied biliary fibrosis in PCLS cultured in the presence of supra-physiological concentrations of bile acids and showed proliferation of biliary epithelial cells and portal fibroblasts, in accordance with effects seen *in vivo* in biliary fibrosis (39). Moreover, the induction of bile duct epithelial cell proliferation *in vivo*, which stimulates remodeling of the portal tract by β-estradiol and epidermal growth factor (EGF), was also found in PCLS. EGF and β-estradiol induced bile duct epithelial cell proliferation and portal fibroblast activation in PCLS. Moreover β-estradiol induced sinusoidal cell proliferation (40). Based on these results it can be concluded that PCLS are a useful tool to study bile duct epithelial cell proliferation and portal fibrosis.

Toxins

Both rat and human PCLS were successfully used to investigate the early onset of fibrosis by incubation with CCl_4. Human PCLS incubated with CCl_4 for 16 h showed increased gene expression of the early HSC activation markers αβ-crystallin and heat-shock protein 47 (HSP47), but the late markers, αSMA and pro-collagen 1a1 were not increased yet (41). After prolonged incubation up to 48h with CCl_4, αSMA and pro-collagen 1a1 expressions were elevated and pentoxifylline, known to have antifibrotic effects *in vivo* and in cell models, significantly reduced the expression of αSMA and pro-collagen 1a1, while it did not reduce the gene expression of the early markers αβ-crystallin and HSP47 (42). PCLS from normal rats were incubated for 3h or 16h with CCl_4 and gene expressions of HSP47, αB-crystallin, KLF6 and desmin were increased, indicating the activation of HSC in these liver slices (30). In human PCLS compared to studies in rat PCLS, a higher concentration of CCl_4 was necessary to provoke a fibrogenic effect, which may be ascribed to a lower metabolic rate of the human livers (43).

Moreover, TAA was used in PCLS to induce HSC activation. TAA is known to be metabolized by centrilobular hepatocytes *in vivo* and induces oxidative liver injury, subsequently followed by HSC activation (44,45). Guyot *et al.* showed that TAA induced HSC activation in rat PCLS, and also provoked toxicity of portal tract cells (40). So, the specific activation of fibrogenic cells in cultured PCLS, makes this model very useful to study the mechanisms involved in early fibrogenic cell activation (40).

Long-term incubation

After long-term incubation of normal rat liver slices up to 96h, fibrogenic pathways are activated, which was shown by an increased collagen deposition and αSMA protein expression (32). Similarly, αSMA and pro-collagen 1a1 mRNA expression increased in normal rat liver slices after 48h of incubation compared to PCLS directly after slicing (34). Furthermore, genes linked with extra-cellular

matrix (cytoskeleton, filaments, collagens and actin genes) were up-regulated after 96h, showing the applicability of long-term incubation of PCLS to study fibrosis (32).
Human liver slices can also be maintained in culture for up to 7 days, enabling the study of injury and repair processes (46). Vickers *et al*. showed that some HSC markers were not affected (αβ-crystallin, synaptophysin), and some were up-regulated (HSP47, αSMA and pro-collagen 1a1) in human liver slices, indicating the involvement of HSC in human liver slices in the induction of regenerative pathways (46). Similar results were found by van de Bovenkamp *et al.*, who even found a decrease in synaptophysin and fibulin-2 mRNA expression, but an increased pro-collagen 1a1 mRNA expression and a small 1.5 fold increase in collagen protein content after 48 h of incubation (42). In addition, Verrill *et al*. described a long-term incubation model of rat and human liver slices to study liver fibrosis (47). Adult rat liver slices were viable up to 2-3 days, while neonatal rat liver slices and adult human liver slices were viable up to 10 days as analysed by light and electron microscopy, although, after 10 days of culture numbers of live hepatocytes declined to 20 % (47). They demonstrated HSC activation and proliferation after 10 days of culture by electron microscopy and αSMA immunostaining (47). Together with the activation of HSC, new matrix was visible by staining of reticulin (fibers composed of type III collagen) and Sirius red (binds to all types of collagen). These combined results indicate that long-term incubation induces the onset of fibrosis in the liver slices. The synthetic drug SDZ-RAD (a rapamycin analog with anti-proliferative properties) could successfully inhibit αSMA expression by HSC (47), and pentoxyfilline reduced the αSMA, procollagen 1a1 and fibulin-2 mRNA expression (42) indicating that the slices represent a useful model to not only study the onset of fibrosis but also to test the effect of anti-fibrotic compounds (42,47). Yoshida *et al.* used hand-cut liver slices of 2mmx2mmx1mm prepared from livers of 8-day-old Wister rats, fixed on a glass slide and continuously rotated in culture medium, and cultured for 21 days with TGFβ and thrombin (48). Despite the relatively thickness of the slices, the viability of the slices was only reduced by 60% after 15 days of culture. After 21 days, both factors induced changes in the tissue that were related to fibrosis, i.e. increase of type 1 collagen and fibronectin in portal tract, whereas slices incubated with TGFβ alone also had elevated αSMA levels (48), suggesting that onset of fibrosis takes place in these slices. In contrast to PCLS of adult rats no activation of fibrosis was seen when these slices were cultured in the absence of TGFβ and thrombin. This may be explained by the fact that these experiments were performed with slices from very young animals and it is known that slices from postnatal animals survive longer in culture than slices from older rats (49).

In summary, both rat and human PCLS are successfully used to study the onset of ethanol, bile acid and toxin induced fibrosis. Furthermore, long-term incubation of PCLS induces fibrosis in these liver slices. The data from these studies confirm that the fibrotic changes in these PCLS resemble the situation *in vivo*, and can elucidate species differences in the mechanisms involved.

End-stage fibrosis and PCLS

Ethanol
Also slices from fibrotic livers were used to study alcohol related fibrosis. Guo *et al.* prepared slices from fibrotic livers from 3 weeks ethanol fed rats that were additionally injected subcutaneously with

CCl_4 during the last 2 weeks (50). In the fibrotic PCLS, phase I and II metabolism was maintained throughout 6h of incubation, indicating that fibrotic PCLS can also be used to study drug metabolism in fibrosis (50).

BDL

Additionally, secondary biliary cirrhosis can be studied in PCLS. Liver slices from 3-weeks BDL rats were used to study the effect of gliotoxin an inducer of apoptosis in HSC and known to cause regression of liver fibrosis. The apoptosis induced by gliotoxin in these slices was found in HSC, but also in Kupffer cells and liver endothelial cells, as shown by both immunohistochemical stainings and real-time PCR (51). In addition, gliotoxin was coupled to mannose-6-phosphate-modified human serum albumin (M6P-HSA) (52). M6P-HSA selectively bound to activated HSC in PCLS derived from 3-week BDL rats (53). This drug targeting preparation gliotoxin-M6P-HSA induced apoptosis in BDL liver slices and also strongly reduced the immunohistochemical staining for desmin, a marker for HSC, while Kupffer cells and liver endothelial cells were not affected, showing the cell-selectivity of this targeting complex (52). Similarly, the tyrosine kinase inhibitor, 4-chloro-N-[4-methyl-3-(4-pyridin-3-yl-pyrimidin-2-ylamino)-phenyl]-benzamide (PAP19), an imatinib derivative, was coupled to M6P-HSA and incubated with fibrotic PCLS from rats 3 weeks after BDL (54). PAP19-M6P-HSA reduced the expression of αSMA and collagen 1a1 and gene-expression of PDGFR-β and TIMP-1 in fibrotic PCLS, this is in contrast to the findings in cultured HSC, where these genes were not affected (54). Furthermore, specific targeting of dexamethasone to Kupffer cells (Dexa5-Man10-HSA) was achieved in fibrotic rat PCLS, resulting in inhibition of TGFβ gene expression in PCLS derived from rat livers subjected to 3 weeks of BDL (55). These studies with drug targeting preparations show that even these relatively large molecules, i.e. modified HSA, are taken up in the fibrotic slice, as was also shown by Olinga *et al.* (56) and these drug targeting carriers deliver the drug to specific liver cells.

Van de Bovenkamp *et al.* described the effects of gleevec, pentoxifylline and dexamethasone on fibrotic PCLS from rats subjected to BDL (3 weeks) (34). All three compounds inhibited the gene expression of αSMA and pro-collagen 1a1 (34).

Numerous compounds and pathways can be investigated with PCLS prepared from a liver of a single BDL rat, demonstrating its use in reducing the number of laboratory animals needed in fibrosis research.

Toxins

Veidal *et al*. studied the presence of a fragment of type III collagen generated by MMP9 (CO3-610) to investigate the molecular pathways leading to MMP activation and liver tissue regeneration (57). Liver slices of rats injected with CCL_4/Intralipid (an emulsion of soy bean oil, egg phospholipids and glycerin) for 8 weeks were cultured during 48 hours and showed increased levels of CO3-610, showing that this liver fibrosis marker CO3-610 in PCLS correlated with the extent of liver fibrosis (57). Furthermore, slices of rats injected with CCl_4 were used to study gene therapy by delivery of a bacterial lacZ gene, which blocks the overproduction of extracellular matrix components (58). A recombinant adenovirus could transmit a foreign gene to septal cells in fibrous septa. These results suggest that genes delivered by adenovirus might be an important tool to inhibit the gene expression of for instance TGFβ, for a successful therapeutic strategy in hepatic cirrhosis (58).

Tissue remodeling, Irradiation and Virus infection

In the work of Guyot *et al*., PCLS from normal and fibrotic human livers were used to study the behavior of different liver fibrogenic cells by immunohistochemistry (59). After a week of incubation of human PCLS in William's E medium supplemented with insulin, dexamethasone and fetal calf serum, sections of PCLS revealed that the myofibroblastic cells derived from HSC lose αSMA expression and thereby reacquire a quiescent phenyotype, without induction of cell death, while the myofibroblastic cells derived from portal fibroblasts undergo apoptosis and fail to reacquire a quiescent phenotype (59). Guyot *et al*. also applied this to rat PCLS and studied the cell fate of fibrogenic cells in different models of fibrosis. In PCLS derived from CCL_4 –treated rats, myofibroblasts dedifferentiate to HSC, while myofibroblasts in PCLS from BDL rats disappear by apoptosis (60). This work shows the applicability of PCLS to study the tissue remodeling present in fibrosis, by comparing different types of fibrotic PCLS directly after slicing and after prolonged culture, where the fibrotic stimulus is no longer present and remodeling could take place (59,60).
Geraci *et al*. prepared and incubated fibrotic rat liver slices from rats with different stages of irradiation damage and showed that 6-keto prostaglandin $F_{1\alpha}$, an early marker of fibrosis, was produced before the production of the fibrosis marker hydroxyproline could be demonstrated (61).
Moreover, recently it was shown that hepatitis C virus (HCV) infection can be studied in human liver slices (62). This opens the possibility to use PCLS to study virus infections that can lead to liver fibrosis.

In summary, liver slices are a useful tool to investigate the different mechanisms of liver fibrosis in both animal and human livers. Both early and established liver fibrosis can be studied in PCLS and it is a promising tool to study the effect of different antifibrotic compounds.

Kidney

Almost all progressive chronic kidney diseases eventually develop into renal fibrosis (63,64). Renal fibrogenesis is considered as an unsuccessful wound healing process, in which almost all the different cell types in the kidney and also infiltrating lymphocytes, macrophages and fibrocytes are involved (64). After injury, inflammatory cells infiltrate, fibroblasts are activated and extracellular matrix is produced (64). The myofibroblast is the key cell type in producing extracellular matrix components, however, mature fibroblasts, tubular epithelial cells, macrophages and fibrocytes are also a source of extracellular matrix in the kidney (63). In fibrosis, the tubular epithelial cells, when released from the basement membrane, can undergo epithelial-mesenchymal transition, forming fibroblasts (65). The interstitial spaces are then filled with matrix components, mostly collagen I, III and fibronectin (65). The two main families of proteases involved in matrix degradation in the kidney are MMPs and members of the plasmin-dependent pathway. These proteases not only fragment the extracellular matrix, but also cleave non-matrix substrates thereby producing profibrotic growth factors (65). Eventually all these cellular and molecular events will lead to renal failure.
To develop therapies for renal fibrosis, detailed knowledge of the mechanisms for this disease is essential. Therefore adequate *in vivo*, but also *in vitro* models, like kidney slices, are necessary.

***In vivo* models for renal fibrosis**

There are several models that can be used to study renal fibrosis characterized by increased synthesis and accumulation of extracellular matrix (66). Fibrosis can be induced by exposure of animals to (toxic) compounds. The chemical N-(3,5-dichlorophenyl)-succinimide can be used to provoke tubular interstitial nephritis, which can serve as a model for interstitial renal fibrosis (67). In the renal cortex of rats exposed to this chemical, an increased activity of proline hydroxylase, elevated hydroxyproline content and an increased water content was found. All these phenomena are associated with chronic renal fibrosis (67).
Exposure of experimental animals to ochratoxin-A (OA), a mycotoxin found in grain, resulted in renal disease, comparable to endemic nephropathy, a chronic interstitial renal pathology correlated to exposure to OA in grains and animal products (68). Four weeks of exposure to OA in piglets resulted in increased collagen formation and fibroblast proliferation, leading to renal fibrosis (68).
A ligation animal model like the unilateral ureteric obstruction (UUO) model, in which one of the two ureters is ligated, can be used to induce renal fibrosis in both rat and mouse. In the UUO model urine accumulates in the kidney, which leads to hydronephrosis, progressive alterations of renal parenchyma and development of renal fibrosis (69,70). The proliferation of interstitial fibroblasts and their transformation to myofibroblast results in accumulation of extracellular matrix components (70).
Furthermore, hypertension can lead to chronic renal failure and renal fibrosis, leading to loss of function (71). Therefore, experimental models of hypertension-induced renal disease were developed. One of them is the NaCl (5%) fed mice, in which the high salt diet induces the development of hypertension (71). Another mice model for hypertension-induced renal disease is subcutaneous infusion of angiotensin II (Ang II), leading to hypertensive nephropathy which mediates progressive kidney injury resulting in renal fibrosis and inflammation (72).
Fibrosis can also occur as complication after kidney transplantation caused by renal lesions due to immune reactions, drug toxicity of cyclosporine administration and ischemia. Klein *et al*. developed a rat kidney transplant model as model for fibrosis: the Interstitial Fibrosis and Tubular Atrophy (IFTA) model (69).
The genetically modified mice strain COL4A3$^{-/-}$ mice, is used as an animal model for the Alport syndrome, which is a type IV collagen disease that leads to hematuria, proteinuria, renal fibrosis and ultimately to renal failure (73).
The abovementioned models for renal fibrosis could be translated into the renal slices system, either to induce fibrosis in slices or to use slices of fibrotic renal tissue to test antifibrotic drugs.

Precision-cut kidney slices (PCKS)

Similar as in the liver, multiple cell types in the kidney are contributing to the development of renal fibrosis. Therefore also in kidney fibrosis precision-cut slices are used as an *in vitro* model with all different cell types present to study the onset and late stage of renal fibrosis.

Early onset of fibrosis and PCKS

Prolonged culture of human kidney slices paves the way to use slices for the study of fibrosis (74). After 72 hours of culture, kidney slices show signaling pathways of repair and a fibrogenic response as seen by an increased deposition of collagen IV and increased gene expression of collagens, laminins, contractile proteins and markers of proliferation (74). Therefore this model is applicable to study mechanisms of fibrotic renal disease (74).

As a model for renal fibrosis, renal cortex slices of transgenic mouse harboring the luciferase reporter gene under the control of collagen I promoter, were used to investigate the mechanisms of collagen up-regulation in renal tissue (75). In renal slices incubated with AngII, the procollagen 1a2 gene was activated, and by using specific inhibitors it could be shown that MAPK/ERK, AP-1 and TGFβ are involved in this process (75). These *in vitro* results indicate that AngII also directly induces the collagen 1 gene expression, not only indirectly by the *in vivo* induction of hypertensive nephropathy.

Renal slices from rats recovered for 5 weeks from an acute kidney injury (AKI) induced by ischemia-reperfusion (I/R) injury, were used to study oxidative stress in renal disease (76). *In vivo* experiments showed that AKI enhances the profibrotic response to AngII, which is released during oxidative stress. Dihydroethidium (DHE) incorporation as parameter for oxidative stress, was increased in renal slices recovered after AKI compared to slices from control rats (76). These data indicate that the kidney slices are an important model for the study of fibrosis in AKI induced by I/R injury.

End-stage fibrosis and PCKS

Nagae *et al*. used fibrotic kidney to prepare whole kidney, medulla or cortex slices, from UUO rats to study the effect of adrenomedullin (ADM), a vasodilating peptide that reduces renal fibrosis in hypertensive animals on cyclic adenosinemonophosphate (cAMP) production (77). In the kidney slices of UUO rats, cAMP production was increased compared to slices of control kidneys and an ADM-neutralizing antibody partially blocked the enhanced cAMP production (77). However, they used rather thick slices (1.5 mm) for a very short incubation time of maximally 45 min. Using thinner PCLS would probably have prolonged the time period that these kidney slices could be used. Still, even in these relatively thick renal fibrotic slices pharmacological intervention studies were possible.

Flamant *et al*. studied the effect of discoidin domain receptor 1 (DDR1), a non-integrin collagen receptor that displays tyrosine-kinase activity, on the development of renal fibrosis, using fibrotic kidney slices besides *in vivo* experiments (71). Renal cortical slices from high-NaCl fed DDR1 null mice showed decreased monocyte chemoattractant protein-1 (MCP-1) secretion upon stimulation with lipopolysaccharide (LPS) compared to slices from high-NaCl fed wild type mice, indicating the importance of DDR1 in the process of renal inflammation and fibrosis (71).

In conclusion, both normal and fibrotic renal slices can be used in renal fibrosis and anti-fibrotic pharmacotherapy research.

Lung

Pulmonary fibrosis is a lung disease characterized by the development of excess fibrous connective tissue in the lung as a result of deposition of extracellular matrix. Pulmonary fibrosis causes lung

scarring and failure of respiratory function, which reduces the oxygen transfer to the bloodstream with death as a consequence (78). Pulmonary fibrosis is a result of both acute and chronic lung injuries including infections, autoimmune response, tuberculosis, or exposure to hazardous environmental factors (78-80). Furthermore, fibrosis with an unknown cause - idiopathic pulmonary fibrosis (IPF) - is a severe form of fibrosis and these IPF patients have a short life expectancy (80-82).
The mechanism of pulmonary fibrosis is complicated and not fully understood, but recent research suggests that also in the lung an imbalance of the wound repair process is probably one of the main causes (83). Moreover, macrophages and immune cells play pivotal roles in pulmonary fibrosis (83). Through type I and type II immune responses, macrophages are activated and produce various cytokines and chemokines, among others IL-12, TNF, CXCL10 (type I response) and IL-10, CCl-18, CCl-22 (type II response) (83,84). These cytokines and chemokines trigger the release of other profibrotic cytokines namely IL1-β, IL-13 and the most important one TGFβ. Once the cytokines are produced, myofibroblasts and fibroblasts are activated or recruited from different sources and the onset of fibrogenesis is underway (83,85,86). As a result, collagen and other extracellular matrix components are produced. The excessive deposition of these proteins results in further tissue damage, scarring and fibrosis in the lung.
Different models for pulmonary fibrosis have been developed both *in vitro* and *in vivo* to mimic the disease in humans. Although these models provide some tools to understand the pathogenesis of the pulmonary fibrosis, they still cannot fully mimic the chronic state as well as indicate the cellular mechanism of the human disease (87).

***In vivo* models for pulmonary fibrosis**

Bleomycin has been commonly used to induce pulmonary fibrosis in rodents (88). Bleomycin is registered to treat various types of cancer (89), but has some side effects on the function and structure of the lung (90). Advantages of the bleomycin induced fibrosis animal model are the reproducibility and the relatively short time frame of treatment and the possibility to administer it via various routes. The bleomycin induced fibrosis shows a similar change in histological alveolar structure as observed during human disease (88,89,91). After the intratracheal administration of bleomycin, tissue injury starts with an inflammatory response in the alveolar epithelial cells. Subsequently, inflammatory cytokines, such as TNF-α and IL-6, are overexpressed and lead to a significant increase of TGFβ as soon as 4 days after administration (92). Fibrosis induced by bleomycin is detected after 14 to 28 days and persists up to 60 days (89,91,93). However, major disadvantages of the bleomycin induced fibrosis model are the reversibility and the absence of hyperplastic type II alveolar epithelial cells (89). Moreover the animals have sustained abundant pain, weight loss and mortality during the experiment (94).
Lung fibrosis can also be induced in laboratory animals by radiation. By applying 5-15 Gy to mice, pulmonary fibrosis develops after 20 weeks, characterized by the up-regulation of fibrosis gene expression markers such as collagen 1, fibronectin and TGFβ (95). In radiation-induced fibrosis, monocyte, lymphocyte, and other immune cells are involved in the release of TNF-α and the activation of TGFβ (96). However, after the radiation intervention, DNA of target cells can be damaged which leads to unpredictable results. Although considered to be a highly clinically relevant

and reliable model, disadvantages of this method are the cost of using radiation and time to achieve a fibrotic organ (87,97).
Different transgenic murine models have been developed to mimic pulmonary fibrosis (Moore and Hogaboam, 2008). These models are based on the fact that the expression of different genes may influence the fibrotic process. TGF-α deficient mice (98) and TGFβ1 gene transferred rats (99) are two examples of the transgenic models for pulmonary fibrosis. Particularly, after TGFβ1 cDNA was delivered by adenovirus into the lung of a rat, progressive collagen deposition and fibrosis was observed, therefore this is a model to evaluate therapies for pulmonary fibrosis (99,100).
All these *in vivo* models for pulmonary fibrosis could be converted into PCPS studies, either to induce fibrosis in slices or to use slices of fibrotic lung to test antifibrotic drugs.

Precision-cut pulmonary slices (PCPS)

There is a shortage of *in vitro* models for pulmonary fibrosis. Up to now, only fibroblast-based cell culture methods have been used as an *in vitro* model for pulmonary fibrosis. Fibroblasts can be isolated from normal or diseased mouse and human lung tissue (101-104). They can be cultured alone or in co-culture with alveolar type II cells (105). Analyzes of collagen and other ECM proteins produced by these cells suggest that there are large differences between the results found with fibroblasts compared to animal models for pulmonary fibrosis (106). This emphasizes again the differences that exist between *cell culture* and *in vivo* studies.
The precision-cut pulmonary slice technique was developed more than 30 years ago and has been used extensively in lung toxicology and drug metabolism studies. Also in PCPS the cell-cell and cell-extracellular matrix interactions are preserved (107,108). The preparation of lung slices and the incubation method were reviewed as early as 1984 by Freeman and O'Neil (107), and repeatedly discussed (108-111). Before preparing lung slices, the lung should be filled and embedded by using 1.2% or 2% agarose solution (109,112,113). Agarose-filled PCPS are usually prepared with a thickness between 250μm-600μm.

Early onset of fibrosis and PCPS
Some groups have successfully induced the early onset of fibrosis by applying different cytokines to PCPS or manually cut slices (114,115). Lin *et al.* cut manually 1-2 mm thick lung slices and incubated them up to 14 days in RPMI-supplement medium (115). When slices were treated for 14 days with 2.5μM $CdCl_2$ and 0.5ng/ml TGFβ, the average thickness of alveolar septa increased. This model was also used to evaluate the antifibrotic effect of the TGFβ inhibitor λ-carrageenan. λ-Carrageenan moderately decreased the thickness of alveolar septa in the fibrosis-induced slice (115).
Kasper *et al.* induced the early onset of lung fibrosis by using 300μm lung slices prepared with the Krumdieck tissue slicer. Three days of incubation with $CdCl_2$ (2.5μM) and TGFβ1 (1ng/mL) resulted in accumulation of extracellular matrix proteins such as collagen type IV and reticulin (114). αSMA was also up-regulated after 3 days of incubation of the lung slices, suggesting the differentiation of myofibroblasts.
Cooper *et al.* also used TGF?1 (10ng/ml) in PCPS, and found no contractile response after 18h and 24h incubation (116). Contractile response is related to the collagen production and associated with

subepithelial fibrosis in the airway (117). The absence of an effect on the contractility may be due to the short-term incubation. In the same study, PCPS were successfully incubated with cigarette smoke to study the parenchymal responses. It might be worthwhile to also study the early onset of fibrosis in lung slices in the presence of tobacco smoke extracts, as Cooper *et al.* found that when rats were exposed to tobacco smoke, various fibrotic markers like IL-13, TGF□1, αSMA and collagen were elevated in the lung at the protein level (116).
Bleomycin has also been used to induce fibrosis in the PCPS model, by incubating PCPS with bleomycin (at concentrations up to 200mU/mL) during 24 and 48h (118). Two fibrotic markers, CD147 and MMP2, were significantly increased in slices after bleomycin treatment. Hoyt *et al.* also incubated lung slices from different murine strains with bleomycin and measured the toxicity in the early events of bleomycin-induced fibrosis (119). Lactate dehydrogenase (LDH), a marker of cell injury, was elevated and Poly(ADP-ribose) polymerase was activated, from which the authors concluded that Poly(ADP-ribose) polymerase activation contributes to acute pneumocyte injury that induced fibrogenesis (119).
Rat lung slices, prepared by Behrsing *et al.,* were viable up to 28 days of incubation, as assessed by measuring LDH and alkaline phosphatase leakage and histology examination. When PCPS were incubated with bleomycin or carmustine, an induction of fibrosis was detected as early as day 8 with the highest concentration of bleomycin. At day 28, the fibrosis and toxicity caused by carmustine were less substantial compared to bleomycin (120).
Kida *et al.* successfully used PCPS from IL6-deficient mice to study the cytoprotective effects of IL6 against oxidative stress induced by hydroperoxide in lung resident cells including the alveolar epithelial cells (121). As there is a strong relationship between alveolar epithelial injury and pulmonary fibrosis (122), these results again support the potential use of PCPS from wild type and knockout mice as a model to study the mechanisms of the early onset of pulmonary fibrosis.

PCPS have mainly been used in the study of the early onset of fibrosis and pharmacological intervention could be investigated with these slices. To study also the end-stage of pulmonary fibrosis, PCPS of fibrotic tissue e.g. induced *in vivo* by bleomycin in experimental animal models or even human fibrotic PCPS may be used. Normal human PCPS can be incubated up to 3 days (123,124), but results obtained with PCPS of fibrotic patients were not published to date to the best of our knowledge. The long-term incubation of human PCPS can be useful to setup an interesting *ex vivo* model used to understand the physiologic and pathologic properties of pulmonary fibrosis (125).

Intestine

Intestinal fibrosis occurs in patients after radiation therapy or as a reaction of intestinal tissue to chronic inflammation. Moreover, intestinal fibrosis is a major complication in inflammatory bowel disease (IBD), represented by ulcerative colitis and Crohn's disease as the two major types of IBD. As described before, fibrosis is an interaction between the innate immune system and multiple cellular sources of excessive extracellular matrix deposition (126). However in the intestine, internal factors such as gut microbiota, external and environmental factors also play important roles (127). Like in other organs, TGFβ is important in the early onset of fibrosis in the intestine, and is overexpressed in

the inflamed areas in the intestine of patients with Crohn's disease (128). Moreover, TGFβ induced a dose-dependent expression of type I collagen and HSP47 in intestinal fibroblasts (129,130). One of the main mysteries in intestinal fibrosis is the source of the mesenchymal cells such as fibroblasts and myofibroblasts. A variety of hypotheses exist about the transition and activation of mesenchymal cells into fibroblasts and myofibroblasts during the onset of fibrosis (131-133). However, none of these hypotheses have been proven, mainly because of the shortage of relevant intestinal fibrosis models.

***In vivo* models for intestinal fibrosis**

Most of the intestinal fibrosis animal models available are based on the models of intestinal inflammation typically induced by toxins to mimic Crohn's disease and ulcerative colitis. In addition, different models based on transgenic animals and gene delivery systems have been developed.

To induce intestinal fibrosis, 2,4,6-trinitrobenzene sulfonic acid *(*TNBS) is administered intrarectally, which results in transmural inflammation and extracellular matrix deposition. Repeated administration of TNBS produces injury similar to chronic colitis and fibrosis (134). The activation of NF-κB and the production of TGFβ1 are both strongly involved in the TNBS-induced fibrosis model (135,136), again pointing to the strong link between chronic inflammation and fibrosis. The TNBS model has been widely used to evaluate the fibrotic/antifibrotic effect of different drugs and cytokines (135,137-139). TNBS has also been utilized in transgenic mouse to understand the mechanism of TNBS-induced fibrosis. Inokuchi *et al.* used TNBS in angiotensin gene knockout mice and found that $Ang^{-/-}$ mice were partly protected against TNBS-induced fibrosis compared to $Ang^{+/+}$ mice (140). In Insulin-like growth factor-I $(IGF\text{-}I)^{+/-}$ mice TNBS-induced colitis, resulted in collagen 1a1 production and fibrosis, which was increased by administration of IGF-I, indicating that IGF-I is a key player in TNBS-induced fibrosis (141).

Another well-known model is the dextran sulfate sodium (DSS) model. DSS induces acute inflammation in the colon, referred to as colitis. The administration of a repeated dose (3-5 cycles) of DSS results in chronic ulcerative colitis (142,143) with increase of extracellular protein and fibrotic cytokines and additionally a thickening of the colon wall (143). Moreover, mesenchymal cells, such as fibroblasts and myofibroblasts, are increased in the mucosa of the colon of DSS-treated mice (143). Pucilowska *et al.* showed that the inflammation is transmural and that collagen production is elevated, both at the gene and protein level (144).

Intestinal fibrosis can also be induced by the administration of peptidoglycan polysaccharide (PG-PS) (145,146). PG-PS directly injected into the intestine of Lewis rats produced a transient acute inflammation (146). After 28 days, PG-PS injected rats developed intestinal fibrosis, measured by elevated pro-collagen gene expression and histologic scores (146).

Induction of fibrosis after radiation treatment has been known for many years (147,148). Small bowel tissue, resected from patients who were treated with radiation therapy showed an increase of the fibrosis marker TGFβ, elevated levels of extracellular matrix proteins, and thickening of submucosal and serosal layer of the intestine (149,150). In a rat model of radiation-induced fibrosis, a strong induction of pivotal fibrotic cytokines such as TGFβ1 (151) was found. However, up to now,

there is no validated protocol for the radiation-induced fibrosis that ensures reproducible elevated fibrosis markers in experimental animals (151-153).
Transgenic animal models for intestinal fibrosis focus on specific genes that may be involved in the different pathways leading to fibrosis. The well-known knockout model for intestinal fibrosis is the IL10$^{-/-}$ mouse model (154,155). In the IL-10$^{-/-}$ mouse, bacterial exposure or surgical intervention results in inflammation and fibrosis that does not occur in the wild type mouse (154,156). Borowiec *et al.* reported an accumulation of collagen in the ileocolonic anastomosis of IL-10 null mice 6 weeks after surgery (156).
Intestinal fibrosis can also be induced by administration of some specific microflora in normal or IL10$^{-/-}$ knockout mice (157-160). As an example, Johnson *et al.* exposed 8–12weeks old CBA/J mice to a *S. typhimurium* strain to induce fibrosis (159). The described *in vivo* models for intestinal fibrosis can be used in precision-cut intestinal slices, either to provoke fibrosis or to use slices of fibrotic intestinal tissue to study antifibrotic drugs.

Precision-cut intestinal slices (PCIS)

In vitro models for intestinal fibrosis are mostly based on fibroblasts using various culture methods and conditions (161-164). Both murine and human intestinal fibroblasts can be used as a model for intestinal fibrosis. Kim *et al.* has succeeded in evaluating the effect of IL-1β on Prostaglandin E2 induction, an antifibrotic mediator, in 5 primary human fibroblasts cultures (165). Simmons *et al.* showed the induction of type I collagen in a human colon fibroblast/myofibroblast (CCD-18Co) cell culture model by using TGFβ1 (166). However, due to the importance of different cell types in intestinal fibrosis, different culture/co-culture methods have been developed. Intestinal epithelial cell and mesenchymal cell co-culture methods were reviewed by Simon-Assmann *et al.* (167). A three-dimensional culture model of intestinal fibroblasts, macrophages and epithelial cells provides a novel cell culture method to understand intestinal fibrosis (168,169).
Precision-cut intestinal slices (PCIS) have been used as a model to study drug metabolism (170), induction of drug metabolism (171), regulation of gene expression of metabolizing enzymes and transporters (172), xenobiotic toxicity and drug transport (108,173).

Early onset of fibrosis and PCIS
We recently established that PCIS can be used as a model to study the early onset of fibrosis in the intestine. PCIS from rat and human small intestine remain viable up to 24h and 48h, respectively. After incubation for 24 and 48 hours, the gene expression of HSP47 was increased in human and rat PCIS (174) which is in line with the observation of Honzawa *et al.* who reported that serum level of HSP47 protein, which is required in the synthesis of normal collagen (175), is higher in Crohn's disease patients than in ulcerative colitis patients (176). When rat PCIS were cultured in the presence of TGFβ, the gene expression of pro-collagen 1A1 and αSMA was up-regulated compared to control slices (174). These results suggest that the early onset of intestinal fibrosis can be mimicked *in vitro* and that the model is a new tool to unravel the complicated mechanisms of intestinal fibrosis.
However, more (human) studies are necessary to validate this *in vitro* model of fibrosis. It would be interesting to investigate whether the TNBS or the DSS model can be applied *in vitro* to induce the

early onset of fibrosis *in vitro*. In addition, the use of animal or human intestine with established intestinal fibrosis can be used to prepare fibrotic PCIS to study the mechanism of end-stage fibrosis and to screen potential antifibrotic drugs.

Conclusions and future perspectives

Precision-cut tissue slices from liver, kidney, lung and intestine, represent a useful tool to investigate the early onset of fibrosis in both human and experimental animals. Utilizing the slice model can lead to new insights into the (human) mechanisms of the onset of organ fibrogenesis. In addition, in the future, incubations of precision-cut tissue slices with the fibrosis-inducing compounds or factors, used to induce fibrosis *in vivo* in the different organs, may help to further elucidate the mechanisms of human fibrosis.
Furthermore, tissue slices from fibrotic liver and kidney from both human and animals were successfully used to study the factors that play a role in established fibrosis. It would certainly be of interest to also utilize slices from fibrotic lung or intestinal tissue, which has not been published, yet.
Moreover, human (fibrotic) tissue slices will pave the way for the testing of novel therapeutic pharmacological interventions for human fibrosis, which up till now only could be performed in animal models.

References

1. Wynn T A. Cellular and molecular mechanisms of fibrosis. J Pathol 2008; 214: 199-210.

2. Guarino M, Tosoni A, Nebuloni M. Direct contribution of epithelium to organ fibrosis: epithelial-mesenchymal transition. Hum Pathol 2009; 40: 1365-76.

3. Ghosh A K, Vaughan D E. PAI-1 in tissue fibrosis. J Cell Physiol 2012; 227: 493-507.

4. Hold G L, Untiveros P, Saunders K A, El-Omar E M. Role of host genetics in fibrosis. Fibrogenesis Tissue Repair 2009; 2: 6.

5. Trojanowska M. Role of PDGF in fibrotic diseases and systemic sclerosis. Rheumatology (Oxford) 2008; 47 Suppl 5: 2-4.

6. Bonner J C. Regulation of PDGF and its receptors in fibrotic diseases. Cytokine Growth Factor Rev 2004; 15: 255-73.

7. Iredale J P. Models of liver fibrosis: exploring the dynamic nature of inflammation and repair in a solid organ. J Clin Invest 2007; 117: 539-48.

8. Wilkening S, Stahl F, Bader A. Comparison of primary human hepatocytes and hepatoma cell line Hepg2 with regard to their biotransformation properties. Drug Metab Dispos 2003; 31: 1035-42.

9. Snowdon V K, Fallowfield J A. Models and mechanisms of fibrosis resolution. Alcohol Clin Exp Res 2011; 35: 794-9.

10. Bataller R, Brenner D A. Liver fibrosis. J Clin Invest 2005; 115: 209-18.

11. Tsukada S, Parsons C J, Rippe R A. Mechanisms of liver fibrosis. Clin Chim Acta 2006; 364: 33-60.

12. Dooley S, ten Dijke P. TGF-beta in progression of liver disease. Cell Tissue Res 2012; 347: 245-56.

13. Friedman S L. Mechanisms of hepatic fibrogenesis. Gastroenterology 2008; 134: 1655-69.

14. Deng Z Y, Li J, Jin Y, Chen X L, Lu X W. Effect of oxymatrine on the p38 mitogen-activated protein kinases signalling pathway in rats with CCl4 induced hepatic fibrosis. Chin Med J (Engl) 2009; 122: 1449-54.

15. Liu Y, Wen X M, Lui E L et al. Therapeutic targeting of the PDGF and TGF-beta-signaling pathways in hepatic stellate cells by PTK787/ZK22258. Lab Invest 2009; 89: 1152-60.

16. Friedman S L. Liver fibrosis -- from bench to bedside. J Hepatol 2003; 38 Suppl 1: S38-53.

17. Hayashi H, Sakai T. Animal models for the study of liver fibrosis: new insights from knockout mouse models. Am J Physiol Gastrointest Liver Physiol 2011; 300: G729-38.

18. Starkel P, Leclercq I A. Animal models for the study of hepatic fibrosis. Best Pract Res Clin Gastroenterol 2011; 25: 319-33.

19. Popov Y, Schuppan D. Targeting liver fibrosis: strategies for development and validation of antifibrotic therapies. Hepatology 2009; 50: 1294-306.

20. Tsukamoto H, Matsuoka M, French S W. Experimental models of hepatic fibrosis: a review. Semin Liver Dis 1990; 10: 56-65.

21. Xie Y, Wang G, Wang H et al. Cytochrome P450 dysregulations in thioacetamide-induced liver cirrhosis in rats and the counteracting effects of hepatoprotective agents. Drug Metab Dispos 2012; 40: 796-802.

22. Galicia-Moreno M, Favari L, Muriel P. Antifibrotic and antioxidant effects of N-acetylcysteine in an experimental cholestatic model. Eur J Gastroenterol Hepatol 2012; 24: 179-85.

23. Fickert P, Stoger U, Fuchsbichler A et al. A new xenobiotic-induced mouse model of sclerosing cholangitis and biliary fibrosis. Am J Pathol 2007; 171: 525-36.

24. Weiler-Normann C, Herkel J, Lohse A W. Mouse models of liver fibrosis. Z Gastroenterol 2007; 45: 43-50.

25. Popov Y, Patsenker E, Fickert P, Trauner M, Schuppan D. Mdr2 (Abcb4)-/- mice spontaneously develop severe biliary fibrosis via massive dysregulation of pro- and antifibrogenic genes. J Hepatol 2005; 43: 1045-54.

26. Ueberham E, Low R, Ueberham U, Schonig K, Bujard H, Gebhardt R. Conditional tetracycline-regulated expression of TGF-beta1 in liver of transgenic mice leads to reversible intermediary fibrosis. Hepatology 2003; 37: 1067-78.

27. Thieringer F, Maass T, Czochra P et al. Spontaneous hepatic fibrosis in transgenic mice overexpressing PDGF-A. Gene 2008; 423: 23-8.

28. Czochra P, Klopcic B, Meyer E et al. Liver fibrosis induced by hepatic overexpression of PDGF-B in transgenic mice. J Hepatol 2006; 45: 419-28.

29. Campbell J S, Hughes S D, Gilbertson D G et al. Platelet-derived growth factor C induces liver fibrosis, steatosis, and hepatocellular carcinoma. Proc Natl Acad Sci USA 2005; 102: 3389-94.

30. van de Bovenkamp M, Groothuis G M, Draaisma A L et al. Precision-cut liver slices as a new model to study toxicity-induced hepatic stellate cell activation in a physiologic milieu. Toxicol Sci 2005; 85: 632-8.

31. Van de Bovenkamp M, Groothuis G M, Meijer D K, Olinga P. Liver fibrosis in vitro: cell culture models and precision-cut liver slices. Toxicol In Vitro 2007; 21: 545-57.

32. Vickers A E, Saulnier M, Cruz E et al. Organ slice viability extended for pathway characterization: an in vitro model to investigate fibrosis. Toxicol Sci 2004; 82: 534-44.

33. Westra I M, Oosterhuis D, Groothuis G M, Olinga P. Induction of Fibrotic Markers in an in Vitro Model of Liver Fibrosis. Hepatology 2011; 54: 754A-5A.

34. van de Bovenkamp M, Groothuis G M, Meijer D K, Olinga P. Precision-cut fibrotic rat liver slices as a new model to test the effects of anti-fibrotic drugs in vitro. J Hepatol 2006; 45: 696-703.

35. Levitsky J, Mailliard M E. Diagnosis and therapy of alcoholic liver disease. Semin Liver Dis 2004; 24: 233-47.

36. Klassen L W, Thiele G M, Duryee M J et al. An in vitro method of alcoholic liver injury using precision-cut liver slices from rats. Biochem Pharmacol 2008; 76: 426-36.

37. Schaffert C S, Duryee M J, Bennett R G et al. Exposure of precision-cut rat liver slices to ethanol accelerates fibrogenesis. Am J Physiol Gastrointest Liver Physiol 2010; 299: G661-8.

38. Guo Y, Wu X Q, Zhang C, Liao Z X, Wu Y, Wang H. Protective Effect of Sodium Ferulate on Acetaldehyde-Treated Precision-Cut Rat Liver Slices. J Med Food 2012; 15: 557-62.

39. Clouzeau-Girard H, Guyot C, Combe C et al. Effects of bile acids on biliary epithelial cell proliferation and portal fibroblast activation using rat liver slices. Lab Invest 2006; 86: 275-85.

40. Guyot C, Combe C, Clouzeau-Girard H, Moronvalle-Halley V, Desmouliere A. Specific activation of the different fibrogenic cells in rat cultured liver slices mimicking in vivo situations. Virchows Arch 2007; 450: 503-12.

41. van de Bovenkamp M, Groothuis G M M, Meijer D K F, Slooff M J H, Olinga P. Human liver slices as an in vitro model to study toxicity-induced hepatic stellate cell activation in a multicellular milieu. Chem Biol Interact 2006; 162: 62-9.

42. van de Bovenkamp M, Groothuis G M, Meijer D K, Olinga P. Liver slices as a model to study fibrogenesis and test the effects of anti-fibrotic drugs on fibrogenic cells in human liver. Toxicol In Vitro 2008; 22: 771-8.

43. Olinga P, Merema M, Hof I H et al. Effect of human liver source on the functionality of isolated hepatocytes and liver slices. Drug Metab Dispos 1998; 26: 5-11.

44. Pallottini V, Martini C, Bassi A M, Romano P, Nanni G, Trentalance A. Rat HMGCoA reductase activation in thioacetamide-induced liver injury is related to an increased reactive oxygen species content. J Hepatol 2006; 44: 368-74.

45. Bruck R, Genina O, Aeed H et al. Halofuginone to prevent and treat thioacetamide-induced liver fibrosis in rats. Hepatology 2001; 33: 379-86.

46. Vickers A E, Fisher R, Olinga P, Dial S. Repair pathways evident in human liver organ slices. Toxicol In Vitro 2011; 25: 1485-92.

47. Verrill C, Davies J, Millward-Sadler H, Sundstrom L, Sheron N. Organotypic liver culture in a fluid-air interface using slices of neonatal rat and adult human tissue--a model of fibrosis in vitro. J Pharmacol Toxicol Methods 2002; 48: 103-10.

48. Yoshida T, Arisaka Y, Nakagawa S, Takahashi H. Rotation culture with a newly developed holder enables long-term liver slice culture for study of liver fibrosis. Hepatol Res 2004; 28: 198-206.

49. Hart A, Mattheyse F J, Balinsky J B. An organ culture of postnatal rat liver slices. In Vitro 1983; 19: 841-52.

50. Guo Y, Wang H, Zhang C. Establishment of rat precision-cut fibrotic liver slice technique and its application in verapamil metabolism. Clin Exp Pharmacol Physiol 2007; 34: 406-13.

51. Hagens W I, Olinga P, Meijer D K, Groothuis G M, Beljaars L, Poelstra K. Gliotoxin non-selectively induces apoptosis in fibrotic and normal livers. Liver Int 2006; 26: 232-9.

52. Hagens W I, Beljaars L, Mann D A et al. Cellular targeting of the apoptosis-inducing compound gliotoxin to fibrotic rat livers. J Pharmacol Exp Ther 2008; 324: 902-10.

53. Beljaars L, Olinga P, Molema G et al. Characteristics of the hepatic stellate cell-selective carrier mannose 6-phosphate modified albumin (M6P(28)-HSA). Liver 2001; 21: 320-8.

54. Gonzalo T, Beljaars L, van de Bovenkamp M et al. Local inhibition of liver fibrosis by specific

delivery of a platelet-derived growth factor kinase inhibitor to hepatic stellate cells. J Pharmacol Exp Ther 2007; 321: 856-65.

55. Melgert B N, Olinga P, Van Der Laan J M et al. Targeting dexamethasone to Kupffer cells: effects on liver inflammation and fibrosis in rats. Hepatology 2001; 34: 719-28.

56. Olinga P, Hof I H, Merema M T et al. The applicability of rat and human liver slices to the study of mechanisms of hepatic drug uptake. J Pharmacol Toxicol Methods 2001; 45: 55-63.

57. Veidal S S, Juul M, Leeming D J, Karsdal M A. An Ex Vivo Model for Liver Fibrosis Resolution. Hepatology 2011; 54: 1219A-.

58. Nakamura T, Akiyoshi H, Saito I, Sato K. Adenovirus-mediated gene expression in the septal cells of cirrhotic rat livers. J Hepatol 1999; 30: 101-6.

59. Guyot C, Lepreux S, Combe C et al. Fibrogenic cell phenotype modifications during remodelling of normal and pathological human liver in cultured slices. Liver Int 2010; 30: 1529-40.

60. Guyot C, Combe C, Balabaud C, Bioulac-Sage P, Desmouliere A. Fibrogenic cell fate during fibrotic tissue remodelling observed in rat and human cultured liver slices. J Hepatol 2007; 46: 142-50.

61. Geraci J P, Mariano M S. Radiation hepatology of the rat: association of the production of prostacyclin with radiation-induced hepatic fibrosis. Radiat Res 1996; 145: 93-7.

62. Lagaye S, Shen H, Saunier B et al. Efficient replication of primary or culture hepatitis C virus isolates in human liver slices: A relevant ex vivo model of liver infection. Hepatology 2012.

63. Boor P, Ostendorf T, Floege J. Renal fibrosis: novel insights into mechanisms and therapeutic targets. Nat Rev Nephrol 2010; 6: 643-56.

64. Liu Y. Cellular and molecular mechanisms of renal fibrosis. Nat Rev Nephrol 2011; 7: 684-96.

65. Zeisberg M, Neilson E G. Mechanisms of tubulointerstitial fibrosis. J Am Soc Nephrol 2010; 21: 1819-34.

66. Zeisberg M, Soubasakos M A, Kalluri R. Animal models of renal fibrosis. Methods Mol Med 2005; 117: 261-72.

67. Barrett M C, Cashman S J, Moss J. Experimental interstitial renal fibrosis in rats: nephritis induced by N-(3,5-dichlorophenyl)succinimide. Br J Exp Pathol 1983; 64: 425-36.

68. Aukema H M, House J D, Bankovic-Calic N, Ogborn M R. Increased renal fibrosis and expression of renal phosphatidylinositol 4-kinase-beta and phospholipase C(gamma1) proteins in piglets exposed to ochratoxin-A. Nephron Physiol 2004; 96: 19-25.

69. Klein J, Kavvadas P, Prakoura N et al. Renal fibrosis: insight from proteomics in animal models and human disease. Proteomics 2011; 11: 805-15.

70. Chevalier R L, Forbes M S, Thornhill B A. Ureteral obstruction as a model of renal interstitial fibrosis and obstructive nephropathy. Kidney Int 2009; 75: 1145-52.

71. Flamant M, Placier S, Rodenas A et al. Discoidin domain receptor 1 null mice are protected against hypertension-induced renal disease. J Am Soc Nephrol 2006; 17: 3374-81.

72. Liu Z, Huang X R, Lan H Y. Smad3 mediates ANG II-induced hypertensive kidney disease in mice. Am J Physiol Renal Physiol 2012; 302: F986-97.

73. Gross O, Girgert R, Beirowski B et al. Loss of collagen-receptor DDR1 delays renal fibrosis in hereditary type IV collagen disease. Matrix Biol 2010; 29: 346-56.

74. Vickers A E, Fisher R, Olinga P. Human liver and kidney slice viability is extended and pathways of fibrosis are characterized. The Toxicologist 2005; 84.

75. Tharaux P L, Chatziantoniou C, Fakhouri F, Dussaule J C. Angiotensin II activates collagen I

gene through a mechanism involving the MAP/ER kinase pathway. Hypertension 2000; 36: 330-6.

76. Basile D P, Leonard E C, Beal A G, Schleuter D, Friedrich J. Persistent oxidative stress following renal ischemia-reperfusion injury increases ANG II hemodynamic and fibrotic activity. Am J Physiol Renal Physiol 2012; 302: F1494-502.

77. Nagae T, Mori K, Mukoyama M et al. Adrenomedullin inhibits connective tissue growth factor expression, extracellular signal-regulated kinase activation and renal fibrosis. Kidney Int 2008; 74: 70-80.

78. Ley K. From lung injury to fibrosis. Nat Med 2008; 14: 20-1.

79. Thannickal V J, Toews G B, White E S, Lynch J P, Martinez F J. Mechanisms of pulmonary fibrosis. Annu Rev Med 2004; 55: 395-417.

80. Gross T J, Hunninghake G W. Idiopathic Pulmonary Fibrosis. N Engl J Med 2001; 345: 517-25.

81. Mutsaers S E, McAnulty R J, Laurent G J, Knight D a. Evaluation of experimental models of idiopathic pulmonary fibrosis. Drug Discovery Today: Disease Models 2004; 1: 329-36.

82. Selman M, King J,Talmadge E., Pardo A. Idiopathic Pulmonary Fibrosis: Prevailing and Evolving Hypotheses about Its Pathogenesis and Implications for Therapy. Ann Intern Med 2001; 134: 136-51.

83. Wynn T A. Integrating mechanisms of pulmonary fibrosis. The Journal of Experimental Medicine} 2011; 208: 1339-50.

84. Homer R J, Elias J a, Lee C G, Herzog E. Modern concepts on the role of inflammation in pulmonary fibrosis. Archives of pathology & laboratory medicine 2011; 135: 780-8.

85. Lee C G, Cho S J, Kang M J et al. Early growth response gene 1-mediated apoptosis is essential for transforming growth factor beta1-induced pulmonary fibrosis. J Exp Med 2004; 200: 377-89.

86. Strieter R M, Mehrad B. New mechanisms of pulmonary fibrosis. Chest 2009; 136: 1364-70.

87. Moore B B, Hogaboam C M. Murine models of pulmonary fibrosis. American journal of physiology.Lung cellular and molecular physiology 2008; 294: 152-60.

88. Moeller A, Ask K, Warburton D, Gauldie J, Kolb M. The bleomycin animal model: a useful tool to investigate treatment options for idiopathic pulmonary fibrosis? The international journal of biochemistry \& cell biology 2008; 40: 362-82.

89. Mouratis M A, Aidinis V. Modeling pulmonary fibrosis with bleomycin. Curr Opin Pulm Med 2011; 17: 355-61.

90. Azambuja E, Fleck J F, Batista R G, Menna Barreto S S. Bleomycin lung toxicity: who are the patients with increased risk? Pulm Pharmacol Ther 2005; 18: 363-6.

91. Degryse A L, Tanjore H, Xu X C et al. Repetitive intratracheal bleomycin models several features of idiopathic pulmonary fibrosis. Am J Physiol Lung Cell Mol Physiol 2010; 299: 442-52.

92. Kolb M, Margetts P J, Galt T et al. Transient transgene expression of decorin in the lung reduces the fibrotic response to bleomycin. American journal of respiratory and critical care medicine 2001; 163: 770-7.

93. Thrall R S, McCormick J R, Jack R M, McReynolds R a, Ward P a. Bleomycin-induced pulmonary fibrosis in the rat: inhibition by indomethacin. The American journal of pathology 1979; 95: 117-30.

94. Corbel M, Caulet-Maugendre S, Germain N, Molet S, Lagente V, Boichot E. Inhibition of bleomycin-induced pulmonary fibrosis in mice by the matrix metalloproteinase inhibitor batimastat. J Pathol 2001; 193: 538-45.

95. Finkelstein J N, Johnston C J, Baggs R, Rubin P. Early alterations in extracellular matrix and transforming growth factor beta gene expression in mouse lung indicative of late radiation fibrosis. Int J Radiat Oncol Biol Phys 1994; 28: 621-31.

96. Johnston C J, Williams J P, Okunieff P, Finkelstein J N. Radiation-induced pulmonary fibrosis: examination of chemokine and chemokine receptor families. Radiat Res 2002; 157: 256-65.

97. Moeller A, Rodriguez-Lecompte J C, Wang L, Gauldie J, Kolb M. Models of pulmonary fibrosis. Drug Discovery Today: Disease Models 2006; 3: 243-9.

98. Madtes D K, Elston a L, Hackman R C, Dunn a R, Clark J G. Transforming growth factor-alpha deficiency reduces pulmonary fibrosis in transgenic mice. American journal of respiratory cell and molecular biology 1999; 20: 924-34.

99. Sime P J, Xing Z, Graham F L, Csaky K G, Gauldie J. Adenovector-mediated gene transfer of active transforming growth factor-beta1 induces prolonged severe fibrosis in rat lung. J Clin Invest 1997; 100: 768-76.

100. Farkas L, Farkas D, Ask K et al. VEGF ameliorates pulmonary hypertension through inhibition of endothelial apoptosis in experimental lung fibrosis in rats. J Clin Invest 2009; 119: 1298-311.

101. Hetzel M, Bachem M, Anders D, Trischler G, Faehling M. Different Effects of Growth Factors on Proliferation and Matrix Production of Normal and Fibrotic Human Lung Fibroblasts. Lung 2005; 183: 225-37.

102. Moodley Y P, Misso N L a, Scaffidi A K et al. Inverse effects of interleukin-6 on apoptosis of fibroblasts from pulmonary fibrosis and normal lungs. American journal of respiratory cell and molecular biology 2003; 29: 490-8.

103. Liu X, Sun S Q, Ostrom R S. Fibrotic lung fibroblasts show blunted inhibition by cAMP due to deficient cAMP response element-binding protein phosphorylation. J Pharmacol Exp Ther 2005; 315: 678-87.

104. Dileto C L, Travis E L. Fibroblast radiosensitivity in vitro and lung fibrosis in vivo: comparison between a fibrosis-prone and fibrosis-resistant mouse strain. Radiat Res 1996; 146: 61-7.

105. Mangum J B, Everitt J I, Bonner J C, Moore L R, Brody A R. Co-culture of primary pulmonary cells to model alveolar injury and translocation of proteins. In vitro cellular \& developmental biology : journal of the Tissue Culture Association 1990; 26: 1135-43.

106. Coker R K, Laurent G J, Shahzeidi S et al. Transforming growth factors-beta 1, -beta 2, and -beta 3 stimulate fibroblast procollagen production in vitro but are differentially expressed during bleomycin-induced lung fibrosis. Am J Pathol 1997; 150: 981-91.

107. Freeman B A, O'Neil J J. Tissue slices in the study of lung metabolism and toxicology. Environ Health Perspect 1984; 56: 51-60.

108. Vickers A E M, Fisher R L. Precision-cut organ slices to investigate target organ injury. Expert opinion on drug metabolism \& toxicology 2005; 1: 687-99.

109. Fisher R L, Smith M S, Hasal S J, Hasal K S, Gandolfi a J, Brendel K. The Use of Human Lung Slices in Toxicology. Hum Exp Toxicol 1994; 13: 466-71.

110. Parrish A, Gandolfi A. Precision-cut tissue slices: applications in pharmacology and toxicology. Life Sci 1995; 57: 1887-901.

111. Umachandran M, Howarth J, Ioannides C. Metabolic and structural viability of precision-cut rat lung slices in culture. Xenobiotica 2004; 34: 771-80.

112. De Kanter R, Monshouwer M, Draaisma A L et al. Prediction of whole-body metabolic clearance of drugs through the combined use of slices from rat liver, lung, kidney, small intestine and colon. Xenobiotica 2004; 34: 229-41.

113. de Graaf I A, de Kanter R, de Jager M H et al. Empirical validation of a rat in vitro organ slice model as a tool for in vivo clearance prediction. Drug Metab Dispos 2006; 34: 591-9.

114. Kasper M, Seidel D, Knels L et al. Early signs of lung fibrosis after in vitro treatment of rat lung slices with CdCl2 and TGF-beta1. Histochem Cell Biol 2004; 121: 131-40.

115. Lin C J, Yang P C, Hsu M T et al. Induction of pulmonary fibrosis in organ-cultured rat lung by cadmium chloride and transforming growth factor-beta1. Toxicology 1998; 127: 157-66.

116. Cooper P R, Poll C T, Barnes P J, Sturton R G. Involvement of IL-13 in tobacco smoke-induced changes in the structure and function of rat intrapulmonary airways. Am J Respir Cell Mol Biol 2010; 43: 220-6.

117. Margulis A, Nocka K H, Wood N L, Wolf S F, Goldman S J, Kasaian M T. MMP dependence of fibroblast contraction and collagen production induced by human mast cell activation in a three-dimensional collagen lattice. Am J Physiol Lung Cell Mol Physiol 2009; 296: L236-47.

118. Barth K, Bläsche R, Kasper M. Lack of evidence for caveolin-1 and CD147 interaction before and after bleomycin-induced lung injury. Histochem Cell Biol 2006; 126: 563-73.

119. Hoyt D G, Lazo J S. Murine strain differences in acute lung injury and activation of poly(ADP-ribose) polymerase by in vitro exposure of lung slices to bleomycin. American journal of respiratory cell and molecular biology 1992; 7: 645-51.

120. Behrsing H, Amin K, Ip C, Tyson C. Induction of fibrosis by bleomycin and carmustine in rat lung slices. The Toxicologist 2004; 78: 50.

121. Kida H, Yoshida M, Hoshino S et al. Protective effect of IL-6 on alveolar epithelial cell death induced by hydrogen peroxide. American journal of physiology.Lung cellular and molecular physiology 2005; 288: 342-9.

122. Adamson I Y, Young L, Bowden D H. Relationship of alveolar epithelial injury and repair to the induction of pulmonary fibrosis. Am J Pathol 1988; 130: 377-83.

123. Ressmeyer A R, Larsson A K, Vollmer E, Dahlèn S E, Uhlig S, Martin C. Characterisation of guinea pig precision-cut lung slices: comparison with human tissues. The European respiratory journal : official journal of the European Society for Clinical Respiratory Physiology 2006; 28: 603-11.

124. Wohlsen a, Martin C, Vollmer E et al. The early allergic response in small airways of human precision-cut lung slices. European Respiratory Journal 2003; 21: 1024-32.

125. Königshoff M, Uhl F, Gosens R. From molecule to man: integrating molecular biology with whole organ physiology in studying respiratory disease. Pulmonary pharmacology & therapeutics 2011; 24: 466-70.

126. Fiocchi C, Lund P K. Themes in fibrosis and gastrointestinal inflammation. Am J Physiol Gastrointest Liver Physiol 2011; 300: G677-83.

127. Lawrance I C, Maxwell L, Doe W. Inflammation location, but not type, determines the increase in TGF-beta1 and IGF-1 expression and collagen deposition in IBD intestine. Inflamm Bowel Dis 2001; 7: 16-26.

128. di Mola F F, Friess H, Scheuren A et al. Transforming growth factor-betas and their signaling receptors are coexpressed in Crohn's disease. Ann Surg 1999; 229: 67-75.

129. Mulsow J J W, Watson R W G, Fitzpatrick J M, O'Connell P R. Transforming growth factor-beta promotes pro-fibrotic behavior by serosal fibroblasts via PKC and ERK1/2 mitogen activated protein kinase cell signaling. Ann Surg 2005; 242: 880,7, dsusson 887--9.

130. Kitamura H, Yamamoto S, Nakase H et al. Role of heat shock protein 47 in intestinal fibrosis of experimental colitis. Biochem Biophys Res Commun 2011; 404: 599-604.

131. Flier S N, Tanjore H, Kokkotou E G, Sugimoto H, Zeisberg M, Kalluri R. Identification of epithelial to mesenchymal transition as a novel source of fibroblasts in intestinal fibrosis. J Biol Chem 2010; 285: 20202-12.

132. Powell D W, Pinchuk I V, Saada J I, Chen X, Mifflin R C. Mesenchymal cells of the intestinal lamina propria. Annu Rev Physiol 2011; 73: 213-37.

133. Rieder F, Kessler S P, West G A et al. Inflammation-induced endothelial-to-mesenchymal transition: a novel mechanism of

intestinal fibrosis. The American journal of pathology 2011; 179: 2660-73.

134. te Velde A a, Verstege M I, Hommes D W. Critical appraisal of the current practice in murine TNBS-induced colitis. Inflamm Bowel Dis 2006; 12: 995-9.

135. Lawrance I C, Wu F, Leite A Z a et al. A murine model of chronic inflammation-induced intestinal fibrosis down-regulated by antisense NF-kappa B. Gastroenterology 2003; 125: 1750-61.

136. Wengrower D, Zanninelli G, Latella G et al. Losartan reduces trinitrobenzene sulphonic acid-induced colorectal fibrosis in rats. Can J Gastroenterol 2012; 26: 33-9.

137. San-Miguel B, Crespo I, Kretzmann N A et al. Glutamine prevents fibrosis development in rats with colitis induced by 2,4,6-trinitrobenzene sulfonic acid. J Nutr 2010; 140: 1065-71.

138. Barrett R, Zhang X, Koon H W et al. Constitutive TL1A expression under colitogenic conditions modulates the severity and location of gut mucosal inflammation and induces fibrostenosis. Am J Pathol 2012; 180: 636-49.

139. Xu X, Weksler-Zangen S, Pikarsky A et al. Mast cells involvement in the inflammation and fibrosis development of the TNBS-induced rat model of colitis. Scand J Gastroenterol 2002; 37: 330-7.

140. Inokuchi Y, Morohashi T, Kawana I, Nagashima Y, Kihara M, Umemura S. Amelioration of 2,4,6-trinitrobenzene sulphonic acid induced colitis in angiotensinogen gene knockout mice. Gut 2005; 54: 349-56.

141. Mahavadi S, Flynn R S, Grider J R et al. Amelioration of excess collagen IαI, fibrosis, and smooth muscle growth in TNBS-induced colitis in IGF-I(+/-) mice. Inflamm Bowel Dis 2011; 17: 711-9.

142. Okayasu I, Hatakeyama S, Yamada M, Ohkusa T, Inagaki Y, Nakaya R. A novel method in the induction of reliable experimental acute and chronic ulcerative colitis in mice. Gastroenterology 1990; 98: 694-702.

143. Suzuki K, Sun X, Nagata M et al. Analysis of intestinal fibrosis in chronic colitis in mice induced by dextran sulfate sodium. Pathol Int 2011; 61: 228-38.

144. Pucilowska J B, Williams K L, Lund P K. Fibrogenesis. IV. Fibrosis and inflammatory bowel disease: cellular mediators and animal models. American journal of physiology.Gastrointestinal and liver physiology 2000; 279: G653-9.

145. Theiss A L, Fuller C R, Simmons J G, Liu B, Sartor R B, Lund P K. Growth Hormone Reduces the Severity of Fibrosis Associated With Chronic Intestinal Inflammation. Gastroenterology 2005; 129: 204-19.

146. Rahal K, Schmiedlin-Ren P, Adler J et al. Resveratrol has antiinflammatory and antifibrotic effects in the peptidoglycan-polysaccharide rat model of Crohn's disease. Inflamm Bowel Dis 2012; 18: 613-23.

147. Donner C S. Pathophysiology and therapy of chronic radiation-induced injury to the colon. Dig Dis 1998; 16: 253-61.

148. Martin M, Lefaix J, Delanian S. TGF-beta1 and radiation fibrosis: a master switch and a specific therapeutic target? Int J Radiat Oncol Biol Phys 2000; 47: 277-90.

149. Richter K K, Fink L M, Hughes B M, Sung C C, Hauer-Jensen M. Is the loss of endothelial thrombomodulin involved in the mechanism of chronicity in late radiation enteropathy? Radiotherapy and oncology : journal of the European Society for Therapeutic Radiology and Oncology 1997; 44: 65-71.

150. Haydont V, Vozenin-Brotons M. Maintenance of radiation-induced intestinal fibrosis: cellular and molecular features. World journal of gastroenterology : WJG 2007; 13: 2675-83.

151. Langberg C W, Hauer-Jensen M, Sung C C, Kane C J. Expression of fibrogenic cytokines in rat small intestine after fractionated irradiation. Radiotherapy and oncology : journal of the European Society for Therapeutic Radiology and Oncology 1994; 32: 29-36.

152. Langberg C W, Sauer T, Reitan J B, Hauer-Jensen M. Relationship between intestinal fibrosis and histopathologic and morphometric changes in consequential and late radiation enteropathy. Acta Oncol 1996; 35: 81-7.

153. Linard C, Billiard F, Benderitter M. Intestinal Irradiation and Fibrosis in a Th1-Deficient Environment. Int J Radiat Oncol Biol Phys 2012.

154. Speck K E, Garrison A P, Rigby R J, von Allmen D C, Lund P K, Helmrath M a. Inflammation enhances resection-induced intestinal adaptive growth in IL-10 null mice. J Surg Res 2011; 168: 62-9.

155. Kühn R, Löhler J, Rennick D, Rajewsky K, Müller W. Interleukin-10-deficient mice develop chronic enterocolitis. Cell 1993; 75: 263-74.

156. Borowiec A M, Sydora B C, Doyle J et al. Small bowel fibrosis and systemic inflammatory response after ileocolonic anastomosis in IL-10 null mice. J Surg Res 2012.

157. van Tol E A, Holt L, Li F L et al. Bacterial cell wall polymers promote intestinal fibrosis by direct stimulation of myofibroblasts. Am J Physiol 1999; 277: G245-55.

158. Mourelle M, Salas A, Guarner F, Crespo E, García-Lafuente A, Malagelada J R. Stimulation of transforming growth factor beta1 by enteric bacteria in the pathogenesis of rat intestinal fibrosis. Gastroenterology 1998; 114: 519-26.

159. Johnson L A, Luke A, Sauder K, Moons D S, Horowitz J C, Higgins P D R. Intestinal fibrosis is reduced by early elimination of inflammation in a mouse model of IBD: Impact of a Top-Down approach to intestinal fibrosis in mice. Inflamm Bowel Dis 2012; 18: 460-71.

160. Rigby R J, Hunt M R, Scull B P et al. A new animal model of postsurgical bowel inflammation and fibrosis: the effect of commensal microflora. Gut 2009; 58: 1104-12.

161. Agrez M V, Chua F K. The role of colon fibroblasts in malignant large bowel obstruction--an experimental in vitro model. Br J Cancer 1990; 62: 567-72.

162. Sellge G, Lorentz A, Gebhardt T et al. Human intestinal fibroblasts prevent apoptosis in human intestinal mast cells by a mechanism independent of stem cell factor, IL-3, IL-4, and nerve growth factor. Journal of immunology (Baltimore, Md.: 1950) 2004; 172: 260-7.

163. Fritsch C, Simon-Assmann P, Kedinger M, Evans G. Cytokines modulate fibroblast phenotype and epithelial-stroma interactions in rat intestine. Gastroenterology 1997; 112: 826-38.

164. Burke J P, Watson R W G, Murphy M, Docherty N G, Coffey J C, O'Connell P R. Simvastatin impairs smad-3 phosphorylation and modulates transforming growth factor beta1-mediated activation of intestinal fibroblasts. Br J Surg 2009; 96: 541-51.

165. Kim E C, Zhu Y, Andersen V et al. Cytokine-mediated PGE2 expression in human colonic fibroblasts. Am J Physiol , Cell Physiol 1998; 275: 988-94.

166. Simmons J G, Pucilowska J B, Keku T O, Lund P K. IGF-I and TGF-beta1 have distinct effects on phenotype and proliferation of intestinal fibroblasts. American journal of physiology.Gastrointestinal and liver physiology 2002; 283: G809-18.

167. Simon-Assmann P, Turck N, Sidhoum-Jenny M, Gradwohl G, Kedinger M. In vitro models of intestinal epithelial cell differentiation. Cell Biol Toxicol 2007; 23: 241-56.

168. Leonard F, Collnot E, Lehr C. A three-dimensional coculture of enterocytes, monocytes and dendritic cells to model inflamed intestinal mucosa in vitro. Molecular pharmaceutics 2010; 7: 2103-19.

169. Spottl T, Hausmann M, Gunckel M et al. A new organotypic model to study cell interactions in the intestinal mucosa. European journal of gastroenterology \& hepatology 2006; 18: 901-9.

170. de Kanter R, Tuin A, van de Kerkhof E et al. A new technique for preparing precision-cut slices from small intestine and colon for drug biotransformation studies. J Pharmacol Toxicol Methods 2005; 51: 65-72.

171. van de Kerkhof E G, de Graaf I A M, Ungell A B, Groothuis G M M. Induction of metabolism and transport in human intestine: validation of precision-cut slices as a tool to study induction of drug metabolism in human intestine in vitro. Drug metabolism and disposition: the biological fate of chemicals 2008; 36: 604-13.

172. Khan A A, Chow E C, Porte R J, Pang K S, Groothuis G M. Expression and regulation of the bile acid transporter, OSTalpha-OSTbeta in rat and human intestine and liver. Biopharm Drug Dispos 2009; 30: 241-58.

173. Possidente M, Dragoni S, Franco G et al. Rat intestinal precision-cut slices as an in vitro model to study xenobiotic interaction with transporters. European Journal of Pharmaceutics and Biopharmaceutics 2011; 79: 343-8.

174. Bao Tung Pham, Westra I, Oosterhuis D, de Graaf I, Olinga P. Rat and human intestinal slices as a model for intestinal fibrosis in Inflammatory Bowel Disease. Inflamm Bowel Dis 2011; 17: S76-.

175. Taguchi T, Razzaque M S. The collagen-specific molecular chaperone HSP47: is there a role in fibrosis? Trends Mol Med 2007; 13: 45-53.

176. Honzawa Y, Nakase H, Takeda Y, Nagata K, Chiba T. Heat shock protein 47 can be a new target molecule for intestinal fibrosis related to inflammatory bowel disease. Inflamm Bowel Dis 2010; 16: 2004-6.

Chapter 2

Scope and outline of the thesis

Scope

In **chapter 1** fibrosis was introduced as a serious disease that can affect various organs. In addition, the use of precision-cut tissue slices (PCTS) was evaluated as *ex vivo* model to study fibrosis in liver, kidney, lung and intestine. The research chapters of this thesis are focused on precision-cut liver slices (PCLS) as *ex vivo* model for liver fibrosis.
Liver fibrosis is characterized by an abundant deposition of extracellular matrix proteins (1,2). It starts as a normal wound healing process, but if this process continues, due to e.g. chronic injury, extracellular matrix accumulates and the liver will become fibrotic. During liver fibrosis, not only hepatic stellate cells (HSC), which are, in activated state, the major contributors of collagen deposition in the liver, but also Kupffer cells, endothelial cells, fibroblasts and hepatocytes are involved in the process of fibrogenesis, by releasing mediators such as platelet- derived growth factor (PDGF) and transforming growth factor beta (TGFβ) (3,4). Since there is no effective pharmacotherapeutic treatment for liver fibrosis yet, the only option for patients with advanced liver fibrosis is a liver transplantation. Therefore, studies investigating possible antifibrotic compounds are of utmost importance (5). To study liver fibrosis and antifibrotics *in vitro* it is pivotal to use a model that contains all the cells of the liver with intact interactions with the extracellular matrix, as is the case in the precision-cut liver slices (PCLS). To strive for the use of a model for liver fibrosis that requires a minimal use of laboratory animals and at the same time resembles the (human) disease as close as possible, we investigated the utilization of human and rat PCLS as an *ex vivo* model for liver fibrosis to study the mechanisms of fibrosis and to test antifibrotic drugs.

Aim

The aims of the studies described in this thesis, are to establish if human and rat PCLS can be utilized 1) to investigate to what extent both the early onset and the late stage of liver fibrosis are reproduced *ex vivo* in PCLS; 2) to study the mechanism of the fibrotic process in liver slices; 3) to investigate antifibrotic properties of compounds during both stages of fibrosis. If these aims are successfully achieved this will lead to the realization of reduction, refinement and replacement in the use of laboratory animals in fibrosis research and pre-clinical testing of antifibrotic drugs for liver fibrosis by the use of this *ex vivo* model for liver fibrosis. Furthermore, because by utilizing human tissue, possibly a better extrapolation to man *in vivo* can be achieved.

Outline

In **chapter 3** prolonged incubation (48 hours) was used to induce the early onset of liver fibrosis *ex vivo* in healthy rat liver tissue. This was assessed by analyzing the gene expression of the fibrosis markers heat shock protein 47, alpha smooth muscle actin and procollagen 1a1 and the protein expression of collagen 1, which were selected in previous studies. Furthermore, the effects of a selection of compounds that were reported to have antifibrotic effects *in vitro* or *in vivo* in animal studies and that were shown to act either via the PDGF or via the TGFβ pathway or directly on the collagen synthesis, were investigated. We verified their antifibrotic effects by assessing their influence on the gene- and protein expression of the fibrosis markers, while taking care that the concentrations used did not affect the viability of the slices.

Subsequently, the effects of the above-mentioned PDGF- and TGFβ pathway inhibitors and a direct effect on collagen expression, were also tested in end-stage rat liver fibrosis using PCLS from fibrotic rat liver tissue, as described in **chapter 4**. In addition, three different methods to quantify different

types of collagen (collagen 1 by western blot, all fibrillar collagens by sirius red staining and total collagen by hydroxyproline measurement) were used in these fibrotic rat PCLS.

To further elucidate the mechanisms which play an important role in the fibrosis process in our models, in **chapter 5**, the effect of several downstream inhibitors of components in the pathways involved in fibrogenesis were investigated in both the early onset and end-stage of liver fibrosis in rat PCLS. Inhibitors of Smad3 (a key enzyme in the TGFβ pathway) (6), Rac-1 (mediates PDGF effects in HSC) (7) and p38-Mapk (important mediator of both the PDGF- and TGFβ pathway) (8) were studied. The effects of these downstream intracellular signaling pathway inhibitors on the gene expression of a more extended number of genes encoding for proteins involved in collagen synthesis and breakdown were investigated using a low density array, together with the effects on the fibrosis markers used in chapter 3 and 4.

Since results of animal experiments often differ from the outcome in patients, in **chapter 6** it was investigated whether both stages of liver fibrosis could also be studied in human PCLS and the effects of the PDGF- and TGFβ pathway inhibitors were assessed. In addition, it was determined which fibrotic pathways are important in human liver fibrosis in PCLS utilizing the downstream signaling pathway inhibitors that were also used in chapter 5.

Finally, in **chapter 7** the outcome of all the studies and the future perspectives of the research on fibrosis with PCLS are discussed.

References

1. Hernandez-Gea V, Friedman S L. Pathogenesis of liver fibrosis. Annu Rev Pathol 2011; 6: 425-56.

2. Schuppan D, Afdhal N H. Liver cirrhosis. Lancet 2008; 371: 838-51.

3. Bonner J C. Regulation of PDGF and its receptors in fibrotic diseases. Cytokine Growth Factor Rev 2004; 15: 255-73.

4. Dooley S, Ten Dijke P. TGF-beta in progression of liver disease. Cell Tissue Res 2012; 347: 245-56.

5. Schuppan D, Kim Y O. Evolving therapies for liver fibrosis. J Clin Invest 2013; 123: 1887-901.

6. Jinnin M, Ihn H, Tamaki K. Characterization of SIS3, a novel specific inhibitor of Smad3, and its effect on transforming growth factor-beta1-induced extracellular matrix expression. Mol Pharmacol 2006; 69: 597-607.

7. Choi S S, Sicklick J K, Ma Q et al. Sustained activation of Rac1 in hepatic stellate cells promotes liver injury and fibrosis in mice. Hepatology 2006; 44: 1267-77.

8. Parsons C J, Takashima M, Rippe R A. Molecular mechanisms of hepatic fibrogenesis. J Gastroenterol Hepatol 2007; 22 Suppl 1: S79-84.

Chapter 3

Precision-cut liver slices as a model for the early onset of liver fibrosis to test antifibrotic drugs

Inge M. Westra[a], Dorenda Oosterhuis[b], Geny M.M. Groothuis[a] and Peter Olinga[b]

Toxicology and Applied Pharmacology 2014;274:328–338

[a]Division of Pharmacokinetics, Toxicology and Targeting, Department of Pharmacy, University of Groningen, The Netherlands
[b]Division of Pharmaceutical Technology and Biopharmacy, Department of Pharmacy, University of Groningen, The Netherlands

Abstract

Induction of fibrosis during prolonged culture of precision-cut liver slices (PCLS) was reported. In this study, the use of rat PCLS was investigated to further characterize the mechanism of early onset of fibrosis in this model and the effects of antifibrotic compounds. Rat PCLS were incubated for 48 hours, viability was assessed by ATP and gene expression of *PDGF-β* and *TGF-β1* and the fibrosis markers *Hsp47*, *αSma* and *Pcol1A1* and collagen1 protein expression were determined. The effects of the antifibrotic drugs imatinib, sorafenib and sunitinib, PDGF-pathway inhibitors, and perindopril, valproic acid, rosmarinic acid, tetrandrine and pirfenidone, TGFβ-pathway inhibitors, were determined. After 48 hours of incubation, viability of the PCLS was maintained and gene expression of *PDGF-β* was increased while *TGF-β1* was not changed. *Hsp47*, *αSma* and *Pcol1A1* gene expressions were significantly elevated in PCLS after 48 hours, which was further increased by PDGF-BB and TGF-β1. The increased gene expression of fibrosis markers was inhibited by all three PDGF-inhibitors, while TGFβ-inhibitors showed marginal effects. The protein expression of collagen 1 was inhibited by imatinib, perindopril, tetrandrine and pirfenidone. In conclusion, the increased gene expression of PDGF-β and the down-regulation of fibrosis markers by PDGF-pathway inhibitors, together with the absence of elevated TGF-β1 gene expression and the limited effect of the TGFβ-pathway inhibitors, indicated the predominance of the PDGF pathway in the early onset of fibrosis in PCLS. PCLS appear a useful model for research of the early onset of fibrosis and for testing of antifibrotic drugs acting on the PDGF pathway.

Introduction

Liver fibrosis is the progressive accumulation of connective tissue that affects the normal function of the liver and eventually leads to liver cirrhosis (1). Hundreds of millions of patients are affected by cirrhosis worldwide (2). As antifibrotic drugs are currently not available, patients can only be treated by organ transplantation. To improve and accelerate the drug discovery and development process, there is an urgent need for reliable *in vitro* methods to test the efficacy of potential antifibrotic compounds, as *in vivo* experiments use a large number of animals with considerable discomfort, and are expensive and time consuming.

During fibrosis, different signaling pathways are activated. The TGFβ/Smad signaling pathway is stimulated by transforming growth factor β (TGFβ), which is secreted by hepatic stellate cells (HSC), Kupffer cells, hepatocytes and platelets (3-6). In addition, upon activation, macrophages and HSC also produce platelet derived growth factor (PDGF), triggering the PDGF signaling pathway (4-7). These pathways are activated upon chronic liver injury, which causes damage of endothelial cells and apoptosis of hepatocytes. In addition to the activation of the TGFβ and PDGF secretion, these injured cells recruit inflammatory cells to the injured liver (8). HSC play an essential role in the onset and progression of liver fibrosis as activation by TGFβ causes them to proliferate and to produce extracellular matrix components (9). In addition, PDGF is a stimulator of HSC growth, which is further stimulated by an increased expression of the PDGF receptor β in activated HSC (9). Thus, there is a continuous interaction between HSC, hepatocytes and Kupffer cells during the onset and progression of liver fibrosis. To study the process of fibrosis in vitro in a physiologic milieu and to test antifibrotic drugs, it is important to use an *in vitro* system, which closely reflects the *in vivo* situation. In precision-cut liver slices (PCLS) all cell types of the liver are present in their original context and remain viable up to 48 hours (10). As each slice contains ca 70-100 lobules, the acinar heterogeneity of the liver or inhomogeneous distribution of portal spaces plays only a minor role in the variability of the results in this ex vivo model. Furthermore, the possibility to make PCLS of human liver tissue makes this model very promising to investigate fibrosis in the human liver. Previously, we and others (11,12) showed that a fibrotic process is initiated during prolonged culture of PCLS. Moreover, van de Bovenkamp *et al.* showed the antifibrotic effect of imatinib, pentoxifyllin and dexamethasone in fibrotic rat PCLS, prepared from bile duct ligated rats, and these compounds decreased the gene expression of specific fibrosis markers heat shock protein 47 (*Hsp47*), α-smooth muscle actin (*αSma*) and pro-collagen 1A1 (*Pcol1A1)* (13).

In the current study, prolonged incubation of the rat PCLS was used to induce the onset of fibrosis (11). Fibrogenesis was measured by determining the expression of genes and proteins that indicate the activation of HSC and (myo)fibroblasts, using gene and protein expression of specific markers of fibrosis as previously described (13). To investigate the involvement of the two main fibrosis pathways, the gene expression of *TGF-β1* and *PDGF- β,* in addition to Ctgf were measured, as well as the effects of exposure of the PCLS to exogenous TGF-β1 and PDGF-BB.

The aim of the present study was to investigate the mechanism of the early onset of fibrosis in prolonged culture of PCLS, and to determine if this *ex vivo* model can be used to test antifibrotic compounds. The antifibrotic compounds used in this study were all selected based on the published effects *in vivo* in animals and/or *in vitro* in cell lines and primary cells. The concentrations used in this

study correspond with the concentrations utilized in experiments with cell cultures. The compounds were selected to represent different modes of action, reflecting the main pathways involved in liver fibrosis, the PDGF and TGFβ signaling pathway. The compounds mainly inhibiting the PDGF pathway (PDGF-inhibitors) were imatinib, sorafenib and sunitinib. Imatinib is a competitive inhibitor of the tyrosine kinases PDGF receptor, Bcr-Abl and c-Kit (14,15). Sorafenib is a receptor tyrosine kinase inhibitor that targets the PDGF receptor and the Raf/ERK signaling pathway (16). Sunitinib, the third tyrosine kinase inhibitor used in this study, targets amongst others the PDGF receptor, c-Kit and the VEGF receptor (17). In this study, rosmarinic acid, perindopril, valproic acid, tetrandrine and pirfenidone were investigated as the inhibitors known to be mainly acting on the TGFβ signaling pathway (TGF-inhibitors). Rosmarinic acid naturally occurs in many medicinal species of the plant Lamiaceae (mint family) (18-20) and it has been shown that rosmarinic acid has antifibrotic effects that were achieved through the inhibitory effect on TGFβ (21,22). In addition, perindopril, an angiotensin converting enzyme (ACE) inhibitor and valproic acid, a histone deacetylase inhibitor, have been shown to decrease the TGFβ expression (23,24). Tetrandrine is an alkaloid that is isolated from the Chinese medicinal herb Stephania tetrandra (25,26). Tetrandrine's antifibrotic effect is at least partially caused by an up-regulation of Smad 7, which in turn blocks the TGFβ expression and its downstream signaling (26). Pirfenidone acts as an antifibrotic agent, by down-regulating the gene expression of TGFβ (27). To investigate the effect of direct inhibition of collagen disposition, the drug colchicine, known to have a direct effect on collagen disposition by causing disruption of microtubule formation and inhibition of collagen transport and synthesis, was investigated (28,29).
The expression of PDGF-β and TGF-β1 and the specific properties of the compounds under investigation, enabled us to assess the involvement of the PDGF and TGFβ pathways in the onset of fibrosis during prolonged incubation of PCLS.

Materials and Methods

Slice experiments
Livers of adult male Wistar rats (Harlan PBC, Zeist, The Netherlands) anaesthetized with isoflurane/O_2 (Nicholas Piramal, London, UK) were freshly isolated and used for preparing liver slices in ice-cold Krebs-Henseleit buffer supplemented with 25 mM D-glucose (Merck, Darmstadt, Germany), 25 mM $NaHCO_3$ (Merck), 10 mM HEPES (MP Biomedicals, Aurora, OH, USA) and saturated with carbogen (95% O_2/5% CO_2) using a Krumdieck tissue slicer as described before in detail (30). PCLS with a diameter of 5 mm and a thickness of 250 µm were incubated individually in 1.3 ml of Williams Medium E (with L-glutamine, Invitrogen, Paisly, Scotland) supplemented with 25 mM glucose and 50 µg/ml gentamycin (Invitrogen) at 37ºC and under continuous supply of 95% O_2/5% CO_2 in 12-wells plates while gently shaken. After 1 hours of preincubation the slices were transferred to fresh medium and further incubated for 24, 48 and 72 hours and for 48 hours with antifibrotic compounds. After 24 and 48 hours the slices were transferred to new 12 wells plates with fresh medium containing the drug. The slices were incubated with the antifibrotic compounds imatinib (1-10 µM) (Novartis, Basel, Switzerland), valproic acid (0.1-1 mM) (Sigma aldrich, Zwijndrecht, Netherlands), perindopril (10 - 100 µM) (Sigma aldrich), pirfenidone (0.5 – 2.5 mM) (Sigma aldrich), rosmarinic acid (120 – 270 µM) (Sigma aldrich), colchicine (30 – 200 nM) (Sigma aldrich), tetrandrine (1 - 10 µM)

(Sigma aldrich), sunitinib (0.5 - 5 µM) (LC laboratories, Woburn, USA) and sorafenib (0.5 - 2 µM) (LC laboratories). Stock solutions of the compounds were prepared in water or DMSO and diluted in the culture medium with a final concentration of the solvent of ≤ 1%. Before the incubations of PCLS with TGF-β1 (1 – 5 ng/ml) (hTGF-β1, Roche Applied Science, Mannheim, Germany) the 12 well plates were pretreated with 10% BSA in milli Q water solution for 20 minutes, whereafter the solution was removed and plates were air dried, in order to prevent aspecific binding of the TGF-β1 to the walls of the plates. Incubations with PDGF-BB (10 and 50 ng/ml) (Recombinant Human PDGF-BB, Peprotech, Bioconnect) were performed as described above for the antifibrotic compounds. All incubations were performed in triplicate (using 3 slices incubated individually in separate wells) and were repeated with livers from 3-x different rats. The rats were housed on a 12 hours light/dark cycle in a temperature-and-humidity-controlled room with food (Harlan chow no 2018, Horst, The Netherlands) and water ad libitum. The animals were allowed to acclimatise for at least seven days before the start of the experiment and all animals received human care. The experiments were approved by the Animal Ethical Committee of the University of Groningen.

Viability

After incubation, slices were transferred to 1 ml sonication solution, containing 70% ethanol and 2 mM EDTA, and snap frozen in liquid nitrogen and stored at -80ºC. To determine the cell viability, ATP levels were measured in the supernatant of samples sonicated for 45 seconds and centrifuged for 2 minutes at 16.000 g, using the ATP bioluminescence kit (Roche diagnostics, Mannheim, Germany). ATP values (pmol) were normalized to the total protein content (µg) of the slice estimated by Lowry (BIO-rad RC DC Protein Assay) (Bio Rad, Veenendaal, The Netherlands) (31). Values displayed are relative values compared to the related controls.

Gene expression

To determine the antifibrotic effect of the drugs, gene expression of fibrosis markers were determined using Real-Time PCR. The triplicate slices were pooled and snap frozen and total RNA was isolated with the use of the RNeasy Mini Kit (Qiagen, Venlo, The Netherlands). The amount of isolated RNA was measured with the ND-1000 spectrophotometer (Fisher Scientific, Landsmeer, The Netherlands).

Reverse transcriptase was performed with 2 µg RNA using Reverse Transcription System (Promega, Leiden, The Netherlands). The RT-PCR reaction was performed in the Eppendorf mastercycler gradient at 25˚C for 10 minutes, 45˚C for 60 minutes and 95˚C for 5 minutes.

The gene expression of *Hsp47*, *αSma*, *Pcol1A1* and *TGF-ß1* was determined using the following primers (50 µM) en probes (5 µM) (Sigma aldrich); 5'- AGACGAGTTGTAGAGTCCAAGAGT -3'(F), 5'-ACCCATGTGTCTCAGGAACCT -3'(R), 5'-CTTCCCGCCATGCCAC-3' (Probe) (Hsp47); 5'-AGCTCTGGTGTGTGACAATGG-3'(F), 5'- GGAGCATCATCACCAGCAAAG-3'(R), 5'- CCGCCTTACAGAGCC-3' (Probe) (αSma); 5'- CCCACCGGCCCTACTG-3'(F), 5'-GACCAGCTTCACCCTTAGCA-3'(R), 5'-CCTCCTGGCTTCCCTG-3' (Probe) (Pcol1A1); 5'- CCTGGAAAGGGCTCAACAC-3'(F), 5'-CAGTTCTTCTCTGTGGAGCTGA-3'(R), 5'- AGAGCCCTGGATACCAACTACTGCT-3'(Probe) (TGF-β1) and the qPCR mastermix plus (Eurogentec, Maastricht, The Netherlands). The Real-Time PCR reaction was performed in a 7900HT Real Time PCR (Applied Biosystems, Bleiswijk, The Netherlands) with 1 cycle

of 10 minutes at 95˚C and 45 cycles of 15 seconds at 95˚C and 1 minute at 60˚C. Ct values were corrected for the Ct values of the housekeeping gene *Gapdh* (ΔCt) (5'- GAACATCATCCCTGCATCCA-3'(F), 5'-CCAGTGAGCTTCCCGTTCA-3'(R), 5'- CTTGCCCACAGCCTTGGCAGC-3'(Probe) (Gapdh) and compared with the control (ΔΔCt). Results are displayed as fold induction of the gene ($2^{-\Delta\Delta Ct}$).
Gene expression of Connective Tissue Growth Factor (*Ctgf*) and *PDGF-β* were determined using the following primers (50 µM); 5'- ACACAAGGGTCTTCTGCGA-3'(F), 5'- TTGCAACTGCTTTGGAAGGAC-3'(R) (Ctgf); 5'- CTGCCTCTCTGCTGCTACCT – 3'(F), 5'- TTCCGACTCGACTCCAGAAT -3'(R) (PDGF-β) and the sybr green mastermix (GC Biotech, Alphen aan de Rijn, The Netherlands). The Real Time PCR reaction was performed on a 7900HT Real Time PCR (Applied Biosystems) with 1 cycle of 10 minutes at 95 ºC and 45 cycles of 15 seconds at 95 ºC and 25 seconds at 60 ºC with a dissociation stage thereafter (95 ºC, 15 sec: 60 ºC, 15 sec: 95 ºC, 15 sec). Ct values were corrected for the Ct values of the housekeeping gene *Gapdh* (ΔCt) (5'- CGCTGGTGCTGAGTATGTCG -3'(F), 5'- CTGTGGTCATGAGCCCTTCC -3'(R) (Gapdh) and compared with the control (ΔΔCt). Results are displayed as fold induction of the gene ($2^{-\Delta\Delta Ct}$).

Collagen 1 protein expression
Following treatment, the triplicate slices were pooled and snap frozen. The slice tissue was lysed for 1 hour on ice with RIPA buffer (1 Protease inhibitor cocktail tablet (Boehringer Ingelheim, Alkmaar, The Netherlands), 50 mM Tris/HCl pH7.5, 150 mM NaCL, 1% Igepal CA-630, 0.5% sodiumdeoxycholaat, 0.1% SDS). The tissue was homogenized on ice by a Potter homogenizer and centrifuged for 1 hour at 4°C at maximum speed. Protein concentrations were determined in the supernatant using a Biorad DC protein assay according to the protocol provided by the manufacturer. Lysates were diluted with 4x SDS sample buffer (50 mM TrisHCl pH 6.8, 2% SDS, 10% glycerol, 5% β-mercaptoethanol, 0.05% Bromophenol Blue) and boiled for 2 minutes. 100 µg of tissue lysate was size fractionated on a 7.5% sodium dodecyl sulphate poly acrylamide gel by electrophoresis and transferred to an activated polyvinylidene difluoride membrane (Biorad). After blocking for 1 hour in Tris buffered saline supplemented with 5% Blocking Grade Powder (Biorad) and 0.1% Tween-20, immunodetection of collagen-1 (1:1000, Rockland Immunochemicals, Gilbertsville, PA, USA) was performed. Binding of the antibody was determined using Horseradish Peroxidase conjugated secondary goat anti-rabbit and tertiary rabbit anti-goat antibody (DAKO, Heverlee, Belgium). Visualization was performed with Western Lightning Plus-ECL, (Perkin Elmer, Groningen, The Netherlands) and equal protein loading was confirmed by immunostaining with Monoclonal anti B-actin (clone AC-74) (Sigma Aldrich). Immunohistochemical staining was performed on cryostat section (4µM) of PCLS incubated for 0 and 48 hours with rabbit anti-collagen I (1:200, Rockland) according to standard immunoperoxidase methods (32).

Statistics
A minimum of three different livers was used for each experiment, using slices in triplicate from each liver. As for each experiment control slices are included, the number of control slices is larger than the number of slices incubated with compounds. The results are expressed as means ± S.E.M. The results of the treatments were compared to the untreated controls using the paired, one-tailed Student's-t-test. A p-value <0.05 was considered significant. Statistical differences in ATP were

determined using the values relative to the control values in the same experiment. Real-time PCR results were compared using the mean ΔΔCt values.

Results

Prolonged incubation of liver slices

PCLS were incubated up to 72 hours. Slices were viable up to 48 hours of incubation, as determined by ATP content (33), and the viability was decreased significantly after 72 hours of incubation compared to the slices after 48 hours of incubation (fig.1A). During incubation the protein content decreases, apparently due to loss of cells. But our ATP per protein data show that the remaining cells in the slices are viable.

The gene expression of the fibrosis markers *Hsp47*, *αSma* and *Pcol1A1* initially decreased during 24 hours of incubation, but was significantly increased after 48 and 72 hours of incubation to values 2-44 fold higher than those of fresh slices directly after slicing (fig. 1B), indicating that there was indeed an early onset of fibrosis in the slices after 48 and 72 hours. In figure 1C a representative immunohistochemical staining of collagen 1 is shown in PCLS incubated for 0 hours en 48 hours. Protein expression of collagen 1, measured by Western blot analysis, was decreased at 1 and 24 hours of incubation. After 48 hours the collagen 1 expression was increased again to the same level as in fresh slices (fig. 1D). Gene expression of *PDGF-β* was increased after 24 and 48 hours of incubation, while the gene expression of *TGF-β1* was not changed during incubation (fig. 1E). Since 72 hours of incubation caused a significant decrease in ATP content of PCLS compared to earlier time points, the experiments with antifibrotic compounds were conducted during 48 hours of incubation.

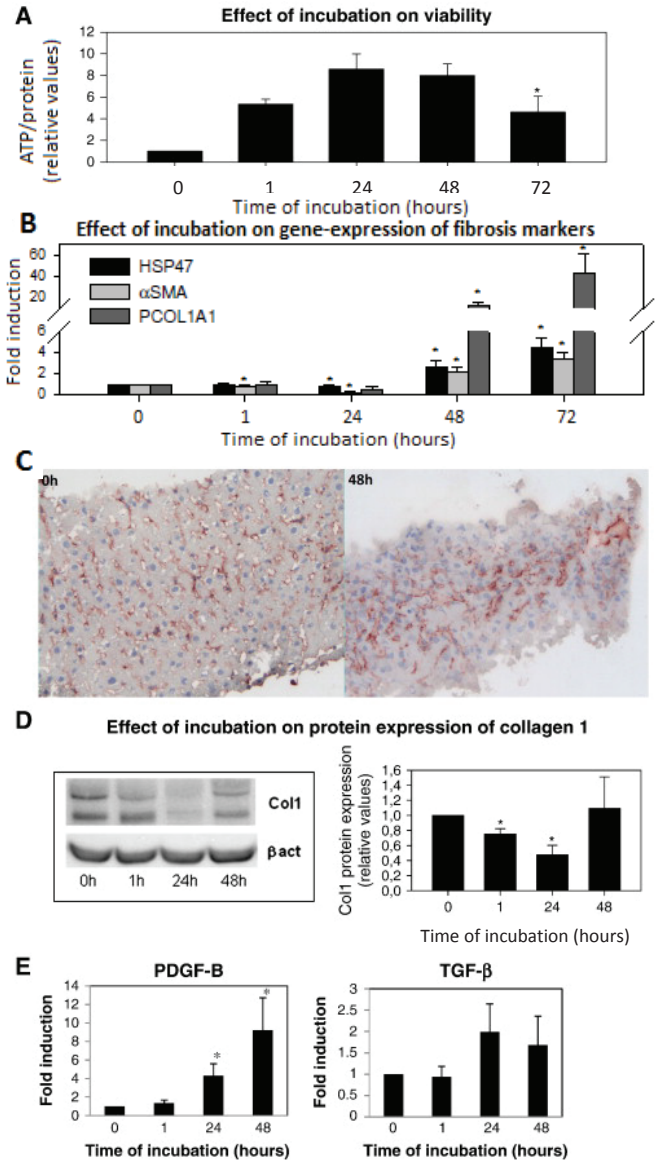

Fig 1. **Prolonged incubation of rat PCLS.** The effect of incubation for 0 hours (n=18), 1 hour (n=10), 24 hours (n=7). 48 hours (n=18) and 72 hours (n=7) of PCLS on the viability of PCLS as measured by ATP content (A), effect of incubation for 0 hours (n=18), 1 hour (n=10), 24 hours (n=7). 48 hours (n=18) and 72 hours (n=7) of PCLS on the gene-expression of fibrosis markers *Hsp47*, *αSma* and *Pcol1A1* (B), microscopic pictures (20x) of cryostat sections of control liver slices incubated for 0 and 48 hours stained for collagen I (C), and the effect of incubation for 0 hours (n=6), 1 hour (n=3), 24 hours (n=3) and 48 hours (n=6) of PCLS on the collagen 1 protein expression measured by Western blot (D) and the effect of incubation for 0, 1, 24 and 48 (n=4) hours on *PDGF-β* and *TGF-β1* gene expression (E). *p<0.05 vs. 0 hours. Data are expressed as mean +/- SEM.

Addition of PDGF-BB and TGF-ß1

To confirm that PDGF-BB and TGF-β1 are able to induce the PDGF and TGFβ signaling pathways in PCLS, PCLS were incubated with PDGF-BB and TGF-β1 and the gene expression of the fibrosis markers was assessed. PCLS incubated for 48 hours without these factors were used as a control and the gene expression of *Hsp47*, *αSma* and *Pcol1A1* in these controls was set at 1 (fig. 2B). Both PDGF-BB (10-100 ng/ml) as well as TGF-β1 (1-5 ng/ml) induced a concentration dependent further increase in the gene-expression of *Hsp47*, *αSma* and *Pcol1A1* in PCLS after 48 hours of incubations (fig. 2B). Slice viability was not changed after addition of PDGF-BB, however, ATP content in PCLS decreased to 50% by TGF-β1 (fig. 2A).

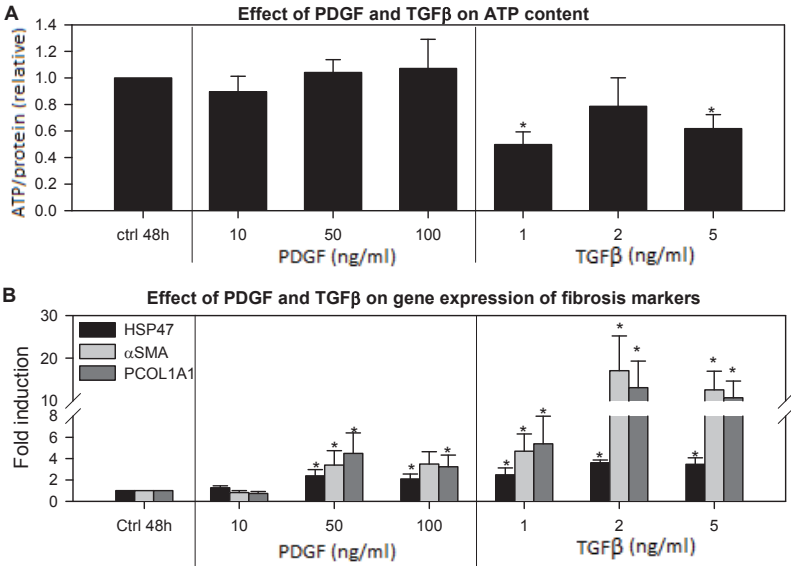

Fig 2. **The effect of PDGF and TGFβ on the viability and expression of fibrosis markers in PCLS.** Viability (ATP content) (A) and gene-expression of fibrosis markers *Hsp47*, *αSma* and *Pcol1A1* (B) of PCLS incubated with 10 (n=3), 50 (n=8), or 100 ng/ml PDGF (n=3) or 1 (n=3), 2 (n=3), or 5 ng/ml TGFβ (n=9) for 48 hours.*p<0.05 vs. ctrl 48 hours. Data are expressed as mean +/- SEM.

The effect of PDGF-inhibitors

Slices were incubated with a range of concentrations of the antifibrotic compounds imatinib (1-10 µM), sorafenib (0.5-2 µM) or sunitinib (0.5-5 µM) during 48 hours. As indicated by the ATP content of the slices, the antifibrotic drugs did not influence the viability of the slices at the concentrations used (fig. 3A), and the protein content per slice was not changed after addition of the compounds compared to the control slices at 48 hours. In PCLS incubated for 48 hours in the presence of imatinib, sorafenib or sunitinib, a significant decrease of the gene expression of *αSma* and *Pcol1A1* was found compared to control slices incubated for 48 hours (fig. 3B). The *Hsp47* expression was also significantly decreased by imatinib or sunitinib (fig. 3B), but not by sorafenib. With 10 µM of imatinib and 1 and 5 µM of sunitinib, the gene expression of fibrosis markers was even significantly lower

than that of the fibrosis markers in PCLS directly after slicing, but not lower than the values after 24 hours of incubation (fig. 3B).

After 48 hours not only the gene expression of *Pcol1A1*, but also the protein expression of collagen 1 was decreased in PCLS by 10 µM imatinib compared to control slices (fig. 4). Collagen 1 protein expression was not changed in slices exposed to sorafenib or sunitinib compared to control slices incubated for 48 hours (fig. 4).

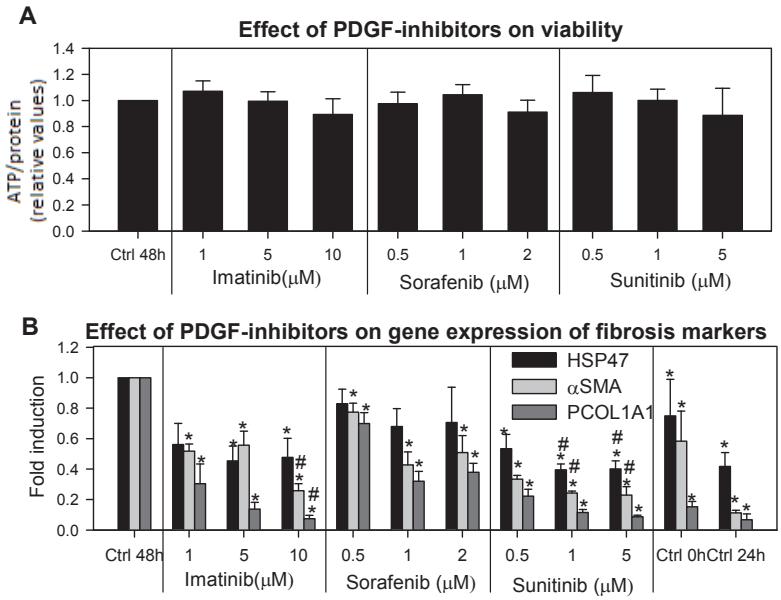

Fig 3. **The effect of PDGF-inhibitors on viability and expression of fibrosis markers in PCLS.** Viability measured by ATP content of PCLS incubated with imatinib, sorafenib or sunitinib (A), gene expression of fibrosis markers *Hsp47*, *αSma* and *Pcol1A1* of PCLS incubated with imatinib, sorafenib or sunitinib (B). *p<0.05 vs. ctrl 48 hours and #p<0.05 vs. ctrl 0 hours. n= 3, data are expressed as mean +/- SEM.

The effect of TGFβ-inhibitors

Incubation with rosmarinic acid (120-270 µM), perindopril (10-100 µM), tetrandrine (1-10 µM) or pirfenidone (0.5-2.5 mM) did not result in a decreased ATP content of slices incubated for 48 hours (fig. 5A). In addition, the protein content per slice was not changed after addition of the compounds compared to the control slices at 48 hours. The viability of slices incubated with valproic acid (0.1-1 mM) was decreased to a minimum of 62 % compared to control slices, however only at 0.5 mM (fig. 5A). Concentrations higher than 1 mM of valproic acid decreased slice viability considerably (data not shown).

The gene expression of *αSma* was inhibited by 120 µM of rosmarinic acid and the *Hsp47* gene expression was decreased after incubation with 120 µM and 200 µM rosmarinic acid (fig. 5B). The gene-expression of *Pcol1A1* was inhibited by 0.5 mM pirfenidone (fig. 5B). Likewise, collagen 1 protein expression was inhibited by pirfenidone (2.5 mM) (fig. 4). The gene expression of *αSma* was

only inhibited by 1 mM of valproic acid, while *Pcol1A1* gene expression was only marginally inhibited by 20% by 100 µM of perindopril and 10 µM of tetrandrine (fig. 5B). However, the collagen 1 protein expression in PCLS was inhibited by almost 50% by these concentrations of perindopril and tetrandrine (fig. 4).

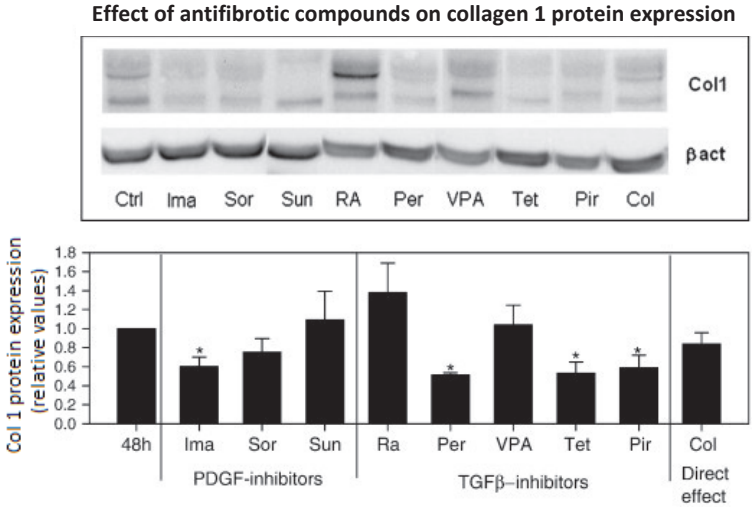

Fig 4. **Collagen 1 protein expression of PCLS.** Collagen 1 protein expression of PCLS, incubated in the presence of PDGF-inhibitors Glv (imatinib 10 µM), Sor (sorafenib 2 µM), Sun (sunitinib 5 µM) and TGFβ-inhibitors RA (rosmarinic acid 270 µM), Per (perindopril 100 µM), VPA (valproic acid 1 mM), Tet (tetrandrine 10 µM), Pir (pirfenidone 2.5 mM) or inhibitor with a direct effect on collagen, Col (Colchicine 200 nM) for 48 hours.*p<0.05 vs. ctrl 48 hours. n= 3, data are expressed as mean +/- SEM.

The effect of colchicine

Slices incubated with colchicine (30-200 nM) resulted in an ATP content decrease of 20 % after 48 hours compared to control slices (fig. 6A). Only 100 nM of colchicine inhibited the gene expression of *αSma* and *Pcol1A1* after 48 hours of incubation (fig. 6B). However, the collagen 1 protein expression in PCLS was not significantly inhibited by colchicine (fig. 4).

The effect of prolonged incubation and antifibrotic compounds on the Ctgf gene expression

As our results showed that the gene expression of TGFβ was not altered during incubation and the addition of TGFβ-inhibitors had only marginal effects on the gene expression of the fibrosis markers, we wanted to investigate whether the TGFβ pathway was activated during culture of the PCLS. Therefore, the effect of prolonged culture on the gene expression of *Ctgf* was investigated, as CTGF is a downstream mediator of TGFβ (34). The results in fig. 7A show that the gene expression of *Ctgf* was increased 2 fold after 24 hours and 8 fold after 48 hours of incubation, indicating the possible activation of the TGFβ pathway (fig. 7A). Addition of TGF-β1 to the incubation medium strongly increased the gene expression of *Ctgf* dose-dependently up to 23 fold compared to the control

incubation at 48 hours and thus 184 fold compared to the 1 hour control, while addition of PDGF did not have an effect (fig. 7B).

Unexpectedly, the alleged TGFβ-inhibitors perindopril and rosmarinic acid caused an increase in the expression of *Ctgf* (fig. 7D), while valproic acid, tetrandrine and pirfenidone had no significant effect on the gene expression of *Ctgf* (fig. 7D). In contrast, colchicine at a concentration of 30 nM decreased the gene-expression of *Ctgf* but higher concentrations did not have an effect (fig. 7E). The *Ctgf* gene expression was also inhibited in PCLS by imatinib and sunitinib but only at the lowest concentrations tested (fig. 7C).

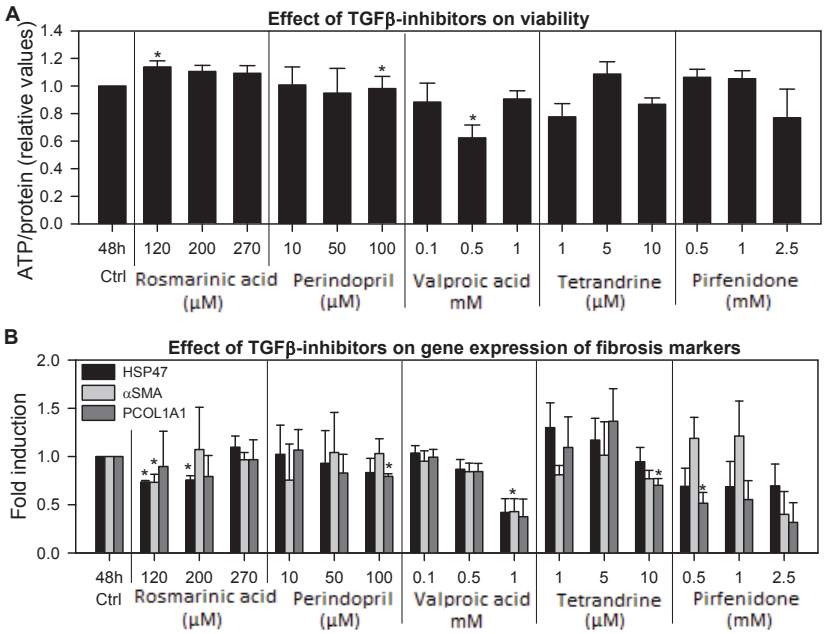

Fig 5. **The effect of TGFβ-inhibitors on viability and expression of fibrosis markers in PCLS.** Viability measured by ATP content (A) and gene expression of fibrosis markers *Hsp47*, *αSma* and *Pcol1A1* (B) of PCLS incubated for 48 hours with TGFβ inhibitors rosmarinic acid (n=3), perindopril (n=3), valproic acid (n=3), tetrandrine (n=3) and pirfenidone (n=4). *p<0.05 vs. ctrl 48 hours. Data are expressed as mean +/- SEM

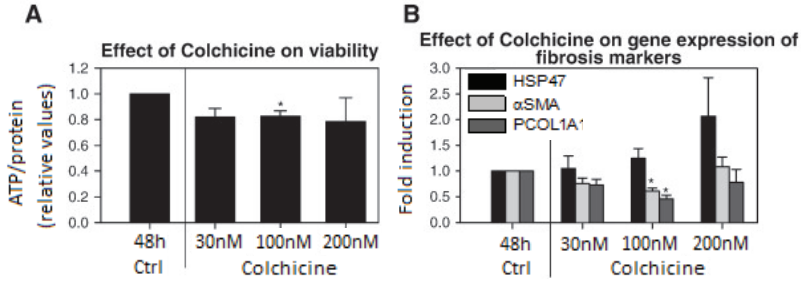

Fig 6. **The effect of colchicine on viability and expression of fibrosis markers in PCLS.** Viability measured by ATP content (A) and gene expression of fibrosis markers *Hsp47*, *αSma* and *Pcol1A1* (B) of PCLS incubated with 30, 100 or 200 nM colchicine for 48 hours. *p<0.05 vs. ctrl 48 hours. n= 3, data are expressed as mean +/- SEM.

Discussion

The aim of this study was to characterize the early onset of fibrosis in PCLS, and determine if this in vitro model can be used to investigate the effect of antifibrotic compounds in order to confirm the use of PCLS as a model to test antifibrotic compounds.

It was shown before that hepatocytes, Kupffer cells and HSC are present and functional in liver slices and this enables the study of inflammatory reactions in its multi-cellular context (35). The increased gene expression of the fibrosis markers *Hsp47*, *αSma* and *Pcol1A1* after 48 and 72 hours of incubation revealed an early onset of fibrosis during culture of PCLS as was also shown earlier (11). A possible explanation for this phenomenon could be that the slice preparation causes damage to the surface of slices which may trigger repair and regenerative responses, resulting in activation of HSC, proliferation of myofibroblasts and increased collagen production (12). The significant increase of *Hsp47* gene expression in liver slices during 48 and 72 hours of incubation suggests activation of HSC. In addition, the increased *αSma* expression suggests further activation of HSC and transformation of HSC into myofibroblasts in the liver slices. Besides an increase in myofibroblasts, increased *αSma* mRNA levels can also indicate an increase in the number of fibroblasts (36). Proliferating myofibroblasts are known to produce large amounts of collagen type I (37), therefore the increased gene expression of *Pcol1A1* in the liver slices is another indication of fibrogenesis in the liver slices during incubation up to 72 hours. Furthermore, after an initial decrease in collagen 1 protein levels, levels were increased again at 48 hours.

In conclusion, these data show that the early onset of fibrosis was induced in rat liver slices incubated for 48 hours, while the viability is maintained. The increase in *PDGF-β* indicated that the PDGF pathway may be involved. However, the involvement of the TGFβ pathway by newly synthesized TGFβ was not confirmed as TGFβ gene expression was not increased. Nevertheless, the Ctgf gene expression, which is a downstream mediator in the TGFβ pathway, was increased. It can be speculated that the increased Ctgf expression is mediated by the release of TGFβ already present in the slice or that Ctgf is induced by another pathway.

Addition of PDGF-BB and TGF-β1

Since PDGF, but not TGFβ gene expression was up-regulated after 48 hours of incubation, we wanted to elucidate whether PDGF-BB and TGF-β1 could activate the PDGF- and TGFβ signaling pathway in the slices. PCLS were cultured in the presence of PDGF-BB or TGF-β1 for 48 hours. Both growth factors could indeed further increase the fibrosis markers after 48 hours of incubation, suggesting that the slices are responsive to both PDGF-BB and TGF-β1. Moreover, the gene expression of Ctgf was increased strongly by the addition of TGF-β1.

The effect of PDGF-inhibitors

To investigate whether these rat liver slices can be used to study the effect of PDGF-inhibitors, the effects of imatinib, sorafenib and sunitinib were determined during 48 hours incubations. The

concentrations of the three compounds used in the current study are in line with plasma concentrations in patients in clinical studies treated for cancer. The C_{max} concentration found in vivo in these patients

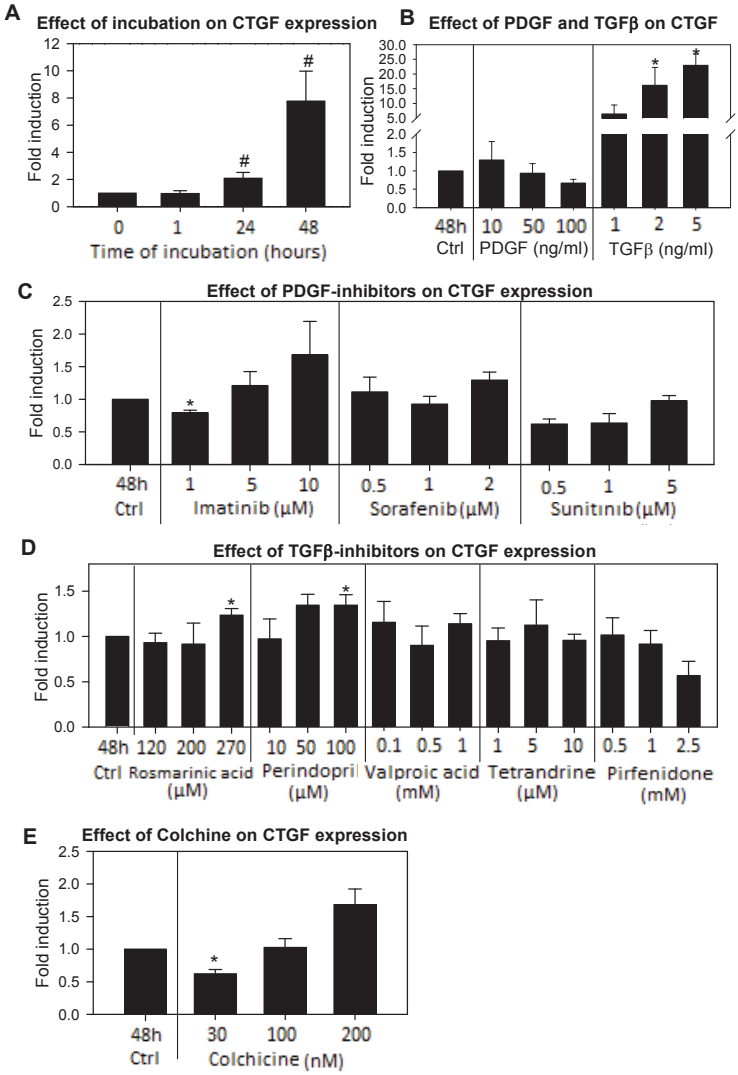

Fig 7. **Gene-expression of *Ctgf* in PCLS.** Gene-expression of *Ctgf* of PCLS incubated up to 48 hours in control PCLS (n=4) (A), PCLS incubated with PDGF (n=3) or TGFβ (n=4) for 48 hours (B), PCLS incubated with PDGF-inhibitors imatinib, sorafenib and sunitinib for 48 hours (n=3) (C), PCLS incubated with TGFβ-inhibitors rosmarinic acid, perindopril, valproic acid, tetrandrine and pirfenidone for 48 hours (n=3) (D) and PCLS incubated with colchicine for 48 hours (n=3) (E). #p<0.05 vs. ctrl 0 h, *p<0.05 vs. ctrl 48 hours. Data are expressed as mean +/- SEM.

administered with the effective dose of imatinib, sorafenib or sunitinib was respectively about 5 μM (38), 9 μM (39) and 14 μM (17).

In this study, all three kinase inhibitors acting on the PDGF pathway caused a significant and substantial decrease in *Hsp47*, *αSma* and *Pcol1A1* gene expression. The gene expression of the fibrosis markers in the presence of imatinib and sunitinib was even lower than in PCLS after incubation for 1 hour, but not different from 24 hours. This indicates that these PDGF-inhibitors inhibit the increase of fibrosis markers from 24 hours up to 48 hours. In addition, imatinib also caused a decrease in collagen 1 protein expression, by preventing the increase of collagen 1 protein expression from 24 hours to 48 hours, which is in line with studies in human dermal fibroblasts (40). The effects of imatinib in PCLS are well in line with the antifibrotic effects found in vivo and in vitro. Imatinib was previously shown to have antifibrotic effects in pig-serum induced fibrosis in rats, in the early phase of BDL-induced fibrosis in rats, in BDL-induced fibrotic rat PCLS and in CCl_4 treated mice (13-15,41,42), and induced apoptosis in hepatic stellate cells in culture (42).

Although both sorafenib and sunitinib showed clear antifibrotic effects on gene expression of the three marker genes, the protein expression of collagen 1 did not change after addition of sorafenib and sunitinib, whereas sorafenib suppressed the protein level of collagen and HSC growth in vivo in rats with established fibrosis (BDL and dimethylnitrosamine) (16), and sunitinib showed a decrease in collagen accumulation in CCl_4 rats (43). This discrepancy may be explained by the longer exposure time in these in vivo experiments, suggesting that these compounds need a longer incubation time to express their effect on the protein level or, alternatively, by the possibility that these compounds are only effective in established fibrosis. In HSC, imatinib has already an effect on *Pcol1A1* gene expression after 12 hours of incubation (44), while the earliest effect of sorafenib on *Pcol1A1* in HSC was described after 24 hours of incubation (16). This earlier effect on *Pcol1A1* mRNA expression with imatinib could imply that also collagen 1 protein is expressed at an earlier time point compared to sorafenib. The same could be the case for sunitinib, however to our knowledge up to now, the time course of the effect of sunitinib on *Pcol1A1* gene expression in HSC has not been studied. Our results are in line with those of Hennenberg *et al.,* who showed reduced gene expression of α*Sma* and *Pcol1A1* by sorafenib after treatment of BDL rats and in culture-activated primary HSC (45). Similarly, Friedman showed antifibrotic effects of sorafenib in vitro in LX2 cells (3.5-15 μM), and in vivo in rats with hepatic fibrosis due to thioacetamide by reducing the gene expression of, among other things, collagen I (46). In line with our studies, 1 μM of sunitinib caused a decrease in LX-2 viability and collagen expression in vitro, and in cirrhotic rats in vivo (40 mg/kg) a decrease in *αSma* abundance, probably through the inhibition of the PDGF signaling pathway in HSC (43).

All these results indicate that these PDGF-inhibitors have similar effects in this ex vivo model of early onset of liver fibrosis as in vivo in animals with hepatic fibrosis. Therefore, it can be concluded that de PDGF pathway is activated in the PCLS and that these PCLS can be used to test antifibrotic effects of PDGF-inhibitors.

The effect of TGFβ-inhibitors

The results of the TGFβ-inhibitors on the gene expression of fibrosis markers in PCLS are less pronounced than the results of the PDGF-inhibitors.

Rosmarinic acid had minor effects on the fibrosis markers. In contrast, in BDL mice in vivo, rosmarinic acid treatment caused a decrease of hepatic gene expression of *αSma* and *Pcol1A1,* Moreover, 270 µM of rosmarinic acid caused a decrease of pro-collagen 1A1 in activated rat HSC (47) and inhibition of proliferation of rat HSC (HSC-T6 cell line) (Zhang et al., 2011).

Also perindopril, an AT-II receptor antagonist, affected the fibrosis process in the PCLS only moderately. Activation of the angiotensin-II (AT-II) receptor induces HSC contraction and proliferation and increases TGFβ gene expression in activated HSC in vitro (48,49). In rat in vivo, perindopril caused inhibition of *Pcol1A1* gene expression in HSC (50) and inhibited the transformation of HSC into myofibroblasts (51). Yeki found only an inhibition of collagen 1 mRNA with a high dose (8mg/kg) of perindopril in BDL rats (52). Despite the marginal effects on the gene expression of fibrosis markers in our study, collagen 1 protein expression was 50% lower after 48 hours incubation with the highest concentration of perindopril (100 µM), whereas *Pcol1A1* gene expression was reduced by only 20%. This might be explained by the fact that perindopril has an effect on MMPs, by inhibiting Timp expression, and these MMPs are involved in the degradation of collagens (53).

Valproic acid reduced the expression of the three fibrosis marker genes in the PCLS only at the highest concentration of 1 mM. Watanabe *et al*. also used a concentration of valproic acid of 1 mM in cultured human HSC, which was slightly toxic, and showed inhibition of col1A1 and TGFβ1 gene- and protein expression (24). Mannaerts *et al.* showed that valproic acid decreased the HSC activation and down-regulated αSma and Pcol1A1 gene and protein expression in mice in vivo and also decreased HSC activation and down-regulated *αSma in vitro* (19). However, valproic acid is a histone deacetylase inhibitor and might inhibit the gene expression of other proteins, and consequently inhibiting their function (54). Therefore, the effect of valproic acid on fibrosis markers could also be caused by hyper acetylation of histones and not only through inhibition of the TGFβ pathway. On the other hand, Fisher et al. studied the effect of 0.7, 2.1 and 3.5 mM valproic acid in rat slices on protein synthesis and found that the protein synthesis was unaffected after 24 hours of incubation (55).

Hsu *et al.* showed that the TGFβ-inhibitor tetrandrine (5 µM) inhibited αSma and collagen protein expression in HSC-T6 cells for at least 50% (25). Our results show an inhibiting effect with 10 µM of tetrandrine on the *Pcol1A1* gene expression by 25% and on the collagen 1 protein expression by 50%. *αSma* and *Hsp47* gene expressions were not changed. A higher concentration of tetrandrine could not be tested due to loss of viability of the slices (data not shown). Chen *et al.* suggested that the effect of tetrandrine might be due to an up-regulation of Smad7, as Smad7 was increased by tetrandrine in TGFβ stimulated HSC, which in turn blocks the TGFβ expression and its downstream signaling (26).

The antifibrotic compound pirfenidone showed effects in experimental and human pulmonary and liver fibrosis (56-59). In PCLS, 0.5-2.5 mM pirfenidone inhibited the *Hsp47* and *Pcol1A1* gene expression. Furthermore, *αSma* gene expression and collagen 1 protein expression was also inhibited with 2.5 mM of pirfenidone. Our results are in line with those found by di Sario *et al.* who showed that pirfenidone (0.1-1 mM) down-regulated the expression of pro-collagen gene expression in rat HSC in culture (60). In addition, it decreased *αSma* and collagen 1 gene expression in either TGFβ or serum activated LX-2 cells (61). Furthermore, in a pilot study with patients with advanced liver fibrosis, pirfenidone treatment (1200 mg/day) for twelve months caused a reduction of fibrosis in

30% of the patients, as determined by down-regulation of protein- and gene expression of collagen 1a, TGFβ and Timp-1 in liver biopsies (56).
In summary, the observation that after spontaneous induction of fibrosis by prolonged incubation the gene expression of fibrosis markers was only slightly inhibited by a few TGFβ-inhibitors and the fact that *TGF-β1* gene expression was not increased after 48 hours might suggest that in the prolonged culture PCLS model the TGFβ pathway is only minimally activated. Therefore, we wanted to elucidate whether the TGFβ-signaling pathway is activated in our model of early onset of fibrosis and can be activated by externally administered TGF-β1. TGF-β1 itself was able to cause an activation of the TGFβ pathway in PCLS, showing that this pathway can be activated in PCLS. As activation of the TGFβ pathway results in increased expression of *Ctgf* (34), we assessed the expression of this gene during culture and whether it could be inhibited by the antifibrotic compounds. CTGF is a cysteine rich protein that has been associated with tissue fibrosis in humans (62) and it is a downstream mediator in the TGFβ pathway (34). In PCLS, the expression of this gene was indeed up-regulated after 48 hours of incubation, which may be an indication that the TGFβ signaling pathway is activated. However, this was relatively small compared to that after addition of exogenous TGF-β1. The fact that TGFβ could further increase the expression of *Ctgf* and PDGF could not, confirms that the expression of *Ctgf* is regulated by the TGFβ-pathway but not by the PDGF pathway. However, the results with the antifibrotic compounds in PCLS were not unambiguous. Some TGFβ-inhibitors reduced the increase in *Ctgf* gene expression, but in contrast, perindopril further increased the *Ctgf* gene-expression after 48 hours in the PCLS. In addition, also some PDGF-inhibitors reduced the *Ctgf* expression. In HSC, Huang *et al.* found that perindopril reduced the protein levels of CTGF (63) and Yeki *et al.* found reduced gene expression of *Ctgf* in 6 weeks BDL rats after perindopril treatment during the last 3 weeks (52). Since in our study perindopril showed the opposite effect, it might be that CTGF is not solely triggered by a TGFβ related pathway but can also be activated by an as yet unknown mechanism.

The effect of colchicine
In our PCLS, the *αSma* and *Pcol1A1* gene expressions were down-regulated in the presence of 30 nM and 100 nM of colchicine, whereas the *Hsp47* gene expression was up-regulated in these slices. Similarly, Chung *et al.* also reported that mRNA expression of pro-collagen 1a1 is inhibited by 1 μM colchicine in human fibroblasts (29). In addition, in activated rat HSC, 30 nM and 100 nM of colchicine caused suppression of αSMA protein- and TGFβ1 mRNA expression (28). These findings may be explained by the work of Vonk *et al*. (64). They showed that endoplasmic reticulum (ER) stress inhibits collagen synthesis, while some collagen-modifying enzymes and chaperones are up-regulated (64). Proper functioning of the ER network requires an intact microtubule system (65). As colchicine causes disruption of microtubule formation, this may induce ER stress, which in turn might decrease the gene-expression of *Pcol1A1* and the up-regulation of gene-expression of the collagen chaperone *Hsp47*. After treatment with colchicine, we found a slight but non-significant decrease of collagen protein in the PCLS, in line with the in vivo results of Rodriquez who showed a significant reduction of collagen amount in CCl_4 treated rats after administration of colchicine (66).

In conclusion

We showed that 48 hours of culture of PCLS induced activation of HSC and the early onset of fibrogenesis, which is mainly mediated by the PDGF pathway. Moreover, our data show that the antifibrotic effect of PDGF-inhibitors can be assessed in this model. However, during incubation, the TGFβ gene expression was not increased and the TGFβ-inhibitors only slightly reduced the fibrotic process, suggesting that the TGFβ pathway plays only a minor role in PCLS during the onset of fibrosis. Further research is needed to elucidate the role of the TGFβ- and PDGF pathway also in established fibrosis in rat PCLS. Moreover, studies in human PCLS are ongoing to assess whether these pathways and inhibitors of fibrogenesis can be investigated in the human liver.

References

1. Bataller R, Brenner D A. Liver fibrosis. J Clin Invest 2005; 115: 209-18.

2. Friedman S L. Liver fibrosis -- from bench to bedside. J Hepatol 2003; 38 Suppl 1: S38-53.

3. Dooley S, Ten Dijke P. TGF-beta in progression of liver disease. Cell Tissue Res 2012; 347: 245-56.

4. Tsukada S, Parsons C J, Rippe R A. Mechanisms of liver fibrosis. Clin Chim Acta 2006; 364: 33-60.

5. Friedman S L. Mechanisms of hepatic fibrogenesis. Gastroenterology 2008; 134: 1655-69.

6. Liu Y, Wen X M, Lui E L et al. Therapeutic targeting of the PDGF and TGF-beta-signaling pathways in hepatic stellate cells by PTK787/ZK22258. Lab Invest 2009; 89: 1152-60.

7. Deng Z Y, Li J, Jin Y, Chen X L, Lu X W. Effect of oxymatrine on the p38 mitogen-activated protein kinases signalling pathway in rats with CCl4 induced hepatic fibrosis. Chin Med J (Engl) 2009; 122: 1449-54.

8. Cong M, Iwaisako K, Jiang C, Kisseleva T. Cell signals influencing hepatic fibrosis. Int J Hepatol 2012; 2012: 158547.

9. Borkham-Kamphorst E, Herrmann J, Stoll D, Treptau J, Gressner A M, Weiskirchen R. Dominant-negative soluble PDGF-beta receptor inhibits hepatic stellate cell activation and attenuates liver fibrosis. Lab Invest 2004; 84: 766-77.

10. van de Bovenkamp M, Groothuis G M, Draaisma A L et al. Precision-cut liver slices as a new model to study toxicity-induced hepatic stellate cell activation in a physiologic milieu. Toxicol Sci 2005; 85: 632-8.

11. van de Bovenkamp M, Groothuis G M, Meijer D K, Olinga P. Liver slices as a model to study fibrogenesis and test the effects of anti-fibrotic drugs on fibrogenic cells in human liver. Toxicol In Vitro 2008; 22: 771-8.

12. Vickers A E, Saulnier M, Cruz E et al. Organ slice viability extended for pathway characterization: an in vitro model to investigate fibrosis. Toxicol Sci 2004; 82: 534-44.

13. van de Bovenkamp M, Groothuis G M M, Meijer D K F, Olinga P. Precision-cut fibrotic rat liver slices as a new model to test the effects of anti-fibrotic drugs in vitro. J Hepatol 2006; 45: 696-703.

14. Buchdunger E, Cioffi C L, Law N et al. Abl protein-tyrosine kinase inhibitor STI571 inhibits in vitro signal transduction mediated by c-kit and platelet-derived growth factor receptors. J Pharmacol Exp Ther 2000; 295: 139-45.

15. Neef M, Ledermann M, Saegesser H et al. Oral imatinib treatment reduces early fibrogenesis but does not prevent progression in the long term. J Hepatol 2006; 44: 167-75.

16. Wang Y, Gao J, Zhang D, Zhang J, Ma J, Jiang H. New insights into the antifibrotic effects of sorafenib on hepatic stellate cells and liver fibrosis. J Hepatol 2010.

17. Minkin P, Zhao M, Chen Z, Ouwerkerk J, Gelderblom H, Baker S D. Quantification of sunitinib in human plasma by high-performance liquid chromatography-tandem mass spectrometry. J Chromatogr B Analyt Technol Biomed Life Sci 2008; 874: 84-8.

18. Osakabe N, Yasuda A, Natsume M, Yoshikawa T. Rosmarinic acid inhibits epidermal inflammatory responses: anticarcinogenic effect of Perilla frutescens extract in the murine two-stage skin model. Carcinogenesis 2004; 25: 549-57.

19. Mannaerts I, Nuytten N R, Rogiers V, Vanderkerken K, van Grunsven L A, Geerts A. Chronic administration of valproic acid inhibits activation of mouse hepatic stellate cells in vitro and in vivo. Hepatology 2010; 51: 603-14.

20. Li G S, Jiang W L, Tian J W, Qu G W, Zhu H B, Fu F H. In vitro and in vivo antifibrotic effects of rosmarinic acid on experimental liver fibrosis. Phytomedicine 2010; 17: 282-8.

21. Zhang J J, Wang Y L, Feng X B, Song X D, Liu W B. Rosmarinic acid inhibits proliferation and induces apoptosis of hepatic stellate cells. Biol Pharm Bull 2011; 34: 343-8.

22. Domitrovic R, Skoda M, Marchesi V V, Cvijanovic O, Pugel E P, Stefan M B. Rosmarinic acid ameliorates acute liver damage and fibrogenesis in carbon tetrachloride-intoxicated mice. Food Chem Toxicol 2012.

23. Helmy A, Jalan R, Newby D E, Hayes P C, Webb D J. Role of angiotensin II in regulation of basal and sympathetically stimulated vascular tone in early and advanced cirrhosis. Gastroenterology 2000; 118: 565-72.

24. Watanabe T, Tajima H, Hironori H et al. Sodium valproate blocks the transforming growth factor (TGF)-beta1 autocrine loop and attenuates the TGF-beta1-induced collagen synthesis in a human hepatic stellate cell line. Int J Mol Med 2011; 28: 919-25.

25. Hsu Y, Chiu Y, Cheng C, Wu C, Lin Y, Huang Y. Antifibrotic effects of tetrandrine on hepatic stellate cells and rats with liver fibrosis. J Gastroen Hepatol 2007; 22: 99-111.

26. Chen Y, Li D, Wu J, Chen Y, Lu H. Tetrandrine inhibits activation of rat hepatic stellate cells stimulated by transforming growth factor-beta in vitro via up-regulation of Smad 7. J Ethnopharmacol 2005; 100: 299-305.

27. Schaefer C J, Ruhrmund D W, Pan L, Seiwert S D, Kossen K. Antifibrotic activities of pirfenidone in animal models. Eur Respir Rev 2011; 20: 85-97.

28. Lee S J, Kim Y G, Kang K W, Kim C W, Kim S G. Effects of colchicine on liver functions of cirrhotic rats: beneficial effects result from stellate cell inactivation and inhibition of TGF beta1 expression. Chem Biol Interact 2004; 147: 9-21.

29. Chung K Y, Kang D S. Regulation of type I collagen and interstitial collagenase mRNA expression in human dermal fibroblasts by colchicine and D-penicillamine. Yonsei Med J 1999; 40: 490-5.

30. de Graaf I A, Olinga P, de Jager M H et al. Preparation and incubation of precision-cut liver and intestinal slices for application in drug metabolism and toxicity studies. Nat Protoc 2010; 5: 1540-51.

31. Lowry O H, Rosebrough N J, Farr A L, Randall R J. Protein measurement with the Folin phenol reagent. J Biol Chem 1951; 193: 265-75.

32. Beljaars L, Molema G, Weert B et al. Albumin modified with mannose 6-phosphate: A potential carrier for selective delivery of antifibrotic drugs to rat and human hepatic stellate cells. Hepatology 1999; 29: 1486-93.

33. Olinga P, Groothuis G M M. Use of Human Tissue Slices in Drug Targeting Research. Drug Targeting: Organ-Specific Strategies 2001; 12: 309-31.

34. Brigstock D R. Connective tissue growth factor (CCN2, CTGF) and organ fibrosis: lessons from transgenic animals. J Cell Commun Signal 2010; 4: 1-4.

35. Olinga P, Merema M T, de Jager M H et al. Rat liver slices as a tool to study LPS-induced inflammatory response in the liver. J Hepatol 2001; 35: 187-94.

36. Desmouliere A, Geinoz A, Gabbiani F, Gabbiani G. Transforming growth factor-beta 1 induces alpha-smooth muscle actin expression in granulation tissue myofibroblasts and in quiescent and growing cultured fibroblasts. J Cell Biol 1993; 122: 103-11.

37. Kawada N, Kuroki T, Kobayashi K et al. Expression of heat-shock protein 47 in mouse liver. Cell Tissue Res 1996; 284: 341-6.

38. Leveque D, Maloisel F. Clinical pharmacokinetics of imatinib mesylate. In Vivo 2005; 19: 77-84.

39. Strumberg D, Clark J W, Awada A et al. Safety, pharmacokinetics, and preliminary antitumor activity of sorafenib: a review of four phase I trials in patients with advanced refractory solid tumors. Oncologist 2007; 12: 426-37.

40. Distler J H, Jungel A, Huber L C et al. Imatinib mesylate reduces production of extracellular matrix and prevents development of experimental dermal fibrosis. Arthritis Rheum 2007; 56: 311-22.

41. Yoshiji H, Noguchi R, Kuriyama S et al. Imatinib mesylate (STI-571) attenuates liver fibrosis development in rats. Am J Physiol Gastrointest Liver Physiol 2005; 288: G907-13.

42. Kuo W L, Yu M C, Lee J F, Tsai C N, Chen T C, Chen M F. Imatinib mesylate improves liver regeneration and attenuates liver fibrogenesis in CCL4-treated mice. J Gastrointest Surg 2012; 16: 361-9.

43. Tugues S, Fernandez-Varo G, Munoz-Luque J et al. Antiangiogenic treatment with sunitinib ameliorates inflammatory infiltrate, fibrosis, and portal pressure in cirrhotic rats. Hepatology 2007; 46: 1919-26.

44. Kim Y, Fiel M I, Albanis E et al. Anti-fibrotic activity and enhanced interleukin-6 production by hepatic stellate cells in response to imatinib mesylate. Liver Int 2012; 32: 1008-17.

45. Hennenberg M, Trebicka J, Kohistani Z et al. Hepatic and HSC-specific sorafenib effects in rats with established secondary biliary cirrhosis. Lab Invest 2010.

46. Friedman S L. Antifibrotic activity of sorafenib in experimental hepatic fibrosis - refinement of targets, dosing and window of efficacy in vivo. Hepatology 2011; 54: 360A-1455A.

47. Yang M D, Chiang Y M, Higashiyama R et al. Rosmarinic acid and baicalin epigenetically derepress peroxisomal proliferator-activated receptor gamma in hepatic stellate cells for their antifibrotic effect. Hepatology 2012; 55: 1271-81.

48. Bataller R, Gines P, Nicolas J M et al. Angiotensin II induces contraction and proliferation of human hepatic stellate cells. Gastroenterology 2000; 118: 1149-56.

49. Yoshiji H, Kuriyama S, Yoshii J et al. Angiotensin-II type 1 receptor interaction is a major regulator for liver fibrosis development in rats. Hepatology 2001; 34: 745-50.

50. Yoshiji H, Kuriyama S, Noguchi R et al. Combination of interferon-beta and angiotensin-converting enzyme inhibitor, perindopril, attenuates the murine liver fibrosis development. Liver International 2005; 25: 153-61.

51. Xu W, Song S, Huang Y, Gong Z. Effects of perindopril and valsartan on expression of transforming growth factor-beta-Smads in experimental hepatic fibrosis in rats. J Gastroenterol Hepatol 2006; 21: 1250-6.

52. Yeki M, Koda M, Matono T, Sugihara T, Maeda K, Murawaki Y. Preventative and therapeutic effects of perindopril on hepatic fibrosis induced by bile duct ligation in rats. Mol Med Report 2009; 2: 857-64.

53. Warner F J, Lubel J S, McCaughan G W, Angus P W. Liver fibrosis: a balance of ACEs? Clin Sci (Lond) 2007; 113: 109-18.

54. Dokmanovic M, Clarke C, Marks P A. Histone deacetylase inhibitors: overview and perspectives. Mol Cancer Res 2007; 5: 981-9.

55. Fisher R, Nau H, Gandolfi A J, Brendel K. Toxicity of valproic acid in liver slices from sprague-dawley rats and domestic pigs. Toxicol In Vitro 1991; 5: 201-5.

56. Armendariz-Borunda J, Islas-Carbajal M C, Meza-Garcia E et al. A pilot study in patients with established advanced liver fibrosis using pirfenidone. Gut 2006; 55: 1663-5.

57. Garcia L, Hernandez I, Sandoval A et al. Pirfenidone effectively reverses experimental liver fibrosis. J Hepatol 2002; 37: 797-805.

58. Navarro-Partida J, Martinez-Rizo A B, Gonzalez-Cuevas J, Arrevillaga-Boni G, Ortiz-Navarrete V, Armendariz-Borunda J. Pirfenidone restricts Th2 differentiation in vitro and limits Th2 response in experimental liver fibrosis. Eur J Pharmacol 2012; 678: 71-7.

59. Iyer S N, Wild J S, Schiedt M J, Hyde D M, Margolin S B, Giri S N. Dietary intake of pirfenidone ameliorates bleomycin-induced lung fibrosis in hamsters. J Lab Clin Med 1995; 125: 779-85.

60. Di Sario A, Bendia E, Baroni G et al. Effect of pirfenidone on rat hepatic stellate cell proliferation and collagen production. J Hepatol 2002; 37: 584-91.

61. Zhao X Y, Zeng X, Li X M, Wang T L, Wang B E. Pirfenidone inhibits carbon tetrachloride- and albumin complex-induced liver fibrosis in rodents by preventing activation of hepatic stellate cells. Clin Exp Pharmacol Physiol 2009; 36: 963-8.

62. Sonnylal S, Shi-Wen X, Leoni P et al. Selective expression of connective tissue growth factor in fibroblasts in vivo promotes systemic tissue fibrosis. Arthritis Rheum 2010; 62: 1523-32.

63. Huang M L, Li X, Meng Y et al. Upregulation of angiotensin-converting enzyme (ACE) 2 in hepatic fibrosis by ACE inhibitors. Clin Exp Pharmacol Physiol 2010; 37: e1-6.

64. Vonk L A, Doulabi B Z, Huang C L, Helder M N, Everts V, Bank R A. Endoplasmic reticulum stress inhibits collagen synthesis independent of collagen-modifying enzymes in different chondrocyte populations and dermal fibroblasts. Biochem Cell Biol 2010; 88: 539-52.

65. Terasaki M, Chen L B, Fujiwara K. Microtubules and the endoplasmic reticulum are highly interdependent structures. J Cell Biol 1986; 103: 1557-68.

66. Rodriguez L, Cerbon-Ambriz J, Munoz M L. Effects of colchicine and colchiceine in a biochemical model of liver injury and fibrosis. Arch Med Res 1998; 29: 109-16.

Chapter 4

The effect of antifibrotic drugs in rat precision-cut fibrotic liver slices

Inge M. Westra[a,b], Dorenda Oosterhuis[b], Geny M.M. Groothuis[a] and Peter Olinga[b]

PLoS One 2014; 9(4):e95462

[a] Division of Pharmacokinetics, Toxicology and Targeting, Department of Pharmacy, University of Groningen, The Netherlands
[b] Division of Pharmaceutical Technology and Biopharmacy, Department of Pharmacy, University of Groningen, The Netherlands

Abstract

Two important signaling pathways in liver fibrosis are the PDGF- and TGFβ pathway and compounds inhibiting these pathways are currently developed as antifibrotic drugs. Testing antifibrotic drugs requires large numbers of animal experiments with high discomfort. Therefore, a method to study these drugs *ex vivo* was developed using precision-cut liver slices from fibrotic rat livers (fPCLS), representing an *ex vivo* model with a multicellular fibrotic environment. We characterized the fibrotic process in fPCLS from rat livers after 3 weeks of bile duct ligation (BDL) during incubation and tested compounds predominantly inhibiting the TGFβ pathway (perindopril, valproic acid, rosmarinic acid, tetrandrine and pirfenidone) and PDGF pathway (imatinib, sorafenib and sunitinib). Gene expression of heat shock protein 47 (*Hsp47*), α smooth muscle actin (*αSma*) and pro-collagen 1A1 (*Pcol1A1*) and protein expression of collagens were determined. During 48 hours of incubation, the fibrosis process continued in control fPCLS as judged by the increased gene expression of the three fibrosis markers, and the protein expression of collagen 1, mature fibrillar collagen and total collagen. Most PDGF-inhibitors and TGFβ-inhibitors significantly inhibited the increase in gene expression of *Hsp47, αSma* and *Pcol1A1.* Protein expression of collagen 1 was significantly reduced by all PDGF-inhibitors and TGFβ-inhibitors, while total collagen was decreased by rosmarinic acid and tetrandrine only. However, fibrillar collagen expression was not changed by any of the drugs. In conclusion, rat fPCLS can be used as a functional *ex vivo* model of established liver fibrosis to test antifibrotic compounds inhibiting the PDGF- and TGFβ signalling pathway.

Introduction

During liver fibrosis, connective tissue accumulates progressively and affects the normal function of the liver. The hepatic stellate cells (HSC) play a pivotal role in the development of liver fibrosis. Upon chronic injury, HSC are activated and transdifferentiate into myofibroblasts that have fibrogenic properties and are the main producers of collagen [1,2].
During fibrosis, different signaling pathways are activated. The two most important pathways in liver fibrosis are the platelet-derived growth factor (PDGF)- and the transforming growth factor beta (TGFβ) signaling pathway. Activation of these pathways results in proliferation of myofibroblasts and excess deposition of collagen [3-5]. Therefore many compounds inhibiting one of these pathways have been developed as potential antifibrotic drugs, some of which entered clinical studies [6]. However no effective medicines against end-stage liver fibrosis are available yet.
PDGF is the most important proliferative factor for HCS and myofibroblasts in liver fibrogenesis. During transition of quiescent HSC into activated HSC with a myofibroblast phenotype, they release PDGF. This PDGF binds to the PDGF receptor on activated HCS and activates the PDGF pathway, but not in quiescent HSC, as they do not express the PDGF receptor [7]. In addition, Kupffer cells and hepatocytes can increase the release of PDGF and the expression of the PDGF receptor in HSC [8]. Furthermore, after HSC activation and differentiation, TGFβ, produced by hepatocytes and Kupffer cells induces a growth stimulatory effect in transdifferentiated myofibroblasts, resulting in extracellular matrix deposition [9].
In order to study the mechanism of fibrosis and the effect of antifibrotic compounds, several *in vitro* models have been developed. The use of precision-cut tissue slices as *ex vivo* model to study fibrosis in different organs has recently been reviewed [10]. The major advantages of the use of precision-cut tissue slices are the presence of the intact organ architecture, cell-cell and cell-matrix interactions and the potential to use human tissue and to contribute to a large reduction in the use of laboratory animals for testing antifibrotic drugs [11,12]. Recently, the early onset of liver fibrosis was investigated using rat precision-cut liver slices (PCLS) [13,14]. Long-term culture for 48 hours of PCLS, prepared from livers from healthy rats, induced activation of HSC and induction of fibrosis markers, which could be inhibited by several antifibrotic compounds acting on the PDGF- signaling pathway but not by compounds acting via the TGFβ pathway [14].
The aim of the present study was to investigate whether PCLS from livers of rats with established fibrosis (fPCLS) can be used to investigate the antifibrotic effects of drugs. Previously we reported that fPCLS from bile-duct ligated (BDL) rats with established fibrosis showed progression of the fibrosis process during incubation which could be inhibited by pentoxifylline, imatinib and dexamethasone [15]. Moreover it was shown that during culture up to 48 hours, both parenchymal and non-parenchymal cells in fPCLS from BDL rats remained functionally active. In the present study, we investigated the efficacy of a series of antifibrotic compounds inhibiting the PDGF- or the TGFβ pathway in fPCLS from BDL rats. The PDGF-inhibitors imatinib, sorafenib and sunitinib are tyrosine kinase inhibitors that have antifibrotic effects *in vitro* and *in vivo* in rats [16-18]. The TGFβ-inhibitors perindopril, an angiotensin converting enzyme (ACE) inhibitor, valproic acid, a histone deacetylase inhibitor, rosmarinic acid and pirfenidone, antifibrotic compounds that inhibit the TGFβ expression, and tetrandrine, which up-regulates smad7, also demonstrated antifibrotic effects *in vitro* and *in vivo*

in liver fibrosis [19-24]. In addition, we also tested colchicine, which antifibrotic effects were shown in HSC and cirrhotic rats [25]. Based on the results, we conclude that fPCLS are an adequate model to test the efficacy of antifibrotic compounds.

Materials and Methods

Ethics statement:
Adult male Wistar rats (Ctrl:WI) were purchased from Charles River (Sulzfeld, Germany).
The rats were housed on a 12 hours light/dark cycle in a temperature-and-humidity-controlled room with food (Harlan chow no 2018, Horst, The Netherlands) and water ad libitum. The animals were allowed to acclimatize for at least seven days before the start of the experiments. The experiments were approved by the Animal Ethical Committee of the University of Groningen. The rats were anaesthetized with isoflurane (Nicholas Piramal, London, UK) and subjected to BDL [26], and all efforts were made to minimize suffering.

Slice experiments
Three weeks after BDL, livers were harvested and used for preparing liver slices in ice-cold Krebs-Henseleit buffer supplemented with 25 mM D-glucose (Merck, Darmstadt, Germany), 25 mM $NaHCO_3$ (Merck), 10 mM Hepes (MP Biomedicals, Aurora, OH, USA) and saturated with carbogen (95% O_2/5% CO_2) using a Krumdieck tissue slicer [11]. fPCLS with a diameter of 5 mm and a thickness of 250 µm were incubated up to 48 hours in 1.3 ml of Williams Medium E (with L-glutamine, Invitrogen, Paisly, Scotland) supplemented with 25 mM glucose and 50 µg/ml gentamycin (Invitrogen), with the antifibrotic compounds, at 37 °C and 95% O_2/5% CO_2 in 12-wells plates while gently shaken [11]. As a control, slices were incubated for 1, 24 and 48 hours with the solvent. After 24 hours the slices were transferred to new 12 wells plates with fresh medium. The slices were incubated with the antifibrotic compounds imatinib (1-10 µM) (Novartis, Basel, Switzerland), valproic acid (0.1-1 mM) (Sigma Aldrich, Zwijndrecht, Netherlands), perindopril (10 – 100 µM) (Sigma Aldrich), pirfenidone (0.5 – 2.5 mM) (Sigma Aldrich), rosmarinic acid (120 – 270 µM) (Sigma Aldrich), colchicine (30 – 200 nM) (Sigma Aldrich), tetrandrine (1 – 10 µM) (Sigma Aldrich), sunitinib (0.5 – 5 µM) (LC laboratories, Woburn, USA) and sorafenib (0.5 – 2 µM) (LC laboratories) and were also transferred after 24 hours to new plates with fresh medium containing the inhibitors. For mature fibrillar and total collagen detection after the addition of antifibrotic drugs, the highest concentration of the compounds was used. Stock solutions of the compounds were prepared in Milli-Q water or DMSO and diluted in the culture medium with a final concentration of the solvent of ≤ 1%.

Viability
After incubation slices were transferred to 1 ml of a sonication solution, containing 70% ethanol and 2 mM EDTA, snap frozen in liquid nitrogen and stored at -80 °C. To determine the viability, ATP levels were measured in the supernatant of samples homogenized for 45 sec in a Mini-BeadBeater-8 (Biospec, Bartlesville, OK, USA) and centrifuged for 2 min. at 16.000 g, using the ATP bioluminescence kit (Roche diagnostics, Mannheim, Germany) [27]. ATP values (pmol) were divided by the total protein content (µg) of the slice estimated by Lowry (Bio-Rad RC DC Protein Assay) [28]. Values for

the control slices are expressed relative to the slices before incubation (t=0). Values displayed for the antifibrotic compounds are relative values compared to the related controls incubated for 48 hours.

Gene expression

To determine the antifibrotic effect of the compounds on the fPCLS, *Hsp47*, *αSma* and *Pcol1A1* gene expression was determined using Quantitative Real-Time PCR. First, the total RNA of three pooled snap-frozen slices was isolated using the RNeasy Mini Kit (Qiagen, Venlo, The Netherlands). The amount of isolated RNA was measured with the ND-1000 spectrophotometer (Fisher Scientific, Landsmeer, The Netherlands). Reverse transcriptase was performed with 1 µg RNA using the Reverse Transcription System (Promega, Leiden, The Netherlands). The RT-PCR reaction was performed in the Eppendorf mastercycler gradient at 25 °C for 10 minutes, 45 °C for 60 minutes and 95 °C for 5 minutes. The gene expression of *Hsp47*, *αSma* and *Pcol1A1* was determined using the primers (50 µM) en probes (5 µM) listed in table 1 and the qPCR mastermix plus (Eurogentec, Maastricht, The Netherlands). The Real Time PCR reaction was performed in a 7900HT Real Time PCR (Applied Biosystems, Bleiswijk, The Netherlands) with 1 cycle of 10 minutes at 95 °C and 45 cycles of 15 seconds at 95 °C and 1 minute at 60 °C.

Ct values were corrected for the Ct values of the housekeeping gene *Gapdh* (ΔCt) and compared with those of slices before incubation (t=0) for the untreated slices and for the slices treated with the antifibrotic compounds with the control slices incubated for 48 hours (ΔΔCt). Results are displayed as fold change ($2^{-\Delta\Delta Ct}$).

Table 1: **Primers and probes**

Primer/Probe	Sequence	Accession number
Hsp47 Forward	5'-AGACGAGTTGTAGAGTCCAAGAGT-3'	NM_017173
Hsp47 Reverse	5'-ACCCATGTGTCTCAGGAACCT-3'	
Hsp47 Probe	5'-CTTCCCGCCATGCCAC-3'	
αSma Forward	5'-AGCTCTGGTGTGTGACAATGG-3'	BC158550
αSma Reverse	5'-GGAGCATCATCACCAGCAAAG-3'	
αSma Probe	5'-CCGCCTTACAGAGCC-3'	
Pcol1A1 Forward	5'-CCCACCGGCCCTACTG-3'	NM_053304
Pcol1A1 Reverse	5'-GACCAGCTTCACCCTTAGCA-3'	
Pcol1A1 Probe	5'-CCTCCTGGCTTCCCTG-3'	
Gapdh Forward	5'-GAACATCATCCCTGCATCCA-3'	XR_008524
Gapdh Reverse	5'-CCAGTGAGCTTCCCGTTCA-3'	
Gapdh Probe	5'-CTTGCCCACAGCCTTGGCAGC-3'	

Collagen 1 protein expression analysis by western blotting.

For the measurement of collagen 1 protein in fPCLS, 3 slices were pooled and snap frozen in liquid nitrogen and stored at -80 °C until analysis. After thawing, the slice tissue was lysed for 1 hour on ice with RIPA buffer (1 protease inhibitor cocktail tablet (Boehringer Mannheim), in 250 µl of buffer pH 7.5, containing 50 mM Tris/HCl, 150 mM NaCl, 1% Igepal CA-630, 0.5% sodium deoxycholate, 0.1% SDS). The tissue was homogenized on ice by a Potter homogenizer and centrifuged for 1 hour at 4 °C

at 16.000 g. Protein concentrations were determined in the supernatant using a Bio-Rad DC protein assay according to the protocol. Lysates were diluted with 4 x SDS sample buffer (50 mM TrisHCl pH 6.8, 2% SDS, 10% Glycerol, 5% β-mercaptoethanol, 0.05% bromophenol blue) and boiled for 2 minutes. Tissue lysate (100 µg of protein) was size fractionated on a 7.5% Sodium Dodecyl Sulphate Poly Acrylamide gel by electrophoresis and transferred to an activated Polyvinylidene Difluoride membrane (Bio-Rad). After blocking for 1 hour in Tris buffered saline supplemented with 5% Blocking Grade Powder (Bio-Rad) and 0.1% Tween-20, immunodetection of collagen-1 (1:1000, Rockland Immunochemicals) was performed. Binding of the antibody was determined using horseradish peroxidase conjugated secondary goat anti-rabbit and tertiary rabbit anti-goat antibody (Dako, Heverlee, Belgium). Visualization was performed with Western Lightning Plus-ECL (Perkin Elmer, Groningen, The Netherlands) and equal protein loading was confirmed by immunostaining with monoclonal anti B-actin (clone AC-74) (Sigma Aldrich Chemie B.V., Zwijndrecht, The Netherlands). The data of the untreated slices were expressed relative to the t=0 value and the data of the slices treated with the antifibrotic compounds were expressed relative to that of slices incubated for 48 hours.

Fibrillar collagen staining

Sirius red staining histochemistry was performed on 4 µm paraffin sections of formalin fixed fPCLS. Staining for fibrillar collagens was performed using the picrosirius red dye (Sigma, Gillingham, UK), which was quantitated using the Cell D computer program (Olympus, Hamburg, Germany). Each bar represents the average of the data of 3 different livers, and of each liver, 3 slices were stained per condition and of each slice the whole area of the section was analyzed for quantification. The data were expressed relative to that of control slices incubated for 48 hours.

Total collagen assay by hydroxyproline measurement

After incubation, triplicate slices were pooled and snap-frozen in liquid nitrogen and stored at -80 °C until analysis. After weighing the tissue, 100 µl of 6 M HCl was added and tissue was hydrolyzed at 95 °C for 20 hours. Hydroxyproline was measured using the QuickZyme Total Collagen Assay (QuickZyme BioSciences, Leiden, The Netherlands) following the manufacturers protocol. Hydroxyproline content (µg) was corrected for the weight of the slices. The data of the untreated slices were expressed relative to the t=0 value and the data of the slices treated with the antifibrotic compounds were expressed relative to that of control slices incubated for 48 hours.

Statistics

A minimum of three different BDL-livers was used for each experiment, using slices in triplicate from each liver. As not all drugs could be tested in the same liver and for each liver control slices were included, the number of livers used for control slices is larger than the number of livers incubated with compounds. The results of the treatments were compared to the untreated controls using the Student's-t-test. The results are expressed as means ± SEM.

A p-value <0.05 was considered significant. Statistical differences were determined on relative ATP-, Western blot, Sirius red and hydroxyproline content values and ΔΔCt values of gene expression data.

Results

Non-treated fibrotic PCLS

Slices from BDL-livers showed increased ATP levels after 1 hour of incubation reflecting the recovery of the ATP levels after the period of cold preservation and slicing. The ATP levels remained constant until 24 hours and were slightly decreased after 48 hours (18 % when compared to the 1 hour control) but were not significantly different from 24 hours samples (fig. 1A). In PCLS from BDL-livers directly after preparation, gene-expression of fibrosis markers *Hsp47*, *αSma* and *Pcol1A1* were significantly higher than those in PCLS from healthy rat livers (data not shown). Incubation of the fibrotic liver slices from the BDL rats was accompanied by a further increase of the gene expression of fibrosis markers after 48 hours compared to slices directly after slicing (fig. 1B). Already after 24 hours of incubation the *Pcol1A1* gene-expression was significantly elevated compared to fPCLS directly after preparation (fig. 1B). Furthermore, after 48 hours, also the protein expression of collagen 1 was increased compared to freshly prepared slices (fig. 1C). Sirius red staining and hydroxyproline content of the slices were increased after 24 and 48 hours of incubation (fig. 2A-D,N and fig. 3A).

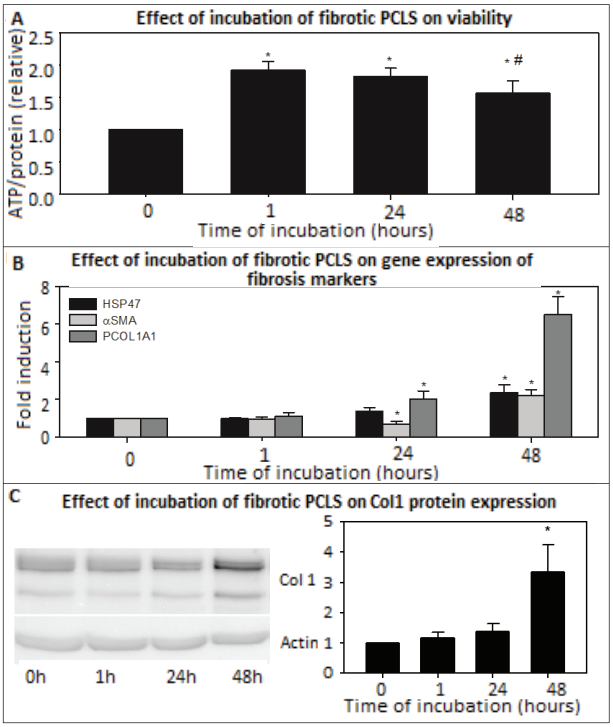

Fig 1: **The effect of incubation of fPCLS on viability, gene expression of fibrosis markers and collagen 1 protein expression.**The effect of incubation up to 48 hours on the viability (A) (n=12), on the gene expression of fibrosis markers *Hsp47*, *αSma* and *Pcol1A1* (B) (n=13) and on the collagen 1 protein expression measured by western blot (pictures are from a representative experiment) (C) (n=10) of fibrotic PCLS from livers of BDL rats. Error bars represent standard error of the mean (SEM). *p<0.05 vs 0 hours. #p<0.05 vs 1 hour.

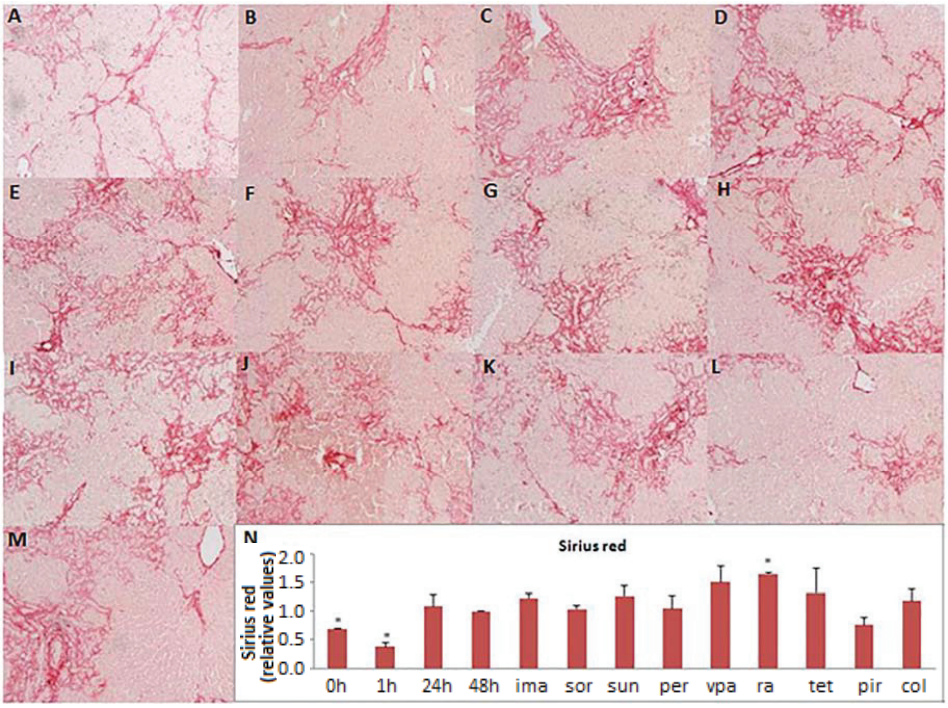

Fig 2: **Sirius red staining of control fPCLS and fPCLS incubated with antifibrotic drugs.**Sirius red staining on paraffin embedded, formalin fixed fibrotic PCLS directly after slicing (A), incubated for 1 hour (B), 24 hours (C) and 48 hours (D) and incubated for 48 hours with the compounds imatinib (ima) (E), sorafenib (sor) (F), sunitinib (sun) (G), perindopril (per) (H), valproic acid (vpa) (I), rosmarinic acid (ra) (J), tetrandrine (tet) (K), pirfenidone (pir) (L) and colchicine (col) (M).Quantification of sirius red staining (N). n=3. Error bars represent SEM. *p<0.05 vs 48 hours.

Effect of PDGF-inhibitors on fibrotic PCLS

The ATP content of the fPCLS indicated that the different concentrations of imatinib, sorafenib and sunitinib used in this study, were not toxic in fPCLS from BDL rats (fig. 4A). Incubation for 48 hours with increasing concentrations of these inhibitors showed a significant concentration dependent decrease in the gene expression of fibrosis markers *Hsp47*, *αSma* and *Pcol1A1* compared to 48 hours incubated control slices (fig. 4B). The gene expression of *Hsp47* in fPCLS, incubated for 48 hours with 5 µM of imatinib, was even significantly lower than in the control fPCLS directly after slicing and fPCLS incubated for 24 hours. Also, the *αSma* gene expression of fPCLS incubated with 5 and 10 µM imatinib, 2 µM sorafenib and 5 µM sunitinib was significantly lower than that of control fPCLS directly after slicing (fig. 4B). Moreover, in fibrotic PCLS incubated for 48 hours in the presence of 5 µM sunitinib, the gene expression of *Hsp47* and *Pcol1A1* was significantly lower than that of control fPCLS incubated for 24 hours (fig. 2B). Collagen 1 protein expression was also significantly decreased after 48 hours of incubation with the PDGF-inhibitors compared to the non-treated fibrotic slices (fig. 4C), while the Sirius red staining and the hydroxyproline content were not changed compared to control incubation (fig. 2 and fig. 3).

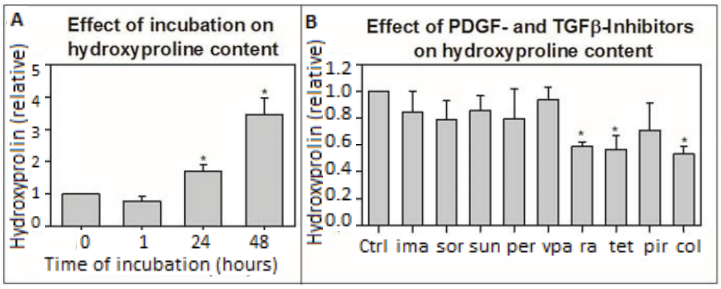

Fig 3: **Hydroxyproline content of control fPCLS and fPCLS incubated with antifibrotic drugs.**Hydroxyproline content in fPCLS incubated up to 48 hours (A) and with addition of 10 µM imatinib (ima), 2 µM sorafenib (sor), 5 µM sunitinib (sun), 100 µM perindopril (per), 1mM valproic acid (vpa) 270 µM rosmarinic acid (ra), 100 µM tetrandrine (tet), 2.5 mM perindopril (pir) and 200 nM colchicine (col) (B). n=3. Error bars represent SEM. *p<0.05 vs 0h (A), *p< 0.05 vs ctrl 48h (B).

Effect of TGFβ-inhibitors on fibrotic PCLS

Perindopril, rosmarinic acid and tetrandrine had no effect on ATP values of fPCLS, however, pirfenidone (0.5 mM) decreased viability by 24 % although only at the lowest concentration and valproic acid showed a concentration dependent decrease in ATP values up to maximally 45 % at 1 mM compared to control fPCLS (fig. 5A). All TGFβ-inhibitors showed a concentration dependent reduction of the gene expression of the 3 fibrosis markers (fig. 5B), while 10 µM tetrandrine even decreased the *αSma* gene expression to a level lower than that of control slices directly after sling and control slices incubated for 24 hours (fig. 5B). On the contrary, 0.5 mM pirfenidone increased the gene expression of *Hsp47* by 20 % in fPCLS. All TGFβ-inhibitors caused a decrease in collagen 1 protein expression (fig. 5C). However, the fibrillar collagen content as detected by the Sirius red staining was not decreased by the TGFβ inhibitors and rosmarinic acid even slightly increased the Sirius red staining compared to control fPCLS (fig. 2). The total collagen content as detected by the hydroxyproline content was only decreased after addition of rosmarinic acid and tetrandrine (fig. 3).

Effect of Colchicine on fibrotic PCLS

Colchicine had no effect on the viability of fPCLS from BDL rats during 48 hours of incubation (fig. 6A). Concentrations of 30 nM and 100 nM significantly increased the gene expression of *Hsp47* (fig. 6B), while *αSma* and *Pcol1A1* gene expression, Sirius red staining and collagen 1 protein expression were not changed after incubation with colchicine (fig. 2 and 6). However, hydroxyproline content was decreased after addition of colchicine (fig. 3).

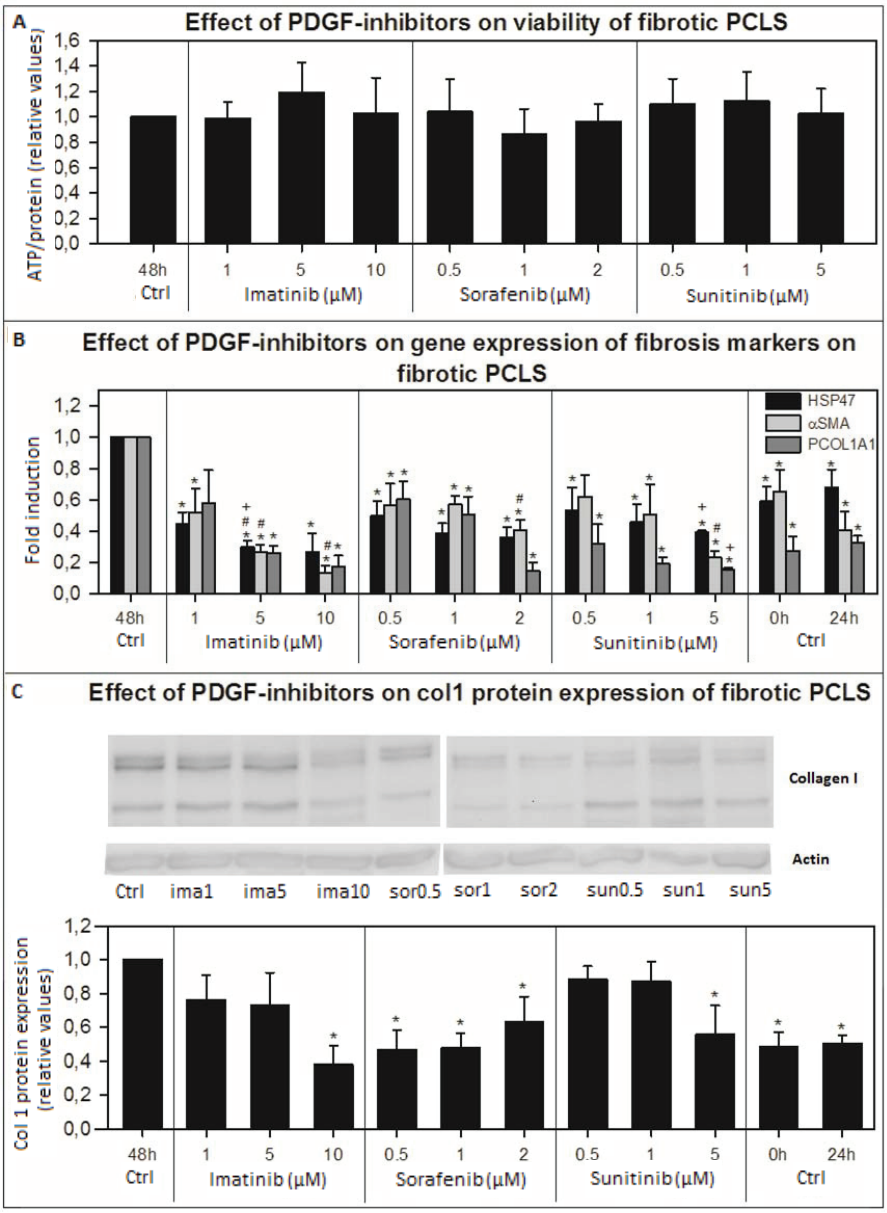

Fig 4: **The effect of PDGF-inhibitors in fPCLS on viability, gene expression of fibrosis markers and collagen 1 protein expression.** The effect of PDGF-inhibitors imatinib (n=4) , sorafenib (n=4) and sunitinib (n=4) on the viability (A), on the gene expression of fibrosis markers *Hsp47*, *αSma* and *Pcol1A1* (B) and on the collagen 1 protein expression (pictures are from a representative experiment) (C) of fibrotic PCLS from livers from BDL rats incubated for 48 hours. Error bars represent SEM. Significant decrease: *p<0.05 vs 48h, #p<0.05 vs 0 hours, +p<0.05 vs 24 hours.

Discussion

Recently, we showed that PCLS from healthy rat livers can be used to study the early onset of liver fibrosis [14]. In this current study we investigated whether this *ex vivo* model could also be utilized to study the end-stage of liver fibrosis, by using fibrotic rat PCLS. Incubation of fPCLS prepared from BDL rat livers resulted in an increase of fibrosis markers in the liver slices after 48 hours. Hence, although fPCLS directly after slicing of a BDL liver are already fibrotic, during incubation an even further increase of gene expression of *Hsp47*, *αSma*, *Pcol1A1,* protein expression of collagen 1, fibrillar collagen and total collagen deposition was observed, suggesting that further HSC activation and fibrogenesis occurs, as was shown before [15]. The initial decrease in *αSma* gene expression at 24 hours might be explained by an initial improvement due to the termination of the bile duct ligation or loss of fibroblasts and again an activation of HSC due to long-term incubation.
In this study we investigated the effect of a series of compounds predominantly inhibiting the TGFβ pathway (TGFβ-inhibitors) or the PDGF pathway (PDGF-inhibitors).
The PDGF-inhibitors imatinib, sorafenib and sunitinib clearly showed antifibrotic effects as they significantly decreased the gene expression of *Hsp47*, *αSma* and *Pcol1A1* in fPCLS after 48 hours of incubation. These compounds also showed antifibrotic effects in the model of early onset of fibrosis in PCLS [14]. Moreover these data confirm the data of Van de Bovenkamp *et al.* who also showed a decrease in *Pcol1A1* and *αSma* gene expression in fPCLS from BDL rats after 24 hours of incubation with imatinib compared to control slices without imatinib [15]. Collagen 1 protein expression was also decreased after 48 hours of incubation, however the PDGF-inhibitors did not decrease the fibrillar collagen and total collagen levels. Suggesting that the decrease in collagen 1 is not large enough to decrease the total collagen content. In the present study the gene expression of *αSma* after 48 hours of incubation of fPCLS with 5 μM imatinib was even lower than in the 24 hours control slices, suggesting that imatinib not only inhibited the increase of the fibrosis marker which occurred between 24 hours and 48 hours of culture, but even further reduced the *αSma* expression. This result is in line with *in vivo* studies where imatinib caused a reduction in the number of proliferating HSC and αSma positive cells 48 hours after BDL surgery in rats [29]. In contrast to the findings with fPCLS, *in vivo* this was accompanied by a reduced Sirius red staining for fibrillar collagen [29], which may be explained by the differences in experimental conditions, as in our studies imatinib was given for 48 hours, 3 weeks after BDL surgery, while *in vivo* imatinib was administered 1 day prior to BDL and treatment was continued for 3 days. This time dependency was also observed in BDL rats *in vivo* where a reduction in fibrillar collagen, assessed by an aniline blue staining, by imatinib was observed during the first 21 days after BDL, but not when administered during 22-35 days after BDL [30]. To our knowledge hydroxyproline has not been measured before after imatinib treatment in BDL rats, but it was decreased after imatinib treatment in a rat model of pig-serum induced fibrosis [16]. However in the latter study imatinib was administered directly at the start of the treatment with pig-serum [16] when fibrosis was not yet established, which might explain the different results of hydroxyproline in fPCLS.
Sorafenib, reduced the gene expression of fibrosis markers in the *ex vivo* fPCLS in accordance with results obtained in rats *in vivo* [31,32]. However, Sirius red was not reduced in fPCLS whereas *in vivo* reduced Sirius red staining was observed after two weeks treatment with sorafenib, starting two

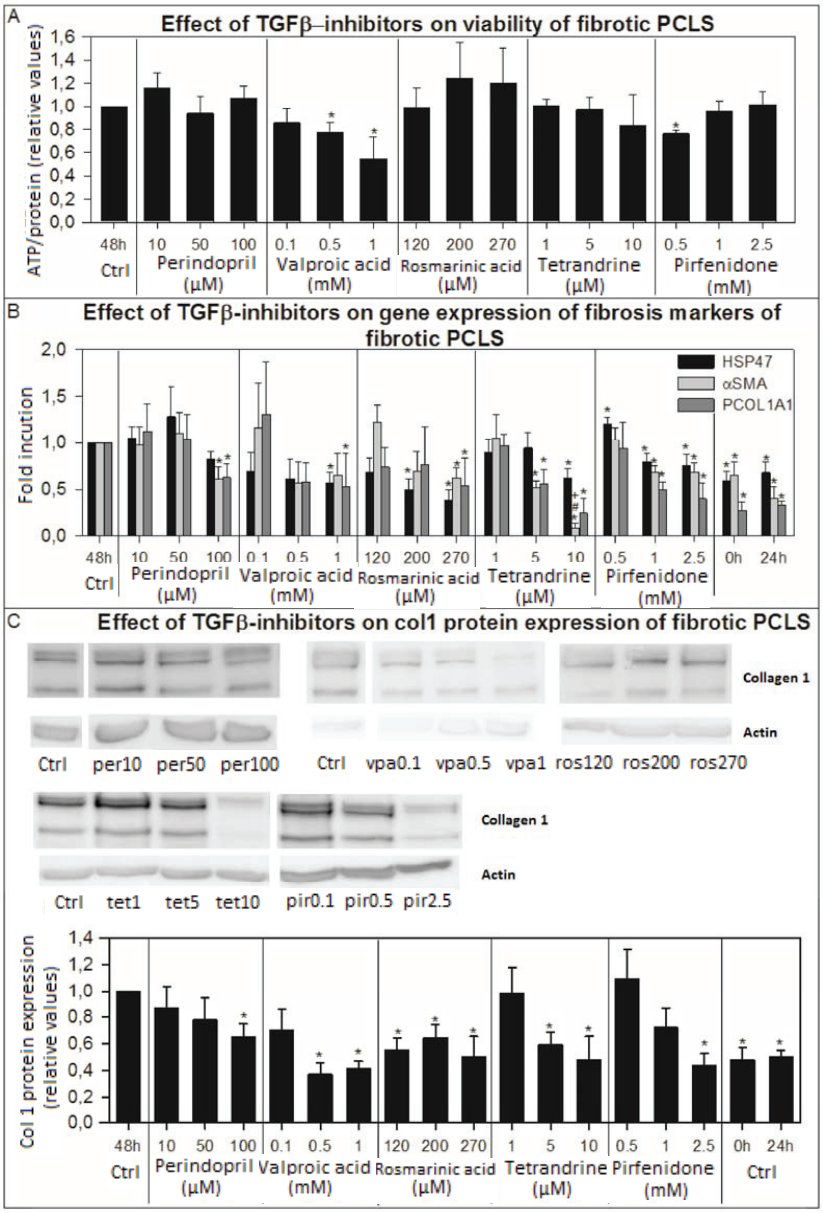

Fig 5: **The effect of TGFβ-inhibitors in fPCLS on viability, gene expression of fibrosis markers and collagen 1 protein expression.** The effect of TGFβ-inhibitors perindopril (n=5), valproic acid (n=4) , rosmarinic acid (n=4), tetrandrine (n=4) and pirfenidone (n=5) on the viability (A), on the gene expression of fibrosis markers *Hsp47*, *αSma* and *Pcol1A1* (B) and on the collagen 1 protein expression (pictures are from a representative experiment) (C) of fPCLS from livers from BDL rats incubated for 48 hours. Error bars represent SEM. Significant decrease: *p<0.05 vs 48h, #p<0.05 vs 0 hours, +p<0.05 vs 24 hours.

weeks after BDL [31], which may indicate that the lack of effect on fibrillar collagen in our studies is due to the relatively short duration of the treatment. Wang *et al.* reported a reduction in both collagen 1 and hydroxyproline content in BDL rats treated with sorafenib during week 3 and 4 of BDL [17], while in fPCLS collagen 1 was reduced, but hydroxyproline content was not, which again may be explained by the short duration of treatment in the fPCLS studies.

To date, sunitinib was not tested *in vivo* in BDL rats, however it was investigated *in vivo* in a model of CCl_4-induced fibrosis [18]. Although the pathophysiology of these two fibrosis models shows some differences, the effect of the PDGF-inhibitor imatinib was similar in both models [29,33]. Sunitinib reduced the collagen deposition (Masson's trichrome staining) and the gene expression of *αSma* and collagens in CCl_4 treated rats [18]. The antifibrotic *ex vivo* effects of sunitinib are therefore in line with these *in vivo* results with respect to the fibrosis markers and the collagen 1 deposition. The lack of effect of sunitinib on the fibrillar and total collagen deposition in the fPCLS could not be compared with *in vivo* data as they are not available.

To summarize, all tyrosine kinase inhibitors reduced the collagen 1 protein and gene expression of fibrosis markers after 48 hours of incubation in fPCLS compared to control fPCLS incubated for 48 hours, however the fibrosis markers were not reduced compared to control slices incubated for 1 hour. Thus, this implies that the antifibrotic compounds inhibited the increase of fibrosis markers during incubation. In addition, PDGF-inhibitors had an effect on collagen 1 only and not on fibrillar and total collagen levels, probably due to the short durations of treatment in the fPCLS studies.

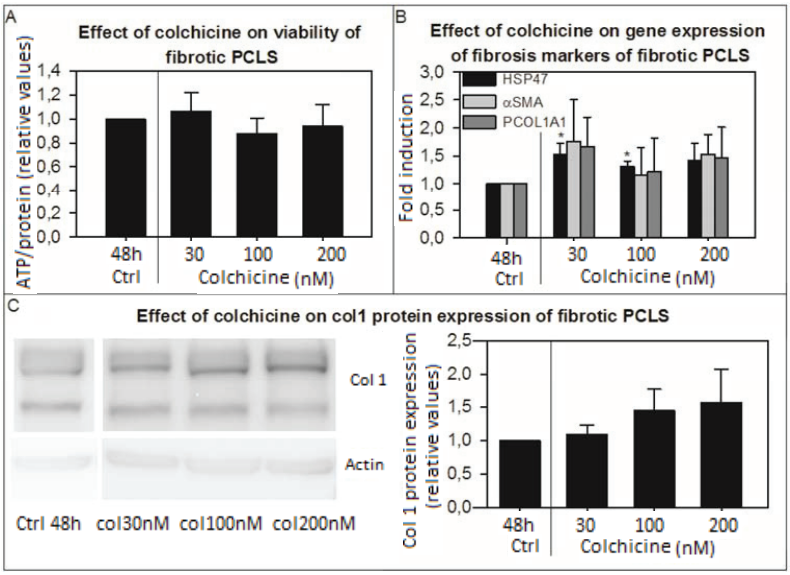

Fig 6: **The effect of colchcine in fPCLS on viability, gene expression of fibrosis markers and collagen 1 protein expression.** The effect of colchicine (n=4) on the viability (A), on the gene expression of fibrosis markers *Hsp47*, *αSma* and *Pcol1A1* (B) and on the collagen 1 protein expression (pictures are from a representative experiment) (C) of fPCLS from livers from BDL rats incubated for 48 hours. Error bars represent SEM. *p<0.05 vs 48h.

To investigate if TGFβ-inhibitors were also effective in the fibrotic PCLS model, the effect of perindopril, valproic acid, rosmarinic acid, tetrandrine and pirfenidone was investigated. *Ex vivo* perindopril treatment decreased *αSma* and *Pcol1A1* gene expression and decreased the amount of collagen 1, in line with results obtained *in vivo* both in BDL induced as well as in CCl_4 induced liver fibrosis [33,34]. Similar to the findings with the PDGF-inhibitors also with perindopril the hydroxyproline content was not decreased in fPCLS, whereas it was decreased *in vivo* which might be explained by the longer treatment period of 21 days.

In vivo valproic acid was not investigated in BDL rats, however it was studied in CCl_4 treated mice [20]. The antifibrotic effect of valproic acid was shown by a down-regulation of *αSma* and *Pcol1A1* in valproic acid treated CCl_4 mice (valproic acid in drinking water starting 2 days before CCl_4 injections) [20]. The *ex vivo* antifibrotic effect of valproic acid in rat fPCLS was comparable with these *in vivo* findings, despite the use of a different species, and was shown by a reduction in the amount of collagen 1, an inhibition of *Hsp47* and *Pcol1A1* expression and a tendency to reduce the *αSma* expression. Again a reduced Sirius red staining was observed *in vivo* after valproic acid treatment [20], and not in the fPCLS, possibly because of the different dosage regimen. The decreased viability of fibrotic PCLS after valproic acid administration was also found before in healthy rat and pig PCLS [14,35], which may have affected the results. Moreover valproic acid is known to have hepatotoxic effects in mice *in vivo* [36]. However, as RNA could be isolated and the expression of the housekeeping gene was constant in time we included the 1 mM valproic acid.

Also rosmarinic acid was not investigated before in a BDL rat fibrosis model, but was investigated in a CCl_4 rat model (6 weeks) for stationary liver fibrosis [21]. As in our fPCLS, hydroxyproline content was reduced in CCl_4 rats treated with rosmarinic acid [21]. The reason why fibrillar collagen was slightly increased in fibrotic PCLS after treatment with rosmarinic acid needs to be further investigated, as no papers about the effect of rosmarinic acid on sirius red in liver fibrosis have been published yet.

A reduced amount of collagen 1, hydroxyproline content and *αSma*, *Hsp47* and *Pcol1A1* was found in fPCLS after tetrandrine addition, which is comparable with *in vivo* studies in BDL rats [37,38]. Treatment of BDL rats with tetrandrine directly after surgery, reduced the number of αSma positive cells [37,38], Sirius red staining [37] hydroxyproline content [38] and the gene expression of *αSma* and *Col1A2* [37]. However, in the fPCLS model, tetrandrine was added when the slices were already fibrotic, which might explain the fact that Sirius red was not reduced after tetrandrine treatment, as it can be assumed that the formation of fibrillar collagen occurs after the synthesis of collagen.

Like the other TGFβ-inhibitors, studies with pirfenidone showed comparable results *in vivo* and *ex vivo*. Pirfenidone treatment was investigated *in vivo* in 4 weeks BDL rats, administered directly after BDL surgery [23] and 2 weeks after BDL surgery [39]. A reduction in Sirius red staining and hydroxyproline content [23] and gene expression of *Col1A* [39] after treatment with pirfenidone was seen.

In conclusion, all five TGFβ-inhibitors showed antifibrotic effects in fibrotic rat PCLS which was comparable with the *in vivo* effects of these compounds on liver fibrosis. Both *Pcol1A1* gene expression and collagen 1 protein expression was decreased after addition of the TGFβ-inhibitors. However, fibrillar collagen levels measured by Sirius red were not decreased and hydroxyproline, a measurement of total collagen was only decreased in slices treated with rosmarinic acid and tetrandrine, indicating that these compounds may also have effects on other collagens. In addition,

the effect of TGFβ-inhibitors on stationary fibrosis is different from the effect of these inhibitors on the early onset of liver fibrosis in PCLS [14]. TGFβ-inhibitors only slightly reduced the fibrosis markers in the early onset of fibrosis in PCLS [14], which suggests that the TGFβ pathway plays a minor role in the early onset of liver fibrosis in PCLS and a larger role in end-stage liver fibrosis in fPCLS.
Colchicine slows down the microtubule mediated transport of procollagen [40], which may explain its antifibrotic effect as observed in BDL rats where colchicine reduced the connective tissue volume (Masson's trichrome staining) [41], reduced the increased collagen deposition (trichrome staining) [42,43] and the hydroxyproline content [43]. Also in the *ex vivo* model of fPCLS, colchicine induced a decrease in total collagen content although fibrillar collagens were not yet changed.
In this study the effect of the antifibrotic drugs on the collagen protein content was assessed on three different levels, the amount of collagen 1 (by western blotting), the total collagen content (by hydroxyproline determination) and the amount of fibrillar collagens (by Sirius red staining). Both PDGF-inhibitors and TGFβ-inhibitors reduced the collagen 1 deposition, while total collagen was only decreased by the TGFβ-inhibitors rosmarinic acid and tetrandrine and fibrillar collagens (mature collagen) were not changed by any of the drugs. Apparently collagen 1 synthesis is primarily affected by these drugs, which is not yet detected by Sirius red or hydroxyproline content as mature fibrillar collagens do not only consist of collagen type I, but also type II, III, V and XI [44] and with a hydroxyproline measurement all collagens are measured [45]. Moreover reduction in mature fibrillar and total collagen is not only dependent on the synthesis of collagen but also on the rate of collagen breakdown, and therefore it may take more than 48 hours for an inhibition of synthesis to become manifest. From the results of this study it can be concluded that collagen 1 detection by western blot is the most sensitive method for the detection of antifibrotic effects on collagen disposition in fibrotic PCLS.
In conclusion, PCLS from fibrotic livers from rats 3 weeks after BDL can be successfully used as a functional *ex vivo* model to study molecular pathways in established liver fibrosis, as these fPCLS remain viable and fibrosis markers continue to increase during incubation. In addition, the *in vivo* observed antifibrotic effects of drugs acting on the PDGF- and TGFβ signaling pathway can successfully be reproduced *ex vivo* on the gene expression of fibrosis related genes and collagen I protein expression, indicating that this *ex vivo* model is a useful model for preclinical studies to test the effect of potential new antifibrotic drugs on these fibrosis markers. This will increase the efficiency of these studies as dose response studies of several drugs can be performed simultaneously with a limited number of rats, which also greatly reduces the number of laboratory animals utilized in fibrosis research. Further studies are ongoing to investigate the application of human PCLS from patients with liver fibrosis, which will be useful to identify species differences and to further reduce the use of experimental animals.

Acknowledgement
The authors would like to thank Natascha Broersma for the BDL surgery.

References

1. Hernandez-Gea V, Friedman SL. Pathogenesis of liver fibrosis. Annu Rev Pathol 2011; 6: 425-456.

2. Schuppan D, Afdhal NH. Liver cirrhosis. Lancet 2008; 371: 838-851.

3. Friedman SL, Sheppard D, Duffield JS, Violette S. Therapy for fibrotic diseases: Nearing the starting line. Sci Transl Med 2013; 5: 167sr1.

4. Friedman SL. Mechanisms of hepatic fibrogenesis. Gastroenterology 2008; 134: 1655-1669.

5. Liu Y, Wen XM, Lui EL, Friedman SL, Cui W, et al. Therapeutic targeting of the PDGF and TGF-beta-signaling pathways in hepatic stellate cells by PTK787/ZK22258. Lab Invest 2009; 89: 1152-1160.

6. Schuppan D, Kim YO. Evolving therapies for liver fibrosis. J Clin Invest 2013; 123: 1887-1901.

7. Andrae J, Gallini R, Betsholtz C. Role of platelet-derived growth factors in physiology and medicine. Genes Dev 2008;22: 1276-1312.

8. Bonner JC. Regulation of PDGF and its receptors in fibrotic diseases. Cytokine Growth Factor Rev 2004; 15: 255-273.

9. Dooley S, Ten Dijke P. TGF-beta in progression of liver disease. Cell Tissue Res 2012; 347: 245-256.

10. Westra IM, Pham BT, Groothuis GM, Olinga P. Evaluation of fibrosis in precision-cut tissue slices. Xenobiotica 2012; 43: 98-112.

11. de Graaf IA, Olinga P, de Jager MH, Merema MT, de Kanter R, et al. Preparation and incubation of precision-cut liver and intestinal slices for application in drug metabolism and toxicity studies. Nat Protoc 2010; 5: 1540-1551.

12. Olinga P, Schuppan D. Precision-cut liver slices: A tool to model the liver ex vivo. J Hepatol 2013; 58: 1252-1253.

13. van de Bovenkamp M, Groothuis GM, Draaisma AL, Merema MT, Bezuijen JI, et al. Precision-cut liver slices as a new model to study toxicity-induced hepatic stellate cell activation in a physiologic milieu. Toxicol Sci 2005; 85: 632-638.

14. Westra IM, Oosterhuis D, Groothuis GMM, Olinga P. Precision-cut liver slices as a model for the early onset of liver fibrosis to test anti-fibrotic drugs. Toxicol Appl Pharmacol 2014; 274: 328-338.

15. van de Bovenkamp M, Groothuis GMM, Meijer DKF, Olinga P. Precision-cut fibrotic rat liver slices as a new model to test the effects of anti-fibrotic drugs in vitro. J Hepatol 2006; 45: 696-703.

16. Yoshiji H, Noguchi R, Kuriyama S, Ikenaka Y, Yoshii J, et al. Imatinib mesylate (STI-571) attenuates liver fibrosis development in rats. Am J Physiol Gastrointest Liver Physiol 2005;288: G907-13.

17. Wang Y, Gao J, Zhang D, Zhang J, Ma J, et al. New insights into the antifibrotic effects of sorafenib on hepatic stellate cells and liver fibrosis. J Hepatol 2010

18. Tugues S, Fernandez-Varo G, Munoz-Luque J, Ros J, Arroyo V, et al. Antiangiogenic treatment with sunitinib ameliorates inflammatory infiltrate, fibrosis, and portal pressure in cirrhotic rats. Hepatology 2007; 46: 1919-1926.

19. Yoshiji H, Kuriyama S, Noguchi R, Yoshii J, Ikenaka Y, et al. Combination of interferon-beta and angiotensin-converting enzyme inhibitor, perindopril, attenuates the murine liver fibrosis development. Liver International 2005;25: 153-161.

20. Mannaerts I, Nuytten NR, Rogiers V, Vanderkerken K, van Grunsven LA, et al. Chronic administration of valproic acid inhibits activation of mouse hepatic stellate cells in vitro and in vivo. Hepatology 2010;51: 603-614.

21. Li GS, Jiang WL, Tian JW, Qu GW, Zhu HB, et al. In vitro and in vivo antifibrotic effects of rosmarinic acid on experimental liver fibrosis. Phytomedicine 2010; 17: 282-288.

22. Di Sario A, Bendia E, Baroni G, Ridolfi F, Casini A, et al. Effect of pirfenidone on rat hepatic stellate cell proliferation and collagen production. J Hepatol 2002; 37: 584-591.

23. Garcia L, Hernandez I, Sandoval A, Salazar A, Garcia J, et al. Pirfenidone effectively reverses experimental liver fibrosis. J Hepatol 2002; 37: 797-805.

24. Hsu Y, Chiu Y, Cheng C, Wu C, Lin Y, et al. Antifibrotic effects of tetrandrine on hepatic stellate cells and rats with liver fibrosis. J Gastroen Hepatol 2007; 22: 99-111.

25. Lee SJ, Kim YG, Kang KW, Kim CW, Kim SG Effects of colchicine on liver functions of cirrhotic rats: Beneficial effects result from stellate cell inactivation and inhibition of TGF beta1 expression. Chem Biol Interact 2004; 147: 9-21.

26. Kountouras J, Billing BH, Scheuer PJ Prolonged bile duct obstruction: A new experimental model for cirrhosis in the rat. Br J Exp Pathol 1984;65: 305-311.

27. Olinga P, Groothuis GMM. Use of human tissue slices in drug targeting research. Drug Targeting: Organ-Specific Strategies 2001; 12: 309-331.

28. Lowry OH, Rosebrough NJ, Farr AL, Randall RJ. Protein measurement with the folin phenol reagent. J Biol Chem 1951; 193: 265-275.

29. Kinnman N, Francoz C, Barbu V, Wendum D, Rey C, et al. The myofibroblastic conversion of peribiliary fibrogenic cells distinct from hepatic stellate cells is stimulated by platelet-derived growth factor during liver fibrogenesis. Lab Invest 2003; 83: 163-173.

30. Neef M, Ledermann M, Saegesser H, Schneider V, Widmer N, et al. Oral imatinib treatment reduces early fibrogenesis but does not prevent progression in the long term. J Hepatol 2006; 44: 167-75.

31. Mejias M, Garcia-Pras E, Tiani C, Miquel R, Bosch J, et al. Beneficial effects of sorafenib on splanchnic, intrahepatic, and portocollateral circulations in portal hypertensive and cirrhotic rats. Hepatology 2009; 49: 1245-1256.

32. Hennenberg M, Trebicka J, Kohistani Z, Stark C, Nischalke HD, et al. Hepatic and HSC-specific sorafenib effects in rats with established secondary biliary cirrhosis. Lab Invest 2010.

33. Yoshiji H, Kuriyama S, Noguchi R, Ikenaka Y, Yoshii J, et al. Amelioration of liver fibrogenesis by dual inhibition of PDGF and TGF-beta with a combination of imatinib mesylate and ACE inhibitor in rats. Int J Mol Med 2006; 17: 899-904.

34. Yeki M, Koda M, Matono T, Sugihara T, Maeda K, et al. Preventative and therapeutic effects of perindopril on hepatic fibrosis induced by bile duct ligation in rats. Mol Med Report 2009; 2: 857-864.

35. Fisher R, Nau H, Gandolfi AJ, Brendel K. Toxicity of valproic acid in liver slices from sprague-dawley rats and domestic pigs. Toxicol In Vitro 1991;5: 201-205.

36. Ikura Y, Iwasa Y, Ueda M. Valproic acid administration for hepatic fibrosis: A balance between antifibrotic efficacy and hepatotoxicity. Hepatology 2010; 51: 2227-8; author reply 2228.

37. Hsu Y, Chiu Y, Lee C, Wu C, Huang Y. Anti-fibrotic effects of tetrandrine on bile-duct ligated rats. Can J Physiol Pharm 2006; 84: 967-976.

38. Park PH, Nan JX, Park EJ, Kang HC, Kim JY, et al. Effect of tetrandrine on experimental hepatic fibrosis induced by bile duct ligation and scission in rats. Pharmacol Toxicol 2000; 7: 261-268.

39. Salazar-Montes A, Ruiz-Corro L, Lopez-Reyes A, Castrejon-Gomez E, Armendariz-Borunda J. Potent antioxidant role of pirfenidone in experimental cirrhosis. Eur J Pharmacol 2008; 595: 69-77.

40. Ehrlich HP, Bornstein P. Microtubules in transcellular movement of procollagen. Nat New Biol 1972; 238: 257-260.

41. Poo JL, Feldmann G, Moreau A, Gaudin C, Lebrec D. Early colchicine administration reduces hepatic fibrosis and portal hypertension in rats with bile duct ligation. J Hepatol 1993; 19: 90-94.

42. Castro V, Muriel P. Comparative study of colchicine and trimethylcolchicinic acid on

prolonged bile duct obstruction in the rat. J Appl Toxicol 1996; 16: 269-275.

43. Muriel P, Deheza R. Fibrosis and glycogen stores depletion induced by prolonged biliary obstruction in the rat are ameliorated by metadoxine. Liver Int 2003; 23: 262-268.

44. Prockop DJ, Kivirikko KI. Collagens: Molecular biology, diseases, and potentials for therapy. Annu Rev Biochem 1995; 64: 403-434.

45. Langrock T, Hoffmann R. Analysis of hydroxyproline in collagen hydrolysates. Methods Mol Biol 2012; 828: 271-280.

Chapter 5

The p38-Mapk pathway is involved in fibrogenesis in rat precision-cut liver slices.

I.M. Westra[a,b], M. Boersema[c], D. Oosterhuis[b], G.M.M. Groothuis[a] and P. Olinga[b]

[a]Division of Pharmacokinetics, Toxicology and Targeting, Department of Pharmacy, University of Groningen, The Netherlands
[b]Division of Pharmaceutical Technology and Biopharmacy, Department of Pharmacy, University of Groningen, The Netherlands
[c]Department of Pathology and Medical Biology, University Medical Centre Groningen, The Netherlands

Abstract

Liver fibrosis is characterized by excessive accumulation of connective tissue in the liver. This leads to serious morbidity and mortality since no successful anti-fibrotic drugs are on the market. Precision-cut liver slices (PCLS) were previously developed as a multicellular ex vivo model for liver fibrosis, which can be used to test the efficacy of antifibrotic compounds in both the early onset and the end-stage of liver fibrosis. Recently, we showed that PDGF-inhibitors were effective in rat PCLS in the early onset of fibrosis and that both PDGF- and TGFβ-inhibitors could inhibit the increase in fibrosis markers in fibrotic rat PCLS. The aim of the current study was to further investigate the mechanism of fibrosis in PCLS by investigating the effect of downstream inhibitors of p38-Mapk (SB203580), Smad 3 (Sis3) and Rac-1 (NSC23766) on the mRNA expression of genes involved in fibrosis and on collagen deposition. These enzymes are part of the main intracellular signaling pathways involved in liver fibrosis.

PCLS of livers from normal rats and from rats who underwent bile duct ligation (BDL) were incubated for 48 hours in the presence of SB203580 (5, 10 μM), Sis3 (0.3 - 3 μM) and NSC23766 (5 – 50 μM). The mRNA expression of genes involved in collagen synthesis and breakdown was determined using a low density gene array (LDA) and for the fibrosis markers *Hsp47*, *αSma* and *Pcol1A1* determined by Real Time PCR. In addition, the total collagen content was determined using a hydroxyproline assay.

SB203580 decreased the gene expression of several genes involved in collagen synthesis and breakdown, including *Lox, Mmp13, Pcol1A1*, *Col3a1, Col5a1, Acta2* and *Pdpn* in the early onset of liver fibrosis and *Lox*, *Plod2, P4ha3*, *PCol1A1*, *Col3a1, Col5a1, Fmod*, *Ace*, *Ace2*, and *Acta2* in fibrotic PCLS (fPCLS). In addition, Real Time PCR analysis confirmed these results as *αSma(=Acta2)* and *Pcol1A1* were down-regulated in normal PCLS and in fPCLS. Furthermore, Hsp47 mRNA expression and hydroxyproline content was decreased by SB203580 in fPCLS. However, NSC23766 and Sis3 showed minimal effects on the markers measured in PCLS and fPCLS.

In conclusion, Smad3 and Rac-1 do not seem to play a significant role in liver fibrosis in PCLS. However, the p38-Mapk pathway plays an important role in the onset and end-stage of liver fibrosis in PCLS. Inhibition of p38-Mapk resulted in a decreased expression of genes involved in collagen deposition and fibrosis.

Introduction

Liver fibrosis is characterized by excessive accumulation of connective tissue in the liver. Hepatic stellate cells (HSC) are activated after liver injury and transdifferentiate into myofibroblasts and start to produce large amounts of collagen (1,2). Many compounds have been developed as potential antifibrotic drugs and some entered clinical studies after successful animal studies. However, up till now, no antifibrotic drugs are available on the market, possibly partly due to species differences. Moreover, research is hampered by the lack of good biomarkers to measure fibrosis (2). Precision-cut tissue slices were shown to be an adequate *ex vivo* model to study fibrosis and the effect of antifibrotic compounds, as was reviewed recently (3). Precision-cut liver slices (PCLS) can be utilized to test antifibrotic compounds for incipient and established liver fibrosis (4-7). We previously showed that the platelet derived growth factor (PDGF) pathway is involved in the early onset of liver fibrosis in rat PCLS, since mRNA expression of PDGF increased during incubation and antifibrotic compounds acting predominantly on the PDGF pathway (PDGF-inhibitors) showed antifibrotic effects (6). The transforming growth factor β (TGFβ) pathway however seemed to be of minor importance in this *ex vivo* model as TGFβ mRNA expression did not increase during incubation and inhibitors mainly acting on the TGFβ pathway (TGFβ-inhibitors) only slightly reduced the fibrosis markers tested (6). In contrast, in the *ex vivo* model for established liver fibrosis, PCLS of fibrotic livers (fPCLS) from rats after bile duct ligation (BDL) for 3 weeks, both PDGF- and TGFβ-inhibitors showed antifibrotic effects assessed by gene- and protein level of fibrosis markers, indicating that both pathways are involved in this model and that the TGFβ-inhibitors do function in PCLS (7).

The aim of the current study was to further investigate the intracellular signaling pathways involved in liver fibrosis that play a role in rat PCLS during the different stages of liver fibrosis. Therefore, the involvement of p38 Mitogen-activated protein kinase (p38 Mapk), SMAD family member 3 (Smad 3) and Ras-related C3 botulinum toxin substrate 1 (Rac-1) was investigated. Both PDGF and TGFβ can activate p38 Mapk signaling and p38 Mapk can increase the synthesis and deposition of collagen I by regulating collagen 1A1 gene expression and increasing collagen 1A1 mRNA stability (8). P38 Mapk can be inhibited by SB203580 (9), which indeed results in a reduction of collagen 1A1 gene expression in HSC (10). Smad 3 is an important component of the TGFβ pathway, and inhibition of Smad 3 by specific inhibitor of Smad3 (Sis3) results in inhibition of TGFβ dependent Smad 3 phosphorylation and signaling with an attenuation of collagen 1 expression as result (11). Rac-1 is involved in the PDGF pathway as it activates NADPH-oxidase. NADPH-oxidase is an important intracellular producer of reactive oxygen species (ROS) during liver injury and ROS is necessary for PDGF to induce proliferation in HSC (12). In addition, Rac-1 is required for myofibroblast differentiation and activity (13). NSC23766 is a specific inhibitor of Rac-1 (14).

In this study, the effect of these three downstream inhibitors of p38-Mapk (SB203580), Smad 3 (Sis3) and Rac-1 (NSC23766) was determined in both the early onset and late stage of liver fibrosis in rat PCLS to elucidate the role of these intracellular signaling pathways in different stages of fibrosis. Hence, it was investigated whether these inhibitors showed effect on the gene expression of the fibrosis markers heat shock protein 47 (*Hsp47*), alpha smooth muscle actin (*αSma*) and pro-collagen 1A1 (*Pcol1A1*), and more specifically which genes, encoding for collagen synthesis and breakdown,

involved in liver fibrosis, were affected in rat PCLS. Furthermore, the effect on collagen protein expression was determined.

Material and Methods

Slice experiments

Adult male Wistar rats (Ctrl:WI) were purchased from Charles River (Sulzfeld, Germany). The rats were housed on a 12 hours light/dark cycle in a temperature-and-humidity-controlled room with food (Harlan chow no 2018, Horst, The Netherlands) and water ad libitum. The animals were allowed to acclimatize for at least seven days before the start of the experiments. The experiments were approved by the Animal Ethical Committee of the University of Groningen.

For experiments with normal livers, rats were anaesthetized with isoflurane (Nicholas Piramal, London, UK) and livers were explanted and immediately used for preparing liver slices. In addition, for experiments with fibrotic livers, rats were anaesthetized with isoflurane and subjected to BDL as described before (15). Three weeks after BDL, rats were anaesthetized with isoflurane and livers were explanted and immediately used for preparing liver slices. Liver slices of both normal and fibrotic livers were prepared in ice-cold Krebs-Henseleit buffer supplemented with 25 mM D-glucose (Merck, Darmstadt, Germany), 25 mM $NaHCO_3$ (Merck), 10 mM Hepes (MP Biomedicals, Aurora, OH, USA) and saturated with carbogen (95% O_2/5% CO_2) using a Krumdieck tissue slicer (16). PCLS with a diameter of 5 mm and a thickness of 250 µm were incubated up to 48 hours in 1.3 ml of Williams Medium E (with L-glutamine, Invitrogen, Paisly, Scotland) supplemented with 25 mM glucose and 50 µg/ml gentamycin (Invitrogen) at 37°C and 95% O_2/5% CO_2 in 12-wells plates while gently shaken (16). After 1 and 24 hours the slices were transferred to new 12 wells plates with fresh medium. The experimental slices were incubated for 1 hour and then transferred to new medium with the inhibitors SB203580 (5, 10 µM) (Bioconnect, Huissen, The Netherlands), Sis3 (0.3 – 3 µM) (Bioconnect) and NSC23766 (5 – 50 µM) (Tocris Bioscience, Bristol, UK) and they were also transferred after 24 hours to new plates with fresh medium containing the inhibitors. As a control, slices were incubated for 1, 24, and 48 hours with the same amount of solvent. Stock solutions of the compounds at 100 times the final concentration were prepared in Milli-Q water or DMSO and diluted in the culture medium with a final concentration of the solvent of ≤ 1%. PCLS were also exposed to TGF-β1 (1 – 5 ng/ml) (hTGF-β1, Roche Applied Science, Mannheim, Germany). For these experiments the 12 well plates were pretreated with 10% BSA in milli Q water solution for 20 minutes, where after the solution was removed and plates were dried on air, in order to prevent aspecific binding of the TGF-β1 to the walls of the plates. Incubations with PDGF-BB (10 and 50 ng/ml) (Recombinant Human PDGF-BB, Peprotech, Bioconnect) were performed as described above for the antifibrotic compounds.

Viability

The viability of the PCLS during incubation with and without the inhibitors was determined by analysis of the ATP content, which was previously shown to be a good marker for viability in PCLS as it correlates with morphological damage (16). After incubation, slices were transferred to 1 ml of 70% ethanol / 2 mM EDTA, snap frozen in liquid nitrogen and stored at -80°C. To determine the viability,

ATP levels were measured (17) in the supernatant of samples homogenized for 45 seconds in a Mini-BeadBeater-24 (Biospec, Bartlesville, OK, USA) and centrifuged for 2 minutes at 4°C at 16.000 g, using the ATP bioluminescence kit (Roche diagnostics, Mannheim, Germany). The ATP values (pmol/slice) were corrected for the possible variation in slice thickness using the total protein content (µg) of the same slice estimated by Lowry (Bio-Rad RC DC Protein Assay) (18), as described previously (19).

RNA isolation and Reverse Transcriptase

The triplicate slices were pooled and snap frozen and total RNA was isolated with the use of the RNeasy Mini Kit (Qiagen, Venlo, The Netherlands). The amount of isolated RNA was measured with the ND-1000 spectrophotometer (Fisher Scientific, Landsmeer, The Netherlands). Reverse transcriptase was performed with 2 µg RNA using Reverse Transcription System (Promega, Leiden, The Netherlands). The RT-PCR reaction was performed in the Eppendorf mastercycler gradient at 25 °C for 10 minutes, 45 °C for 60 minutes and 95 °C for 5 minutes

Gene expression analysis by Low Density Array (LDA)

Custom-made TaqMan Array microfluidic cards (Applied Biosystems) with 384 wells preloaded with primers were used to measure the expression of genes involved in deposition and breakdown of collagen (listed in table 1), to determine the effects of incubation and of the inhibition of p38 Mapk, Smad 3 and Rac-1 in PCLS on the fibrosis process in PCLS. 8 µl of cDNA (40 ng/µl) was mixed with 42 µl RNase free water and 50 µl 2x Taqman PCR master mix (Applied Biosystems). Thermal cycling and fluorescence detection was performed on a ViiA™ 7 Real-Time PCR System (Applied Biosystems, Bleiswijk, The Netherlands) with 1 cycle of 50°C for 2 minutes and 95°C for 10 minutes and 40 cycles of 90°C for 15 seconds and 60°C for 1 minute. Ct values were corrected for the Ct values of the housekeeping gene β actin (ΔCt). The effect of incubation on gene expression in both PCLS and fPCLS were displayed as $2^{-\Delta Ct}$. Results of the experiments with the inhibitors are displayed as fold induction of the gene ($2^{-\Delta\Delta Ct}$) after incubation with 10 µM SB203580 in healthy and fibrotic PCLS, with 50 µM NSC23766 in healthy PCLS and 25 µM NSC23766 in fibrotic PCLS (50 µM tended to decrease the ATP values), and with 3 µM of Sis3 in healthy and fibrotic PCLS, for 48 hours, relative to control PCLS incubated for 48 hours without the inhibitors.

Gene expression analysis by Real Time PCR

To confirm the results of the LDA, the gene expression of 3 of the genes present on the LDA were also determined by quantitative Real Time PCR. The gene expression of *Hsp47 (serpinh1)*, *αSma* (*acta2*) and *Pcol1A1* was determined using the following primers (50 µM) en probes (5 µM) (Sigma aldrich); 5'-AGACGAGTTGTAGAGTCCAAGAGT-3'(F), 5'-CCCATGTGTCTCAGGAACCT-3'(R), 5'-CTTCCCGCCATGCCAC-3' (Probe, FAM) (*Hsp47*); 5'-AGCTCTGGTGTGTGACAATGG-3'(F), 5'-GGAGCATCATCACCAGCAAAG-3'(R), 5'-CCGCCTTACAGAGCC-3' (Probe, FAM) (*αSma*); 5'-CCCACCGGCCCTACTG-3'(F), 5'-GACCAGCTTCACCCTTAGCA-3'(R), 5'-CCTCCTGGCTTCCCTG-3' (Probe, FAM) (*Pcol1A1*) and the qPCR mastermix plus (Eurogentec, Maastricht, The Netherlands). The Real-Time PCR reaction was performed in a 7900HT Real Time PCR (Applied Biosystems, Bleiswijk, The Netherlands) with 1 cycle of 10 minutes at 95 °C and 45 cycles of 15 seconds at 95 °C and 1 minute at 60 °C. Ct values were corrected for the Ct values of the housekeeping gene *Gapdh* (ΔCt) (5'-

GAACATCATCCCTGCATCCA-3'(F), 5'-CCAGTGAGCTTCCCGTTCA-3'(R), 5'-CTTGCCCACAGCCTTGGCAGC-3') (Probe, VIC) which remained constant during incubations in absence and presence of the inhibitors and compared with the control (ΔΔCt). Results are displayed as fold induction of the gene ($2^{-\Delta\Delta Ct}$).

Hydroxyproline measurement

After incubation, triplicate slices were pooled and snap-frozen in liquid nitrogen and stored at -80°C until analysis. After weighing the tissue, 100 µl of 6 M HCl was added and tissue was hydrolyzed at 95°C for 20 hours. Hydroxyproline was measured using the QuickZyme Total Collagen Assay (QuickZyme BioSciences, Leiden, The Netherlands) following the manufacturers protocol. Hydroxyproline content was expressed per mg wet weight of the slices and the values are displayed as relative to the control slices incubated without inhibitor.

Statistics

All incubations were performed in triplicate (using 3 slices incubated individually in separate wells) and were repeated with a minimum of three different normal or fibrotic livers for each experiment. The results of the Real Time PCR, ATP and hydroxyproline analysis were compared to the untreated controls using the Student's-t-test. A *p*-value <0.05 was considered significant. Differences in values derived from gene expressions from the LDA were analyzed using ANOVA and corrected for multiple comparison (using the Tukey's test).

Table 1: Specifications of genes measured by Low Density Array.

Assay ID	Gene Symbol(s)	Gene Name(s)	Gene Alias(es)	RefSeq(s)	GenBank mRNA(s)	Species	Amplicon Length
Rn00561094_m1	Ace	angiotensin I converting enzyme (peptidyl-dipeptidase A) 1	Dcp1;StsRR92	NM_012544.1	U03708.1;AF201331.1;AF539425.1;BC085760.1;L36664.1;AF532784.1;AF201332.1;AF532783.1;U03734.1	Rat	90
Rn01416293_m1	Ace2	angiotensin I converting enzyme (peptidyl-dipeptidase A) 2	-	NM_001012006.1	GQ262788.1;AY881244.1	Rat	90
Rn01759928_g1	Acta2	smooth muscle alpha-actin	-	NM_031004.2	DN934985.1;CB608976.1;BC158550.1;X06801.1	Rat	65
Rn00667869_m1	Actb	actin, beta	Actx	NM_031144.2	BC063166.1;AB028846.1;EF156276.1	Rat	91
Rn00571880_m1	Adam17	ADAM metallopeptidase domain 17	TACE	NM_020306.1	AJ012603.1	Rat	143
Rn01435427_m1	Agtr1a	angiotensin II receptor, type 1a	AT1;AT1A;AT1R;Agtr1	NM_030985.4	AY585653.1;BC078810.1;AY585654.1	Rat	99
Rn00560677_s1	Agtr2	angiotensin II receptor, type 2	AT2-R;AT2R;AT₂R	NM_012494.3	D16840.1;BC161802.1	Rat	71
Rn01466024_m1	Bmp1	bone morphogenetic protein 1	-	NM_031323.1	AB073100.1	Rat	85
Rn00560930_m1	Cat	catalase	CS1;Cas1;Cs-1;RATCAT01;RATCATL	NM_012520.1	BC081853.1;M11670.1	Rat	107
Rn00580109_m1	Cdh1	cadherin 1	-	NM_031334.1	AB017696.1	Rat	105
Rn01463848_m1	Col1a1	collagen, type I, alpha 1	COLIA1	NM_053304.1	Z78279.1;BC133728.1;CB693258.1	Rat	115
Rn01437681_m1	Col3a1	collagen, type III, alpha 1	-	NM_032085.1	AJ005395.1;BC087039.1;M21354.1	Rat	71
Rn01482927_m1	Col4a1	collagen, type IV, alpha 1	-	NM_001135009.1	BC089096.1	Rat	69
Rn00593170_m1	Col5a1	collagen, type V, alpha 1	-	NM_134452.1	AF272662.1	Rat	61
Rn00580723_m1	Ctsk	cathepsin K	-	NM_031560.2	BC078793.1;AF010306.1	Rat	69
Rn00432253_m1	Ddr1	discoidin domain receptor tyrosine kinase 1	Cak;Drd1;PTK3D	NM_013137.2;NM	DN935615.1;BC166604.1;CB613563.1	Rat	68
Rn01467728_m1	Fkbp10	FK506 binding protein 10	-	NM_001014120.1	BC085854.1	Rat	74
Rn00589918_m1	Fmod	fibromodulin	-	NM_080698.1	X82152.1	Rat	99
Rn00569575_m1	Fn1	fibronectin 1	FIBNEC;fn-1	NM_019143.2	X15906.1	Rat	97
Rn99999916_s1	Gapdh	glyceraldehyde-3-phosphate dehydrogenase	Gapd	NM_017008.3	M17701.1;BC059110.1;BC087743.1;DQ403053.1;X02231.1;AB017801.1	Rat	87
Rn01419840_g1	Glt25d1	glycosyltransferase 25 domain containing 1	RGD1309002	NM_001106067.2	BC160899.1	Rat	85
Rn00597703_m1	Havcr1	hepatitis A virus cellular receptor 1	KIM-1;Kim1	NM_173149.1	BC061820.1;AF035963.1	Rat	60
Rn00566984_m1	Lox	lysyl oxidase	H-rev142;Rrg1	NM_017061.2	U11038.1;BC078861.1	Rat	96
Rn01418038_m1	Loxl1	lysyl oxidase-like 1	-	NM_001012125.1	BC089224.1	Rat	82
Rn01466080_m1	Loxl2	lysyl oxidase-like 2	-	NM_001106047.2	BC168900.1	Rat	76
Rn00562673_s1	Mas1	MAS1 oncogene	c-mas	NM_012757.2	BC078884.1	Rat	67

Rn01448194_m1	Mmp13	matrix metallopeptidase 13	-	NM_133530.1	M60616.1	Rat	65
Rn00579172_m1	Mmp14	matrix metallopeptidase 14 (membrane-inserted)	Mt1-mmp	NM_031056.1	X83537.1;X91785.1;BC072509.1	Rat	62
Rn01538170_m1	Mmp2	matrix metallopeptidase 2	-	NM_031054.2	U65656.1;BC074013.1	Rat	63
Rn00579162_m1	Mmp9	matrix metallopeptidase 9	-	NM_031055.1	U24441.1	Rat	72
Rn01456616_m1	Mrc2	mannose receptor, C type 2	Endo180	NM_001024687.1	DQ058624.1	Rat	110
Rn00597082_m1	P4ha1	prolyl 4-hydroxylase, alpha polypeptide	PHalphaI	NM_172062.2	BC078703.1;X78949.1	Rat	67
Rn01649308_m1	P4ha3	prolyl 4-hydroxylase, alpha polypeptide III	-	NM_198775.1	AY313450.1	Rat	129
Rn00564459_m1	P4hb	prolyl 4-hydroxylase, beta polypeptide	PDI;PDIR	NM_012998.1	M21018.1;BC061857.1;X02918.1	Rat	58
Rn00570318_m1	Pcolce	procollagen C-endopeptidase enhancer	PCPE	NM_019237.1	U94710.1;AB008534.1;BC086572.1;AF016503.1	Rat	70
Rn00571195_m1	Pdpn	podoplanin	E11;Gp38;OTS-8;RTI40;T1-alpha	NM_019358.1	U32115.1;U96449.1;U07797.1;BC072492.1	Rat	97
Rn00587606_m1	Plod1	procollagen-lysine, 2-oxoglutarate 5-dioxygenase 1	Plod	NM_053827.1	L25331.1	Rat	77
Rn00598533_m1	Plod2	procollagen lysine, 2-oxoglutarate 5-dioxygenase 2	-	NM_001142915.1;	AJ430860.1;AJ430861.1	Rat	67
Rn00710210_m1	Plod3	procollagen-lysine, 2-oxoglutarate 5-dioxygenase 3	-	NM_178101.3	BC085683.1;AJ430859.1	Rat	73
Rn03302274_m1	Ppib	peptidylprolyl isomerase B	CypB;Scylp	NM_022536.1	BC061971.1;AF071225.1	Rat	70
Rn00567777_m1	Serpinh1	serine (or cysteine) peptidase inhibitor, clade H, member 1	Cbp2;Serpinh2	NM_017173.1	M69246.1;BC086529.1	Rat	76
Rn01485759_m1	Slc39a13	solute carrier family 39 (zinc transporter), member 13	-	NM_001039196.1	BC112321.1	Rat	60
Rn00580659_m1	Tagln	transgelin	Sm22	NM_031549.2	M83107.1;X71070.1;BC061770.1	Rat	77
Rn00572010_m1	Tgfb1	transforming growth factor, beta 1	Tgfb	NM_021578.2	X52498.1;AY550025.1;BC076380.1	Rat	65
Rn00587558_m1	Timp1	TIMP metallopeptidase inhibitor 1	TIMP-1;Timp	NM_053819.1	BC099821.1;L31883.1;AY550026.1;U06179.1	Rat	91
Rn00579738_m1	Vim	vimentin	-	NM_031140.1	BC061847.1;X62952.1	Rat	105
Rn00755072_m1	Ywhaz	tyrosine 3-monooxygenase /tryptophan 5-monooxygenase activation protein, zeta polypeptide	14-3-3z	NM_013011.3	D30740.1;U37252.1;D17615.1;BC094305.1;BC070941.1	Rat	104

Results

Gene expression of fibrosis related genes analyzed by LDA

The effect of 48 hours of incubation on genes related to collagen production and degradation was investigated using a low density gene array (LDA) (see Table 1 for all the genes that were measured). During incubation of normal PCLS up to 48 hours, the gene expression of *Agtr1a*, *Cat*, *Fn1*, *Loxl2* and *Plod1* were significantly down-regulated and the expression of *Timp1* and *Havcr1* were increased during incubation, compared to freshly prepared slices (Table 2).

Furthermore, incubation of fPCLS for 48 hours caused an increase in the gene expression of *Acta2, Pcol1A1, Lox, Mmp2, P4ha3* and *Plod2* compared with fPCLS directly after slicing (Table 2).The gene

expression of *Ace2*, *Cat*, *Col4a1*, *Fkbp10*, *Fn1*, *Pcolce*, *Serpinh1*, *Tgfb1* and *Vim* in fPCLS were significantly different at basic level (0h) for fPCLS compared to normal PCLS (Table 2).

Table 2. Gene expression (2^-dCT) during incubation in PCLS and fPCLS measured by low density array (LDA) of collagen related genes corrected for β actin gene expression. x= below detection level. n=3. *p<0.05 vs. 0 hours, #p<0.05 vs. 24 hours, +p<0.05 end-stage vs. early onset.

	Early-onset						End-stage			
	0h		24h		48h		0h		48h	
	2^-dCT (*10^-3)	sem	2^-dCT (*10^-3)	sem	2^-dCT (*10^-3)	sem	2^-dCT (*10^-3)	sem	2^-dCT (*10^-3)	sem
Ace	0.09	0.03	0.14	0.02	0.22	0.05	0.58	0.05	3.36	0.94
Ace2	0.07	0.02	0.01	0.00	0.00	0.00	0.21 +	0.03	0.12	0.02
Acta2	0.83	0.05	0.18	0.04	0.48	0.17	4.29	1.16	8.25 *	1.47
Adam17	1.55	0.28	2.76	0.14	2.52	0.62	1.44	0.30	1.79	0.16
Agtr1a	27.62	1.00	4.78 *	0.69	3.24 *	1.15	8.07	5.15	2.40	0.98
Agtr2	0.01	0.01	0.00	0.00	0.00	0.00	0.03	0.02	0.00	0.00
Bmp1	54.56	9.05	63.95	13.66	80.66	31.98	28.68	11.98	23.40	3.15
Cat	2023.31	193.34	1055.17 *	204.73	249.99 *#	144.95	322.23 +	208.04	194.48	71.92
Cdh1	44.23	6.70	39.95	4.20	18.23	6.21	50.05	10.75	26.63	6.40
Col1a1	0.65	0.10	0.21	0.06	0.51	0.16	9.38	3.06	47.97 *	11.40
Col3a1	53.19	18.23	10.46	4.18	4.92	2.21	120.64	44.11	202.57	80.98
Col4a1	11.75	1.85	7.52	1.35	6.73	2.05	47.99 +	7.47	47.85	0.38
Col5a1	5.10	0.74	1.27	0.24	0.64	0.19	8.89	0.70	12.48	2.12
Ctsk	0.34	0.10	0.17	0.02	0.24	0.05	0.43	0.07	0.57	0.06
Ddr1	0.07	0.02	0.16	0.05	0.38	0.09	1.06	0.18	1.19	0.20
Fkbp10	0.10	0.03	0.24	0.02	0.21	0.08	0.54 +	0.09	1.82	0.19
Fmod	0.04	0.01	0.01	0.00	0.02	0.01	0.08	0.06	0.10	0.04
Fn1	687.55	139.75	246.34 *	0.50	98.19 *	21.57	213.94 +	74.67	212.88	35.68
Glt25d1	7.24	2.38	5.96	0.60	2.95	0.48	6.27	1.76	5.21	0.69
Havcr1	0.05	0.01	0.23	0.07	0.85 *#	0.24	0.04	0.02	0.04	0.02
Lox	10.75	6.41	4.17	1.86	4.23	1.93	7.56	2.64	31.70 *	8.52
Loxl1	0.09	0.01	0.03	0.00	0.03	0.02	3.21	1.06	2.33	0.53
Loxl2	6.10	0.65	1.48 *	0.24	0.96 *	0.19	9.69	1.07	10.72	1.72
Mas1	0.03	0.02	0.02	0.00	0.01	0.00	0.05	0.03	0.01	0.00
Mmp13	x	x	0.85	0.30	5.09	2.62	0.00	0.00	0.06	0.01
Mmp14	11.40	1.61	14.96	1.22	10.50	1.90	9.39	2.78	17.37	1.69
Mmp2	0.71	0.07	0.39	0.09	0.55	0.23	3.43	0.40	13.24 *	2.86
Mmp9	0.10	0.02	4.71	0.89	4.64	2.21	0.08	0.02	0.35	0.04
Mrc2	0.09	0.01	0.08	0.03	0.07	0.05	1.33	0.05	1.92	0.28
P4ha1	1.59	0.24	1.56	0.19	1.08	0.23	1.75	0.29	1.95	0.14
P4ha3	0.01	0.01	0.04	0.01	0.05	0.01	0.03	0.01	0.64 *	0.19
P4hb	199.72	32.22	164.88	22.41	93.07	4.71	106.53	54.12	104.12	46.21
Pcolce	1.00	0.17	0.82	0.10	0.73	0.22	5.10 +	1.16	12.00	1.87
Pdpn	0.01	0.01	0.09	0.03	0.35	0.24	0.71	0.26	0.37	0.02
Plod1	8.01	1.08	7.61	0.36	3.60 *#	0.31	6.84	1.13	7.88	0.32
Plod2	0.13	0.02	0.57	0.10	0.69	0.20	3.31	0.87	10.51 *	2.28
Plod3	6.28	0.89	9.64	1.01	5.94	1.07	6.15	1.95	5.31	0.92
Ppib	17.52	4.16	11.62	2.94	7.40	0.80	10.72	4.63	7.43	1.87
Serpinh1	4.93	0.76	2.39	0.48	2.07	0.64	18.27 +	2.76	20.10	1.16
Slc39a13	0.64	0.09	0.54	0.10	0.41	0.11	0.87	0.12	0.86	0.10
Tagln	0.52	0.06	0.07	0.04	0.30	0.09	2.74	0.77	3.19	0.78
Tgfb1	5.55	0.32	7.69	0.91	5.42	1.45	10.54 +	0.81	21.30	0.77
Timp1	0.44	0.04	5.24	0.21	10.58 *	3.28	2.11	0.53	9.11	0.62
Vim	7.59	1.23	10.07	1.11	14.06	5.18	47.95 +	15.74	56.94	7.72

The effect of inhibition of p38-Mapk, Smad 3 and Rac-1 on the selected genes related to collagen production and degradation was also investigated using the LDA. The three compounds were non-toxic at the applied concentrations in the early onset and end-stage *ex vivo* models of liver fibrosis as determined by ATP (data not shown). 10 µM of SB203580 decreased the gene expression of *Lox, Mmp13, Pcol1A1*, *Col3a1, Col5a1, Acta2* and *Pdpn* in the early onset of liver fibrosis in rat PCLS (Table 3). In fPCLS, the gene expression of *Lox*, *Plod2, P4ha3*, Pcol1A1, *Col3a1, Col5a1, Fmod*, *Ace*, *Ace2*, and *Acta2* was down-regulated after addition of SB203580 (Table 3). In contrast, the Smad 3 and Rac-1 inhibitors had hardly any effect on the gene expression. NSC23766 only decreased the gene expression of *Ace2* in the early onset of fibrosis, and did not significantly change any of the genes

presented on the LDA in fibrotic PCLS (fPCLS) (Table 4). In addition, Sis3 down-regulated only the gene expression of *Loxl1* in the early onset of fibrosis and up-regulated *Mas1* in the fPCLS (Table 4).

Table 3. Low density array (LDA) results after incubation of PCLS with 10 μM SB203580 for 48 hours in the early onset of liver fibrosis (Early onset) and end-stage liver fibrosis (End-stage). Gene expressions were corrected for the housekeeping gene β actin. Fold induction values (2^-ddCT) are relative to control healthy PCLS incubated for 48 hours or control fibrotic PCLS incubated for 48 hours. x= below detection level. n=3, *p<0.05 vs. ctrl is considered significant after correction for multiple comparison.

		Early onset		End-stage	
Gene		SB10 (fold induction)	sem	SB10 (fold induction)	sem
Ace	Angiotensin I converting enzyme	0.97	0.22	0.42*	0.06
Ace2		x	x	0.16*	0.06
Acta2	α smooth muscle actin	0.19*	0.04	0.43*	0.08
Adam17	Adam metallopeptidase	1.06	0.19	1.36	0.32
Agtr1a	Angiotensin II receptor	0.48	0.15	1.41	0.47
Bmp1	Bone morphogenetic protein	0.89	0.29	1.18	0.2
Cat	Catalase	0.65	0.05	2.03	0.84
Cdh1	Cadherin 1	1.51	0.22	1.51	0.32
Col1a1	Collagen	0.42*	0.04	0.38*	0.06
Col3a1		0.49*	0.01	0.46*	0.11
Col4a1		0.75	0.1	0.88	0.28
Col5a1		0.64*	0.07	0.56*	0.11
Ctsk	Cathepsin K	0.79	0.21	0.74	0.12
Ddr1	Discoidin domain receptor tyrosine kinase	0.54	0.08	0.85	0.1
Fkbp10	FK506 binding protein	0.76	0.21	0.6	0.07
Fmod	Fibromodulin	x	x	0.19*	0.04
Fn1	Fibronectin	0.79	0.18	0.61	0.13
Glt25d1	Glycosyltransferase	1.22	0.11	1.17	0.25
Havcr1	Hepatitis A virus cellular receptor	0.03	0.01	0.85	0.41
Lox	Lysyl oxidase	0.37*	0.15	0.41*	0.12
Loxl1		0.71	0.17	0.55	0.05
Loxl2		1.17	0.18	0.67	0.08
Mas1	Receptor for angiotensin	0.78	0.58	2.14	0.68
Mmp13	Matrix metallopeptidase	0.19*	0.05	0.65	0.18
Mmp14		0.59	0.07	1.11	0.29
Mmp2		1.18	0.46	0.7	0.13
Mmp9		1.32	0.2	4.41	1.96
Mrc2	Mannose receptor	1.71	0.32	0.53	0.17
P4ha1	Prolyl hydroxylase	0.95	0.15	1.05	0.25

P4ha3		0.48	0.21	0.32*	0.1
P4hb		0.94	0.16	1.65	0.55
Pcolce	Procollagen C-endopeptidase enhancer	0.5	0.12	0.74	0.25
Pdpn	Podoplanin	0.34*	0.11	0.76	0.07
Plod1	Lysyl hydroxylase	1.14	0.05	0.95	0.05
Plod2		0.43	0.1	0.46*	0.07
Plod3		0.96	0.13	1.23	0.16
Ppib	Peptidylprolyl isomerase	0.69	0.04	1.37	0.27
Serpinh1	Heat Shock Protein 47	0.93	0.11	0.66	0.1
Slc39a13	Zinc transporter	1.33	0.17	1.05	0.15
Tagln	Transgelin	0.78	0.24	0.51	0.11
Tgfb1	Transforming growth factor, beta 1	0.93	0.07	1.2	0.19
Timp1	Metallopeptidase inhibitor	1.77	0.58	0.71	0.09
Vim	Vimentin	0.58	0.03	1.28	0.49

Table 4. Low density array (LDA) results after incubation of NSC23766 and Sis3 for 48 hours in the early onset of liver fibrosis (Early onset) and end-stage liver fibrosis (End-stage) in rat PCLS. Gene expressions were corrected for the housekeeping gene β actin. Fold induction values (2^-ddCT) are relative to control healthy PCLS incubated for 48 hours or control fibrotic PCLS incubated for 48 hours. x= below detection level. n=3, except for Sis3 early onset (n=2). *p<0.05 vs. ctrl is considered significant after correction for multiple comparison

	Early onset		End-stage	
Gene	NSC	sem	NSC	sem
Ace2	0.19*	0.09	0.56	0.16
	Early onset		End-stage	
Gene	Sis3	sd	Sis3	sem
Loxl1	0.14*	0.02	0.96	0.21
Mas1	x	x	2.49*	0.35

Gene expression of Hsp47, αSma and Pcol1A1 by Real Time PCR

The p38-Mapk inhibitor SB203580 inhibited the gene expression of *aSma* and *Pcol1A1* in PCLS in both the early onset and end-stage of liver fibrosis (Fig. 1A, B) as was also shown with the LDA (Table 3, Acta2 and Pcol1A1). In the end-stage of liver fibrosis in fPCLS the gene expression of *Hsp47* was also significantly decreased to 70 % (p=0.004) (Fig. 1B) by SB203580, in line with the 66% decrease in the LDA, although this was not significant (p=0.069) (Table 3, Serpinh1). Addition of PDGF had no effect on the viability of the liver slices (data not shown), and increased the *Hsp47* gene expression significantly compared to control PCLS (Fig. 1A). When SB203580 was added together with PDGF, 10 µM SB203580 reduced the increase of the gene expression of *aSma* compared with PCLS incubated with PDGF alone and it tended (p=0.07) to decrease the *Pcol1A1* gene expression compared to the control with PDGF alone (Fig. 1A).

Inhibition of Smad 3 by Sis3 only slightly affected the fibrotic process by decreasing the gene expression of *Pcol1A1* in the early onset of liver fibrosis in PCLS (0.3 µM) and in fPCLS (3 µM) (Fig. 1C, D). Addition of TGFβ for 48 hours increased the gene expression of the three fibrosis markers in PCLS, despite a decrease in viability by 34% (data not shown). Addition of Sis3 did not inhibit this TGFβ- induced increase in Pcol1a1 gene expression (Fig. 1C). A high variance in the results with Sis3 together with TGFβ was observed (Fig. 1C), however in each of the individual experiments an

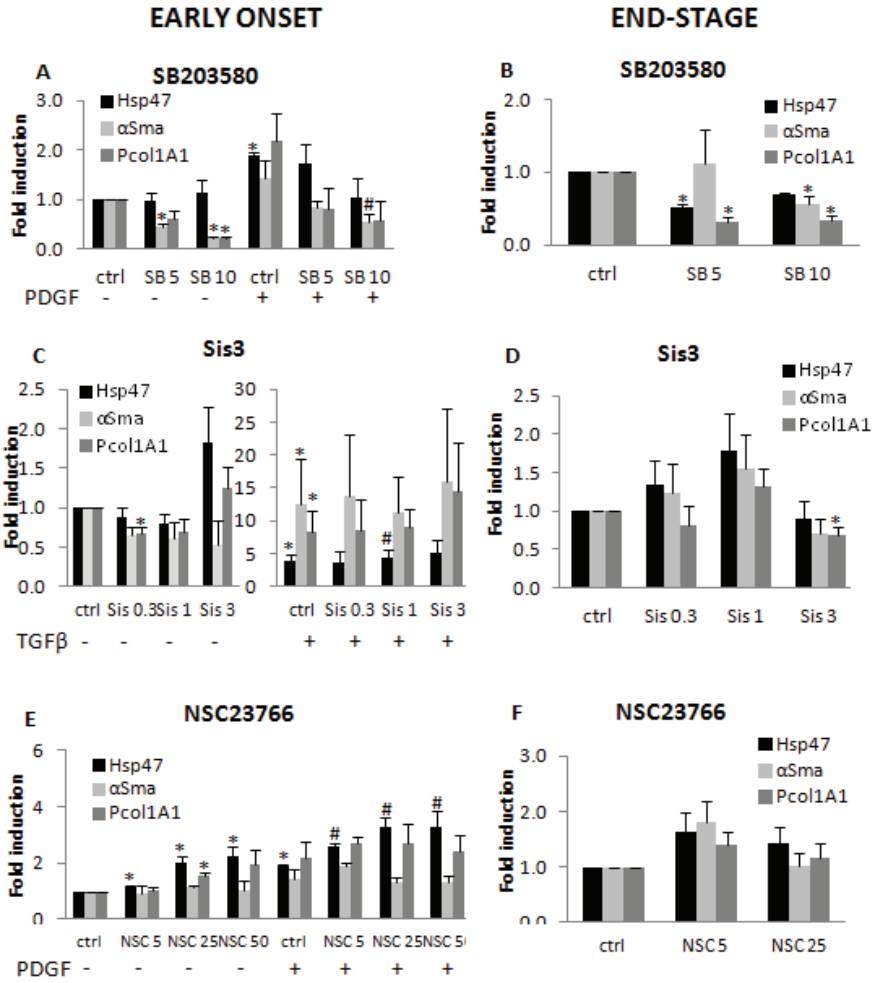

Fig. 1. Gene expression of *Hsp47*, *αSma* and *Pcol1A1,* corrected for *Gapdh*, of healthy and fibrotic rat PCLS incubated for 48 hours, with addition of SB203580 (A, B), Sis3 (C, D) and NSC23766 (E, F). ctrl: control 48 hours; SB 5: SB203580 5 µM; SB 10: 10 µM; Sis 0.3: Sis3 0.3 µM; Sis 1: 1 µM; Sis 3: 3 µM; NSC 5: NSC23766 5 µM; NSC 25: 25 µM; NSC 50: 50 µM; PDGF: platelet derived growth factor 50 ng/ml; TGFβ: Transforming Growth Factor β 5 ng/ml. n=3-4. *p<0.05 vs. ctrl. #p<0.05 vs. ctrl + PDGF or TGFβ.

increase in Pcol1A1 expression was found in the TGFβ +Sis3 stimulated slices compared to the non-stimulated control. The specific inhibitor of Rac-1, NSC23766, increased the gene expression of *Hsp47* in a concentration dependent manner, while the gene expression of *Pcol1A1* was only increased with 25 µM of NSC23766 but *αSma* expression was not changed (Fig. 1E). In the fPCLS, NSC23766 did not influence the gene expression of the measured fibrosis markers (Fig. 1F).

Hydroxyproline

In addition, to investigate the effects of the inhibition of p38 Mapk, Smad 3 and Rac-1 on fibrosis in the fPCLS, hydroxyproline was measured as marker of the total collagen content. During incubation of fPCLS the hydroxyproline content increased up to 48 hours compared to fPCLS directly after slicing (Fig. 2A). Addition of 10 µM SB203580 and 25 µM NSC23766 reduced the increased hydroxyproline content after 48 hours of incubation in fPCLS, while Sis3 did not have an effect on the hydroxyproline content (Fig. 2B).

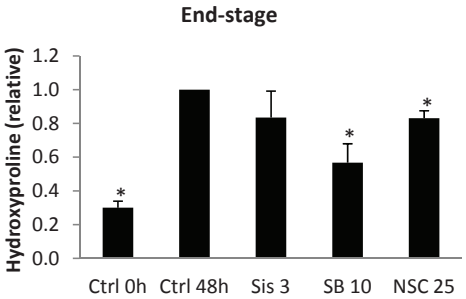

Fig. 2 Hydroxyproline measurement of fibrotic rat PCLS incubated for 0 and 48 hours and after incubations with SB203580, Sis 3 and NSC23766 for 48 hours. ctrl: control; SB 10: SB203580 10 µM; Sis 3: Sis3 3 µM; NSC 25: NSC23766 25 µM. n=3. *p<0.05 vs. ctrl 48h.

Discussion

Rat PCLS are a useful tool to study liver fibrosis and the effects of antifibrotic compounds *ex vivo* (3). Previously, the early onset and end-stage of fibrosis was studied in rat PCLS from normal and fibrotic liver tissue by incubating the slices for 48 hours, after which the gene expression of fibrosis markers *Hsp47*, *αSma* and *Pcol1A1* were increased (6) and the effect of inhibitors mainly acting on the PDGF- and TGFβ-pathway were studied (6,7). The results showed that although both PDGF and TGFβ can induce the fibrosis markers in PCLS, during extended culturing of normal PCLS the PDGF pathway plays a more important role than the TGFβ pathway, whereas in fibrotic PCLS both pathways seem to be involved. As PDGF and TGFβ share common intracellular signaling pathways, the aim of the current study was to further elucidate which intracellular signaling pathways are involved in the onset and end-stage of liver fibrosis in PCLS. This was investigated with control incubations of normal and fibrotic PCLS and by studying the effect of downstream inhibitors of p38-Mapk, Smad 3 and Rac-1 on these PCLS. These enzymes are important in the pathways involved in liver fibrosis (8,12).

In line with our previous studies (6,7) the Real Time PCR analysis showed an increased expression of *αSma*, *PCol1A1* and *Hsp47* expression by extended incubation of normal and fibrotic PCLS for 48 hours. However, in the current LDA measurements, no significant increase of gene expression of *Hsp47*, *αSma* and *Pcol1A1* in PCLS was found, but the inhibition by SB203580 of these fibrosis markers in PCLS was found in both Real Time-PCR and LDA analyses. One of the differences in the two platforms is the primer sequence of *Hsp47*, *αSma* and *Pcol1A1*, currently we are studying these discrepancies.

In this current study the gene expression of *Timp1* and *Havcr1*, also known as kidney injury molecule 1 (KIM1), were increased during incubation. Previously, *in vivo* it was shown that *Timp1* is up-regulated during the onset of fibrosis (20). In the kidney KIM1 is strongly induced by ischemia and toxic injury (21). To our knowledge this is the first time that an increase of *Kim1* is reported in liver during the onset of fibrosis. Therefore, in future studies *Timp1* and *Kim1* may be used as early markers of fibrogenesis in PCLS.

Catalase expression was down-regulated in PCLS during incubation, Dong et al. suggested that catalase expression is reduced by reactive oxygen species (ROS) (22), until now no indications have been found for the presence of ROS during PCLS in culture (23), therefore more in depth studies with PCLS are necessary to elucidate if ROS are produced in cultured PCLS.

The genes important for collagen matrix formation, *Loxl2* (24) and *Plod1* (25) that promote cross-linking of fibrillar collagen I, and *FN1*, that seems to be essential *in vitro* for the assembly of collagen matrix (26), were down-regulated during 48 hours of culturing in PCLS. Assembly of collagen may therefore be impaired during the early onset of fibrosis in PCLS. Furthermore, down-regulation of the gene expression of *Agtr1a* in PCLS may indicate that angiotensin II receptor, type 1a*,* which is important in liver fibrogenesis, plays a minor role in the induction of fibrosis in PCLS (27).

During incubation of fPCLS, gene expression of the *Lox, P4ha3* and *Plod2* genes were increased, these are genes that encode for proteins essential for collagen production (28). Up-regulation of *Acta2* and Pcol1A1 in fPCLS was in line with previous studies (5,7). Moreover, *Mmp2*, which plays a major role in ECM remodeling and is up-regulated in human liver fibrosis (29), was also up-regulated during incubation in fPCLS. These results indicate that during culture of fPCLS fibrogenesis is still ongoing.

Firstly, the role of p38-Mapk, which is activated by both PDGF and TGFβ, during the early onset of liver fibrosis in PCLS, was evaluated by studying the effect of the inhibitor SB203580. *αSma* expression is increased during incubation for 48 hours (4,6) but when p38-Mapk is inhibited, this gene is down-regulated compared to the control incubated for 48 hours without the inhibitor, indicating an inhibition in the increase of activated HSC and (myo)fibroblasts. Also, Lysyl oxidase (*Lox*) gene expression is down-regulated when p38-Mapk is inhibited, indicating a decrease in collagen cross-linking (30), together with a decrease in the gene expression of genes encoding collagen itself (*Col1a1*, *Col3a1, Col5a1*). Down-regulation of these genes may cause a reduction in the production, amount or stability of the extracellular matrix (ECM). In contrast to these genes that are down-regulated, causing a reduction in the production, amount or stability of the extracellular matrix (ECM), the gene encoding Mmp13, a protease that degrades the ECM, is also down-regulated when p38-Mapk is inhibited by SB203580. Suggesting, an inhibition of the degradation of the ECM. However, Uchinami et al. showed that Mmp13 caused an increase in fibrogenesis in BDL mice by mediating inflammation of the liver and that fibrosis is attenuated in Mmp13-deficient mice after

BDL (31). Furthermore, when Mmp13 is increased by endoplasmic reticulum stress, inhibiting p38 Mapk by SB203580 resulted in a complete attenuation of the up-regulated Mmp13 expression (32). However, Mmp13 only seems to play a role in the early onset of fibrosis, since the expression of Mmp13 in fPCLS is very low compared to the expression in normal PCLS. Podoplanin (*Pdpn*), is a marker for mesothelial cells, who can differentiate into HSC and myofibroblasts during liver fibrogenesis and also for lymphatic endothelial cells (33). Since mesothelial cells are present on the liver surface, it is unlikely that the Pdpn expression in slices reflects the mesothelial cells as the liver surface is not present in the liver slices. Yokomori et al. showed that podoplanin is also a marker for lymphatic endothelial cells and they showed a strong expression of podoplanin in cirrhotic human liver (34). Podoplanin is down-regulated after inhibition of p38-Mapk in PCLS, which could suggest that inhibition of Mapk inhibited the increase of lymphatic endothelial cells found in fibrosis.

Secondly, the role of p38-Mapk was investigated in established liver fibrosis in fPCLS of BDL rats by analyzing the effect of the inhibitor SB203580 on the expression of the genes involved in the production and degradation of collagen. Inhibition of p38-Mapk led to inhibition of the gene expression of genes encoding collagen prolyl and lysyl hydroxylases (*P4ha* and *Plod*), which are required for collagen deposition (*P4ha*) and ECM stiffness and fiber alignment (*Plod*) (28), and were increased after 48 hours of incubation in fPCLS. ECM stiffness is also regulated by the gene expression of *Lox,* which is highly expressed in fPCLS incubated for 48 hours compared to 0 hours, and *Loxl1* (30,35). Both these genes were down-regulated after inhibition of p38-Mapk in fibrotic PCLS. Inhibition of p38 Mapk also decreased the gene expression of collagens (*Col1a1* (which was increased after incubation)*, Col3a1, Col5a1*) and of fibromodulin (*Fmod*), a proteoglycan that regulates ECM organization (36). In addition, the gene expression of *Ace* (angiotensin converting enzyme) and *Ace2* (a homologue of *Ace*) was also down-regulated after inhibition of p38-Mapk. Zhang et al. showed that in experimental liver fibrosis in rats (induced by CCl_4) *Ace* and *Ace2* are significantly up-regulated (37). The gene expression of *Acta2* (αSma) was increased after incubation and is also down-regulated after inhibition of p38-Mapk in fPCLS, which indicates less activated HSC and/or (myo)fibroblasts.

These results of the LDA were confirmed by the data of Real Time PCR of *HSp47*, *αSma* and *Pcol1A1* gene expression. *Ex vivo* in PCLS SB203580 effectively reduced the gene expression of these fibrosis markers in both the early onset and end-stage of liver fibrosis.

To investigate the effect of the inhibitors on the amount of collagen in the liver, the ultimate marker for fibrosis, the amount of hydroxyproline in the slices was measured. The collagen content increased in the fibrotic slices during 48 hours of incubation and this increase was inhibited after incubation with SB203580. These results are also in line with *in vitro* results in rat HSC where SB203580 inhibited the gene expression of *Col1A,* αSma protein expression (10) and *Pcol1A1* gene expression (38). In addition, *in vitro* in HSC from cirrhotic rats, SB203580 reduced the ^{3}H-proline incorporation into collagen (39).

These results indicate an active role of the p38-Mapk pathway in the fibrotic processes in (f)PCLS as the inhibition of p38-Mapk leads to a decrease in expression of genes related to the activation of HSC and ECM production and organization. Tsukada et al. showed that the p38 Mapk pathway is independent from the Smad 3 pathway, since blocking of Smad signaling did not affect the phoshorylation of p38 Mapk and blocking of p38 Mapk did not affect the phosphorylation of Smad 2

(10). Therefore, since in PCLS inhibition of p38 Mapk by SB203580 resulted in a decrease in *Pcol1A1* expression, and Smad 3 inhibition by Sis3 only slightly decreased *Pcol1A1* gene expression and *LoxI* in the onset of liver fibrosis and had no effect in end-stage fibrosis it can be concluded that the effect of TGFβ on collagen expression in PCLS is mediated via the p38 Mapk and not via the Smad signaling pathway. The *ex vivo* results of Sis3 also correspond with the findings that in the early onset of liver fibrosis the TGFβ pathway did not seem to be involved, because the TGFβ pathway inhibitors only slightly reduced the fibrosis markers in PCLS (6). However in end-stage liver fibrosis in PCLS this pathway is activated and the TGFβ-inhibitors did show antifibrotic effects (7). TGFβ could act through p38-Mapk and not via Smad in this case. To elucidate this, Smad 3 phosphorylation will be measured in future experiments.

Inhibition of the Rac-1 pathway does not seem to have an antifibrotic effect in the early onset and end-stage of fibrosis in PCLS. It even seems profibrotic, since Hsp47 is increased after inhibition of Rac-1. In the studies of Vonk *et al.* ER stress was shown to up-regulate collagen-modifying enzymes like Hsp47 (40), and inhibition of Rac-1 seemed to reduce both ER stress and the concomitant Hsp47 expression (41), therefore the increase of Hsp47 gene expression after inhibition of Rac-1 in our experiments remains to be explained. Rac-1 is a member of the Rho family of small GTPases and regulates cell proliferation and organization of the actin cytoskeleton (42). It plays a role in the activation of NADPH oxidase and ROS derived from NADPH oxidase is necessary to induce proliferation in HSC by PDGF (43). ROS can also activate the p38 Mapk pathway (43). *In vitro*, treatment of LX-2 cells with the Rac-1 inhibitor NSC23766 resulted in decreased expression of plasminogen activator inhibitor (PAI)-1 mRNA which is a marker of activated HSC (12). Moreover in fibrotic dermal fibroblasts the Rac-1 inhibitor caused a decrease in the gene expression of αSma and Col1A2 (13). However, *ex vivo* in PCLS, inhibition of Rac-1 only resulted in a down-regulation of *Ace2* gene expression in the early onset of liver fibrosis and in fPCLS none of the genes measured in the LDA were changed after addition of NSC23766 compared with control. Furthermore, inhibition of Rac-1 did not result in reduction of fibrosis markers and the hydroxyproline content was only slightly reduced. Therefore we conclude that probably Rac-1 signaling plays a minor role in fibrogenesis in PCLS.

In conclusion, in the onset and end-stage of liver fibrosis in rat PCLS, an *ex vivo* model for liver fibrosis, Rac-1 and Smad 3 seem to be of minor importance during fibrogenesis in PCLS. However, the p38-Mapk pathway plays an important role in the increase of the fibrosis markers during culture. Either PDGF, TGFβ or ROS, or all together could in principle play a role in the activation of p38-Mapk. However, since we showed that Rac-1 plays a minor role in fibrogenesis in PCLS, it is more likely that p38-Mapk is activated by PDGF and TGFβ in the fPCLS, whereas in the early onset PCLS model the activation of p38-Mapk is mediated by PDGF only. Inhibition of p38-Mapk in normal and fibrotic PCLS resulted in a decrease of expression of profibrotic genes with a function in collagen deposition and fibrosis. Therefore, antifibrotic compounds acting on p38-Mapk could be successful in the treatment of liver fibrosis.

Acknowledgement

The authors would like to thank Natascha Broersma for the BDL surgery.

References

1. Hernandez-Gea V, Friedman S L. Pathogenesis of liver fibrosis. Annu Rev Pathol 2011; 6: 425-56.

2. Schuppan D, Kim Y O. Evolving therapies for liver fibrosis. J Clin Invest 2013; 123: 1887-901.

3. Westra I M, Pham B T, Groothuis G M, Olinga P. Evaluation of fibrosis in precision-cut tissue slices. Xenobiotica 2012; 43: 98-112.

4. van de Bovenkamp M, Groothuis G M, Draaisma A L et al. Precision-cut liver slices as a new model to study toxicity-induced hepatic stellate cell activation in a physiologic milieu. Toxicol Sci 2005; 85: 632-8.

5. van de Bovenkamp M, Groothuis G M M, Meijer D K F, Olinga P. Precision-cut fibrotic rat liver slices as a new model to test the effects of anti-fibrotic drugs in vitro. J Hepatol 2006; 45: 696-703.

6. Westra I M, Oosterhuis D, Groothuis G M M, Olinga P. Precision-cut liver slices as a model for the early onset of liver fibrosis to test anti-fibrotic drugs. Toxicol Appl Pharmacol 2014; 274: 328-38.

7. Westra I M, Oosterhuis D, Groothuis G M M, Olinga P. The effect of antifibrotic drugs in rat precision-cut fibrotic liver slices. PloS One 2014;9(4):e95462.

8. Parsons C J, Takashima M, Rippe R A. Molecular mechanisms of hepatic fibrogenesis. J Gastroenterol Hepatol 2007; 22 Suppl 1: S79-84.

9. Cuenda A, Rouse J, Doza Y N et al. SB 203580 is a specific inhibitor of a MAP kinase homologue which is stimulated by cellular stresses and interleukin-1. FEBS Lett 1995; 364: 229-33.

10. Tsukada S, Westwick J K, Ikejima K, Sato N, Rippe R A. SMAD and p38 MAPK signaling pathways independently regulate alpha1(I) collagen gene expression in unstimulated and transforming growth factor-beta-stimulated hepatic stellate cells. J Biol Chem 2005; 280: 10055-64.

11. Jinnin M, Ihn H, Tamaki K. Characterization of SIS3, a novel specific inhibitor of Smad3, and its effect on transforming growth factor-beta1-induced extracellular matrix expression. Mol Pharmacol 2006; 69: 597-607.

12. Choi S S, Sicklick J K, Ma Q et al. Sustained activation of Rac1 in hepatic stellate cells promotes liver injury and fibrosis in mice. Hepatology 2006; 44: 1267-77.

13. Xu S W, Liu S, Eastwood M et al. Rac inhibition reverses the phenotype of fibrotic fibroblasts. PLoS One 2009; 4: e7438.

14. Gao Y, Dickerson J B, Guo F, Zheng J, Zheng Y. Rational design and characterization of a Rac GTPase-specific small molecule inhibitor. Proc Natl Acad Sci U S A 2004; 101: 7618-23.

15. Kountouras J, Billing B H, Scheuer P J. Prolonged bile duct obstruction: a new experimental model for cirrhosis in the rat. Br J Exp Pathol 1984; 65: 305-11.

16. de Graaf I A, Olinga P, de Jager M H et al. Preparation and incubation of precision-cut liver and intestinal slices for application in drug metabolism and toxicity studies. Nat Protoc 2010; 5: 1540-51.

17. Olinga P, Groothuis G M M. Use of Human Tissue Slices in Drug Targeting Research. Drug Targeting: Organ-Specific Strategies 2001; 12: 309-31.

18. Lowry O H, Rosebrough N J, Farr A L, Randall R J. Protein measurement with the Folin phenol reagent. J Biol Chem 1951; 193: 265-75.

19. Hadi M, Westra I M, Starokozhko V, Dragovic S, Merema M T, Groothuis G M. Human precision-cut liver slices as an ex vivo model to study idiosyncratic drug-induced liver injury. Chem Res Toxicol 2013; 26: 710-20.

20. Wang H, Lafdil F, Wang L, Yin S, Feng D, Gao B. Tissue inhibitor of metalloproteinase 1 (TIMP-1) deficiency exacerbates carbon tetrachloride-induced liver injury and fibrosis in mice:

involvement of hepatocyte STAT3 in TIMP-1 production. Cell Biosci 2011; 1: 14,3701-1-14.

21. Ichimura T, Bonventre J V, Bailly V et al. Kidney injury molecule-1 (KIM-1), a putative epithelial cell adhesion molecule containing a novel immunoglobulin domain, is up-regulated in renal cells after injury. J Biol Chem 1998; 273: 4135-42.

22. Dong Y, Qu Y, Xu M, Wang X, Lu L. Catalase ameliorates hepatic fi brosis by inhibition of hepatic stellate cells activation. Front Biosci (Landmark Ed) 2014; 19: 535-41.

23. Schaffert C S, Duryee M J, Bennett R G et al. Exposure of precision-cut rat liver slices to ethanol accelerates fibrogenesis. Am J Physiol Gastrointest Liver Physiol 2010; 299: G661-8.

24. Kagan H M, Li W. Lysyl oxidase: properties, specificity, and biological roles inside and outside of the cell. J Cell Biochem 2003; 88: 660-72.

25. Myllyharju J, Kivirikko K I. Collagens and collagen-related diseases. Ann Med 2001; 33: 7-21.

26. Kawelke N, Vasel M, Sens C, Au A, Dooley S, Nakchbandi I A. Fibronectin protects from excessive liver fibrosis by modulating the availability of and responsiveness of stellate cells to active TGF-beta. PLoS One 2011; 6: e28181.

27. Karimian G, Buist-Homan M, Mikus B, Henning R H, Faber K N, Moshage H. Angiotensin II protects primary rat hepatocytes against bile salt-induced apoptosis. PLoS One 2012; 7: e52647.

28. Gilkes D M, Bajpai S, Chaturvedi P, Wirtz D, Semenza G L. Hypoxia-inducible Factor 1 (HIF-1) Promotes Extracellular Matrix Remodeling under Hypoxic Conditions by Inducing P4HA1, P4HA2, and PLOD2 Expression in Fibroblasts. J Biol Chem 2013; 288: 10819-29.

29. Milani S, Herbst H, Schuppan D et al. Differential expression of matrix-metalloproteinase-1 and -2 genes in normal and fibrotic human liver. Am J Pathol 1994; 144: 528-37.

30. Perepelyuk M, Terajima M, Wang A Y et al. Hepatic stellate cells and portal fibroblasts are the major cellular sources of collagens and lysyl oxidases in normal liver and early after injury. Am J Physiol Gastrointest Liver Physiol 2013; 304: G605-14.

31. Uchinami H, Seki E, Brenner D A, D'Armiento J. Loss of MMP 13 attenuates murine hepatic injury and fibrosis during cholestasis. Hepatology 2006; 44: 420-9.

32. Hamamura K, Goldring M B, Yokota H. Involvement of p38 MAPK in regulation of MMP13 mRNA in chondrocytes in response to surviving stress to endoplasmic reticulum. Arch Oral Biol 2009; 54: 279-86.

33. Li Y, Wang J, Asahina K. Mesothelial cells give rise to hepatic stellate cells and myofibroblasts via mesothelial-mesenchymal transition in liver injury. Proc Natl Acad Sci U S A 2013; 110: 2324-9.

34. Yokomori H, Oda M, Kaneko F et al. Lymphatic marker podoplanin/D2-40 in human advanced cirrhotic liver--re-evaluations of microlymphatic abnormalities. BMC Gastroenterol 2010; 10: 131,230X-10-131.

35. Kim Y, Peyrol S, So C K, Boyd C D, Csiszar K. Coexpression of the lysyl oxidase-like gene (LOXL) and the gene encoding type III procollagen in induced liver fibrosis. J Cell Biochem 1999; 72: 181-8.

36. Mormone E, Lu Y, Ge X, Fiel M I, Nieto N. Fibromodulin, an oxidative stress-sensitive proteoglycan, regulates the fibrogenic response to liver injury in mice. Gastroenterology 2012; 142: 612,621.e5.

37. Zhang W, Miao J, Li P, Wang Y, Zhang Y. Up-regulation of components of the renin-angiotensin system in liver fibrosis in the rat induced by CCL4. Res Vet Sci 2013; 95: 54-8.

38. Cao Q, Mak K M, Lieber C S. DLPC decreases TGF-beta1-induced collagen mRNA by inhibiting p38 MAPK in hepatic stellate cells. Am J Physiol Gastrointest Liver Physiol 2002; 283: G1051-61.

39. Zhang Y, Yao X. Role of c-Jun N-terminal kinase and p38/activation protein-1 in interleukin-1beta-mediated type I collagen synthesis in rat hepatic stellate cells. APMIS 2012; 120: 101-7.

40. Vonk L A, Doulabi B Z, Huang C L, Helder M N, Everts V, Bank R A. Endoplasmic reticulum stress inhibits collagen synthesis independent of collagen-modifying enzymes in different chondrocyte populations and dermal fibroblasts. Biochem Cell Biol 2010; 88: 539-52.

41. Li J, Zhu H, Shen E, Wan L, Arnold J M, Peng T. Deficiency of rac1 blocks NADPH oxidase activation, inhibits endoplasmic reticulum stress, and reduces myocardial remodeling in a mouse model of type 1 diabetes. Diabetes 2010; 59: 2033-42.

42. Bosco E E, Mulloy J C, Zheng Y. Rac1 GTPase: a "Rac" of all trades. Cell Mol Life Sci 2009; 66: 370-4.

43. Adachi T, Togashi H, Suzuki A et al. NAD(P)H oxidase plays a crucial role in PDGF-induced proliferation of hepatic stellate cells. Hepatology 2005;41:1272-81

Chapter 6

Human precision-cut liver slices as an *ex vivo* model to test antifibrotic drugs in the early onset and end-stage of liver fibrosis

Inge M. Westra[a,b], Mackenzie Hadi[a], Dorenda Oosterhuis[b], Koert P. de Jong[c], Geny M.M. Groothuis[a] and Peter Olinga[b]

[a]Division of Pharmacokinetics, Toxicology and Targeting, Department of Pharmacy, University of Groningen, The Netherlands

[b]Division of Pharmaceutical Technology and Biopharmacy, Department of Pharmacy, University of Groningen, The Netherlands

[c]Department of Surgery, Division of Hepato-Pancreatico-Biliary Surgery and Liver Transplantation, University Medical Center Groningen, University of Groningen, The Netherlands

Abstract

Recently, rat precision-cut liver slices (PCLS) were used to study the mechanisms of liver fibrosis and the effects of antifibrotic compounds in the early- and end-stage of liver fibrosis. Since results of animal experiments often are poorly predictive for the human situation, in the present study, human PCLS were used to study both stages of liver fibrosis and the effect of potential antifibrotic compounds. In addition, pathways that are activated in human PCLS during the onset of liver fibrosis were determined.

PCLS of healthy and cirrhotic human liver tissue were incubated for 48 and 24 hours respectively, during which viability of the PCLS was retained as judged by the ATP content, with compounds possessing antifibrotic activity in animal studies, such as the PDGF pathway inhibitors; imatinib, sorafenib and sunitinib and the TGFβ-pathway inhibitors; perindopril, valproic acid, rosmarinic acid, tetrandrine and pirfenidone. In addition, downstream inhibitors of Smad 3, Rac-1 and p38 Mapk were used in healthy human PCLS to elucidate the downstream mechanisms of the pathways involved in fibrosis in PCLS. Gene expression of HSP47, αSMA and PCOL1A1 and the protein expression of collagen 1 were determined as markers for fibrosis.

During incubation for 48 hours the gene expression of HSP47 and PCOL1A1 was increased in human PCLS of healthy liver, indicating the onset of fibrosis. Addition of PDGF-BB and TGF-β1 together further increased these fibrosis markers in human PCLS. Gene expression of PCOL1A1 was downregulated with sunitinib, valproic acid, rosmarinic acid, tetrandrine and pirfenidone, while col1 protein expression was downregulated by sorafenib, valproic acid and rosmarinic acid. SB203580, a specific inhibitor of p38-Mapk showed a marked decrease in HSP47 and PCOL1A1 gene expression, while downstream inhibitors of Smad 3 and Rac-1 showed no or only minor effects. In cirrhotic human PCLS the fibrosis markers were highly expressed but did not further increase during incubation. Sorafenib and rosmarinic acid were the only compounds that decreased the PCOL1A1 gene expression in cirrhotic human PCLS, all other compounds did not reduce any of the fibrosis markers.

In conclusion, human PCLS appear to be an adequate *ex vivo* model to study the early onset and end-stage of liver fibrosis. In healthy human PCLS, TGFβ-inhibitors are more effective to prevent the early onset of fibrosis than PDGF-inhibitors, which is in contrast to what was found in healthy rat PCLS. In addition, the p38 Mapk pathway seems to play an important role in the onset of fibrosis in human PCLS. In cirrhotic human PCLS most of the selected antifibrotic compounds had minor effects, again indicating possible species differences. This *ex vivo* model has the potential to be used to select those compounds that showed antifibrotic activity in animals, for further testing in patients.

Introduction

Liver fibrosis is considered a serious complication associated with chronic injury and is characterized by excessive deposition of extracellular matrix proteins. Research on the mechanism and potential pharmacotherapeutic treatment of liver fibrosis has been ongoing for decades and a considerable amount of knowledge about this disease has been acquired. However, despite these efforts, currently there is no antifibrotic drug available and liver transplantation is the only treatment for liver cirrhosis. Recently, precision-cut liver slices (PCLS) have been used as an *ex vivo* model for incipient and established fibrosis (1). This *ex vivo* model replicates most of the multicellular characteristics of the liver and antifibrotic efficacy of several putative anti-fibrotic drugs was studied in rat PCLS (2-4).

Particularly the possibility of using (healthy and cirrhotic) human liver tissue to study the mechanisms of fibrosis and to test antifibrotic drugs has the potential to become a great asset of the PCLS technique. Previously, it was shown that incubation of healthy human PCLS with CCl_4 resulted in induction of early hepatic stellate cell (HSC) activation (5). Furthermore, the antifibrotic compound pentoxifylline inhibited the induction of HSC activation in human PCLS (6). The aim of this study was to further investigate the use of human PCLS as a model for both the early onset and the end-stage of liver fibrosis, cirrhosis. The major pathways involved in liver fibrosis are the platelet-derived growth factor (PDGF) and the transforming growth factor beta (TGFβ) signaling pathway (7). Recently, we tested the effects of several antifibrotic compounds affecting these two pathways in both early and end-stage *ex vivo* models of liver fibrosis using rat PCLS. In the early onset model for rat liver fibrosis, antifibrotic compounds predominantly inhibiting the PDGF pathway (PDGF-inhibitors) showed antifibrotic effects, while antifibrotic compounds mainly inhibiting the TGFβ pathway (TGFβ-inhibitors) only slightly reduced the fibrosis markers tested (3). We concluded that the PDGF signaling pathway plays an important role in the early onset of liver fibrosis in rat PCLS, however the TGFβ-pathway seems to play a minor role during the early onset of liver fibrosis in rat PCLS (3). In addition, in the *ex vivo* model for established liver fibrosis, PCLS from fibrotic livers of rats 3 weeks after bile duct ligation (BDL), both PDGF- and TGFβ-inhibitors showed antifibrotic effects on gene- and protein level of fibrosis markers (4). In the current study, we aimed to investigate the effect of these inhibitors on the process of fibrosis in human PCLS. PDGF-inhibitors used in this study were the tyrosine kinase inhibitors imatinib, sorafenib and sunitinib, which showed antifibrotic efficacy both *in vivo* in rats and *in vitro* in rat and human HSC (8-10). As TGFβ-inhibitors, we used perindopril (angiotensin converting enzyme (ACE) inhibitor), valproic acid (histone deacetylase inhibitor), tetrandrine (upregulates smad7), rosmarinic acid and pirfenidone (antifibrotic compounds that inhibit TGFβ itself). All these compounds demonstrated antifibrotic effects in liver fibrosis *in vitro* in isolated mouse and rat HSC and *in vivo* in mice and rats (11-16). In addition, pirfenidone also showed antifibrotic effects *in vitro* in human HSC and *in vivo* in patients with advanced liver fibrosis (17,18).

To further study the downstream mechanisms of the pathways, which are involved in the early onset of liver fibrosis in human PCLS, downstream inhibitors of Smad 3, Rac-1 and p38 Mapk were used. Specific Inhibitor of Smad 3 (Sis3) is known to inhibit the TGFβ-dependent Smad 3 phosphorylation (19). Rac-1 is involved in the response to PDGF-β, as it is important for the activation of NADPH-

oxidase, which produces reactive oxygen species (ROS) that are necessary for PDGF to induce proliferation in HSC (20). To investigate the involvement of Rac-1 we used its specific inhibitor NSC23766 (21). P38 Mapk is involved in the regulation of collagen 1A1 gene expression and mRNA stability, and it can be activated by both PDGF and TGFβ (22). To study its involvement in the early onset of liver fibrosis in human PCLS we used SB203580 as a specific inhibitor of p38 Mapk (23). Using these inhibitors, it was shown that the P38 Mapk pathway plays an important role in liver fibrosis in both the early and end-stage, while Smad 3 phosphorylation and Rac-1 seemed to play a minor role in the fibrotic process in rat PCLS (24). In this current study, the roles of these pathways were investigated utilizing healthy human PCLS.

Materials and methods

Human liver tissue

For the study of the early onset of fibrosis, human liver tissue was obtained from patients after partial hepatectomy because of liver metastasis of colorectal carcinoma (PH-livers) or from liver tissue from multi-organ donors, remaining as surgical waste after split liver transplantation (TX), as described previously (25). Cirrhotic human liver tissue was obtained from explanted cirrhotic livers from patients undergoing liver transplantation. Characteristics of patients and donors of both healthy and cirrhotic human liver tissue are shown in table 1. The experimental protocols were approved by the Medical Ethical Committee of the University Medical Center Groningen.

Table 1: Human liver donor characteristics. PH is liver tissue after partial hepatectomy, TX is liver tissue remaining from donor liver after transplantation. PCOL1A1 is Pro-collagen 1A1 gene expression after 48 of incubation compared to slices directly after slicing (average fold induction +/- sem). NASH is Nonalcoholic Steatohepatitis, PFIC is Progressive Familial Intrahepatic Cholestasis and ITBL is Ischemic Type Biliary Lesions

Healthy		**Cirrhotic**	
No. of livers	27	No. of livers	10
PH/TX	10/17		
Female/Male	20/7	Female/Male	6/4
Age (median, range)	51 (10-82)	Age (median, range)	34 (1-59)
PCOL1A1 48h vs. 0h:			
*All donors	5.8 +/- 1.2	PCOL1A1 24h vs. 0h	0.7 +/- 0.1
*PH	5.8 +/- 2.3	Disease:	
*TX	5.6 +/- 1.4	Bile duct atresia	1
		Primary sclerosing cholangitis	1
		Acute liver failure	1
		Alcoholic liver cirrhosis	3
		cirrhosis NASH	1
		cirrhosis PFIC	1
		ITBL	1
		cirrhosis	1

Precision-cut liver slice experiments

Liver tissue obtained from PH-livers was perfused via veins at the cutting surface with cold University of Wisconsin (UW) organ preservation solution (DuPont Critical Care, Waukegab, IL, USA) immediately after excision (26). Liver tissue obtained from TX-livers was perfused with cold UW *in situ* before explantation and stored in cold UW until the liver was reduced. During reduction, the liver remained in ice-cold UW and after reduction, the liver tissue was stored in ice-cold UW solution until the start of the slicing procedure. Liver tissue from explanted human cirrhotic livers was also stored in ice-cold UW solution (< 12 hours) until the start of the slice experiments. Liver slices were prepared in ice-cold Krebs-Henseleit buffer supplemented with 25 mM D-glucose (Merck, Darmstadt, Germany), 25 mM $NaHCO_3$ (Merck), 10 mM HEPES (MP Biomedicals, Aurora, OH, USA) and saturated with carbogen (95% O_2/5% CO_2) using a Krumdieck tissue slicer as described before in detail (26). PCLS with a diameter of 5 mm and a thickness of 250 µm were incubated individually in 1.3 ml of Williams Medium E (with L-glutamine, Invitrogen, Paisly, Scotland) supplemented with 25 mM glucose and 50 µg/ml gentamycin (Invitrogen) at 37°C and under continuous supply of 95% O_2/5% CO_2 in 12-wells plates while gently shaken. After 1 hour of preincubation the slices were transferred to fresh medium and further incubated for 24 and 48 (healthy human PCLS) and for 24 (cirrhotic human PCLS) hours in the presence or absence of antifibrotic compounds. For the experiments conducted for 48 hours, after 24 hours the slices were transferred to new 12 wells plates with fresh medium containing the drug. The slices were incubated with a range of concentrations of the antifibrotic compounds which were shown to be effective in previous studies (human) in vitro or in animal studies in vivo (3,19,27,28): imatinib (1-10 µM) (Novartis, Basel, Switzerland), valproic acid (0.1-1 mM) (Sigma Aldrich, Zwijndrecht, Netherlands), perindopril (10 - 100 µM) (Sigma Aldrich), rosmarinic acid (120 – 270 µM) (Sigma aldrich), tetrandrine (1 - 10 µM) (Sigma aldrich), sunitinib (0.5 - 5 µM) (LC laboratories, Woburn, USA), sorafenib (0.5 - 2 µM) (LC laboratories), pirfenidone (0.5 – 2.5 mM) (Sigma Aldrich) and the specific Mapk inhibitor SB203580 (5, 10 µM) (Bioconnect, Huissen, The Netherlands), the SMAD 3 inhibitor Sis3 (0.3 – 3 µM) (Bioconnect) and the Rac1 inhibitor NSC23766 (5 – 50 µM) (Tocris Bioscience, Bristol, UK). Furthermore, healthy PCLS were incubated with the growth factors PDGF-BB (10 and 50 ng/ml) (Recombinant Human PDGF-BB, Peprotech, Bioconnect) and TGF-β1 (1 – 5 ng/ml) (hTGF-β1, Roche Applied Science, Mannheim, Germany). Stock solutions of the compounds were prepared in water or DMSO and diluted in the culture medium with a final concentration of the solvent of ≤ 1%. In order to prevent aspecific binding of the TGF-β1 to the walls of the plates, the 12 well plates were pretreated with 10% BSA in milli Q water solution for 20 minutes, whereafter the solution was removed and plates were dried at room temperature. All incubations were performed in triplicate (using 3 slices incubated individually in separate wells) and were repeated with random livers from 3-5 different patients.

Viability

After incubation, slices were transferred to 1 ml sonication solution, containing 70% ethanol and 2 mM EDTA, snap frozen in liquid nitrogen and stored at -80°C. To determine the cell viability, the samples were thawed on ice and ATP levels were measured in the supernatant of samples homogenized for 45 sec in a Mini-BeadBeater-8 (Biospec, Bartlesville, OK, USA) and centrifuged for 2 minutes at 16.000 g, using the ATP bioluminescence kit (Roche diagnostics, Mannheim, Germany).

ATP values (pmol) were normalized to the total protein content (µg) of the slice estimated by Lowry (BIO-rad RC DC Protein Assay) (Bio Rad, Veenendaal, The Netherlands) (29) as described previously (30).

Gene expression

To determine the antifibrotic effect of the drugs on the gene expression of the fibrosis markers heat shock protein 47 (HSP47), alpha smooth muscle actin (αSMA) and pro-collagen 1A1 (PCOL1A1), the mRNA expression was determined using Real-Time PCR. The triplicate slices were pooled and snap frozen and total RNA was isolated with the use of the RNeasy Mini Kit (Qiagen, Venlo, The Netherlands). The amount of isolated RNA was measured with the ND-1000 spectrophotometer (Fisher Scientific, Landsmeer, The Netherlands). Reverse transcriptase was performed with 2 µg RNA using Reverse Transcription System (Promega, Leiden, The Netherlands). The RT-PCR reaction was performed in the Eppendorf mastercycler gradient at 25 °C for 10 minutes, 45 °C for 60 minutes and 95 °C for 5 minutes. The gene expression of HSP47, αSMA and PCOL1A1 was determined using the following primers (50 µM) en probes (5 µM) (Sigma aldrich); for HSP47 5'- GCCCACCGTGGTGCCGCA -3'(F), 5'- GCCAGGGCCGCCTCCAGGAG -3'(R), 5'- CTCCCTCCTGCTTCTCAGCG -3'(probe); for αSMA 5'- AGGGGGTGATGGGTGGGAA -3'(F), 5'- ATGATGCCATGTTCTATCGG -3'(R), 5'- GGGTGACGAAGCACAGAGCA -3' (probe); for PCOL1A1 5'- CAATCACCTGCGTACAGAACGCC -3'(F), 5'- CGGCAGGGCTCGGGTTTC -3'(R), 5'- CAGGTACCATGACCGAGACGTG -3'(probe) and the qPCR mastermix plus (Eurogentec, Maastricht, The Netherlands). The Real-Time PCR reaction was performed in a 7900HT Real Time PCR (Applied Biosystems, Bleiswijk, The Netherlands) with 1 cycle of 10 minutes at 95 °C and 45 cycles of 15 seconds at 95 °C and 1 minute at 60 °C. Ct values were corrected for the Ct values of the housekeeping gene *Gapdh* (ΔCt) (5'- ACCAGGGCTGCTTTTAACTCT -3'(F), 5'- GGTGCCATGGAATTTGCC -3'(R), 5'- TGCCATCAATGACCCCTTCA -3'(probe)) and compared with the control (ΔΔCt). Results are displayed as fold induction of the gene ($2^{-\Delta\Delta Ct}$). The gene expression of PDGF-BB and TGF-β1 was determined using the primers (50µM) 5'- CTGGCATGCAAGTGTGAGAC-3' (F), 5'-CGAATGGTCACCCGAGTTT-3' (R) (PDGF-β) and 5'- GCAGCACGTGGAGCTGTA-3' (F), 5'-CAGCCGGTTGCTGAGGTA-3' (R) (TGF-β1) and the sybr green mastermix (GC Biotech, Alphen aan de Rijn, The Netherlands). The Real Time PCR reaction was performed on a 7900HT Real Time PCR (Applied Biosystems) with 1 cycle of 10 minutes at 95°C and 45 cycles of 15 seconds at 95°C and 25 seconds at 60°C with a dissociation stage thereafter (95 ºC, 15 sec: 60 ºC, 15 sec: 95 ºC, 15 sec). Ct values were corrected for the Ct values of the housekeeping gene Gapdh (ΔCt) (5'- CGCTGGTGCTGAGTATGTCG -3'(F), 5'- CTGTGGTCATGAGCCCTTCC -3'(R) (Gapdh) and compared with the control (ΔΔCt). Results are displayed as fold induction of the gene (2-ΔΔCt).

Western blot

Collagen 1 protein expression was determined by western blot. Following treatment, the triplicate slices were pooled and snap frozen. The slice tissue was lysed for 1 hour on ice in 250 µl of RIPA buffer (1 Protease inhibitor cocktail tablet (Boehringer Ingelheim, Alkmaar, The Netherlands)), in 10 ml of 50 mM Tris/HCl pH7.5, 150 mM NaCl, 1% Igepal CA-630, 0.5% sodiumdeoxycholaat, 0.1% SDS). The tissue was homogenized on ice by a Potter homogenizer and centrifuged for 1 hour at 4°C at

16.000 g. Protein concentrations were determined in the supernatant using a Biorad DC protein assay according to the protocol provided by the manufacturer. Lysates were diluted 4 fold in SDS sample buffer (50 mM TrisHCl pH 6.8, 2% SDS, 10% glycerol, 5% β-mercaptoethanol, 0.05% Bromophenol Blue) and boiled for 2 minutes. 100 µg of protein was size fractionated on a 7.5 % sodium dodecyl sulphate polyacrylamide gel by electrophoresis and transferred to an activated polyvinylidene difluoride membrane (Biorad). After blocking for 1 hour in Tris buffered saline supplemented with 5 % Blocking Grade Powder (Biorad) and 0.1 % Tween-20, immunodetection of collagen-1 (1:1000, Rockland Immunochemicals, Gilbertsville, PA, USA) was performed. Binding of the antibody was determined using Horseradish Peroxidase conjugated secondary goat anti-rabbit and tertiary rabbit anti-goat antibody (DAKO, Heverlee, Belgium). Addition of Western Lightning Plus-ECL, (Perkin Elmer, Groningen, The Netherlands) to the membrane resulted in light emission captured on an imaging system. Results were displayed as relative values compared to the control.

Statistics

3-5 livers were used for each experiment, using slices in triplicate from each liver. The results are expressed as means ± S.E.M. The results of the treatments were compared to the untreated controls using the paired, one-tailed Student's-t-test. A *p*-value <0.05 was considered significant. Real-time PCR results were compared using the mean ΔΔCt values.

Results

Viability and expression of fibrosis markers during incubation of healthy and cirrhotic human PCLS

Incubation up to 24 hours of healthy and cirrhotic human PCLS increased the viability as assessed by ATP compared to slices directly after slicing (0 hours) (fig. 1A). Directly after slicing, human PCLS have a low ATP and 1 hour preincubation restores it to normal values, whereafter it remains constant for at least 24 h (26). After 24 hours the ATP content of healthy human PCLS was 7.3 +/- 0.6 pmol/g protein (n=23) and of cirrhotic human PCLS 2.9 +/- 0.5 pmol/µg protein (n=10) (fig. 1B). After 48 hours of incubation the ATP content of healthy human PCLS was somewhat decreased by 28% compared to 24 hours (fig. 1A). The PCLS from healthy livers were cultured for 48 hours but the cirrhotic human liver slices were cultured for 24 hours instead of 48 hours, since the amount of RNA that could be isolated was already low after 24 hours compared to cirrhotic human PCLS at the start of the incubation period. In healthy PCLS, the αSMA gene expression was decreased after 24 hours, but increased again significantly between 24 and 48 hours, while HSP47 gene-expression was increased at all time points compared to 0 hours (fig. 1B). The gene-expression of PCOL1A1 in healthy PCLS was unchanged after 24 hours but was 4.4 fold increased after 48 hours of incubation compared to slices directly after slicing (fig. 1B). Since αSMA was not increased after 48 hours in healthy human PCLS compared to 0 hours, we focused on the effect of the antifibrotic compounds in healthy human PCLS on the gene expression of HSP47 and PCOL1A1.

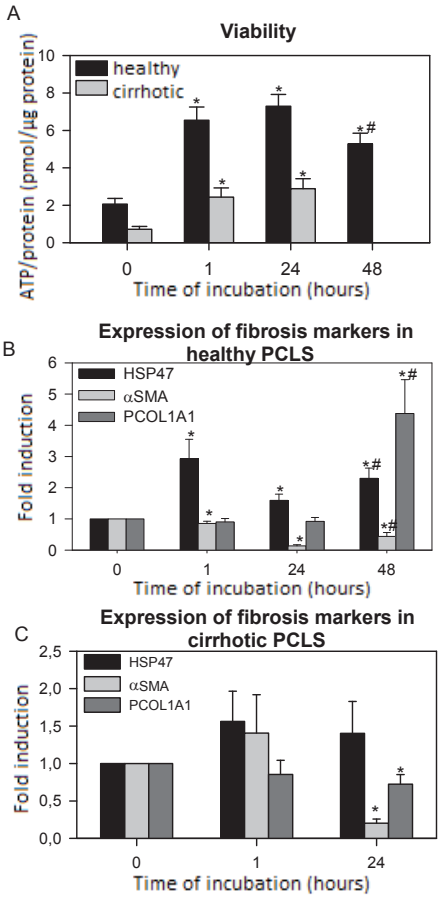

Fig.1 The effect of incubation on the viability and gene expression of fibrosis markers of healthy (n=23) and cirrhotic (n=10) human PCLS. Viability was measured by ATP content (A). Gene-expression of HSP47, αSMA and PCOL1A1 of healthy human PCLS (B) and cirrhotic human PCLS (C) after incubation. *p<0.05 vs 0h; #p<0.05 vs 24h.

In cirrhotic human PCLS incubated for 24 hours, the gene-expression of αSMA and PCOL1A1 decreased to 24 and 66 % respectively compared to 0 hours, while HSP47 was not significantly changed (fig. 1C). We tested the effect of the antifibrotic compounds on the expression of these three fibrosis markers in cirrhotic human PCLS.

The effect of anti-fibrotic drugs in fibrosis onset and in cirrhosis in human PCLS

The concentrations of PDGF-inhibitors incubated with healthy human PCLS were non-toxic, as determined by the ATP content of the slices, except for 10 µM of imatinib, which caused a significant decrease in slice viability of 46 % (data not shown). Sunitinib decreased the gene expression of HSP47

and PCOL1A1 at all concentrations (fig. 2A). In contrast, sorafenib had no effect on the gene expression of the fibrosis markers (fig. 2A). Also imatinib did not show an effect on the fibrosis markers except for a small but significant decrease of HSP47 expression at the lowest concentration (1 µM) (fig. 2A).

In cirrhotic human PCLS, the PDGF-inhibitor sunitinib was not toxic and imatinib and sorafenib decreased the viability of the slices only slightly, but significantly, by 13 % at the highest concentrations used compared to control cirrhotic human PCLS incubated for 24 hours (data not shown). Among the PDGF-inhibitors, only sorafenib significantly decreased the gene expression of HSP47 and PCOL1A1 in the cirrhotic human PCLS to 39 and 38 % respectively, but αSMA expression was not affected by any of the PDGF inhibitors. (fig. 2B).

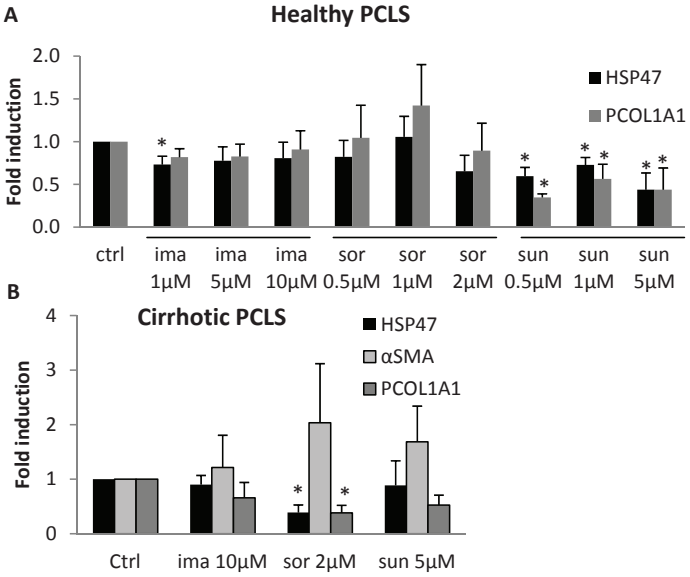

Fig.2 The effect of PDGF-inhibitors imatinib (ima), sorafenib (sor) and sunitinib (sun) on the gene-expression of HSP47 and PCOL1A1 of healthy human PCLS (A) and on the gene-expression of HSP47, αSMA and PCOL1A1 of cirrhotic human PCLS (B) after incubation for 48 hours. n=4-5. *p<0.05 vs control slices incubated without inhibitors

The concentrations of the TGFβ-inhibitors that were used in healthy PCLS were non-toxic, except for 1 mM of valproic acid, it decreased the ATP content by 37 % and 1 and 2.5 mM of pirfenidone decreased the ATP content by 31 and 51 % (data not shown), however Gapdh expression was constant in PCLS with these ATP decreasing compounds. In healthy human PCLS, the gene expression of HSP47 was decreased by valproic acid (at 0.5 and 1 mM), whereas the gene expression of PCOL1A1 was decreased by valproic acid and pirfenidone at all concentrations and by rosmarinic acid and tetrandrine at the two highest concentrations, while perindopril had no effect on both of these fibrosis markers (fig. 3A).

The concentrations of TGFβ-inhibitors were not toxic in the cirrhotic human PCLS (data not shown). In general the TGFβ-inhibitors had no significant influence on the expression of the fibrosis markers, only rosmarinic acid decreased the gene expression of PCOL1A1 in cirrhotic PCLS (fig. 3B).
The effect of incubation and of the antifibrotic compounds on the protein expression of collagen 1 (col1) was determined by western blot in human PCLS during the early onset of liver fibrosis. During incubation for 1 and 24 hours, the col1 protein expression was decreased compared to slices directly after slicing (fig. 4A), but increased again between 24 and 48 hours of incubation, although it did not reach the same level as the tissue directly after slicing (fig. 4A). Among the PDGF-inhibitors, sorafenib significantly decreased the col1 protein expression and in the group of the TGFβ-inhibitors, valproic acid and rosmarinic acid also decreased the col1 protein expression in human PCLS (fig. 4B). Due to the limited amount of cirrhotic human tissue, the collagen I protein expression could not be determined in cirrhotic human PCLS.

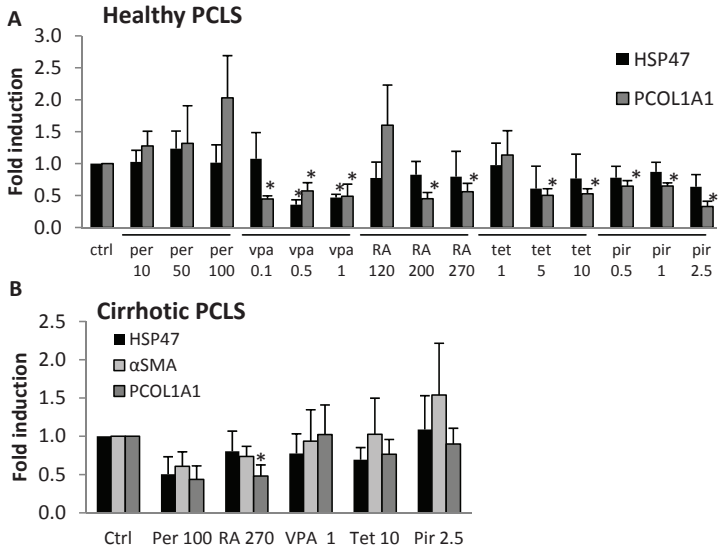

Fig.3 The effect of TGFβ-inhibitors perindopril (per, μM), valproic acid (vpa, mM), rosmarinic acid (RA, μM), tetrandrine (tet, μM) and pirfenidone (pir, mM) on the gene-expression of HSP47 and PCOL1A1 of healthy human PCLS (A) and cirrhotic human PCLS (B) after incubation with TGFβ-inhibitors for 48 hours. n=3-5. *p<0.05 vs 48h.

The effect of PDGF, TGFβ and downstream inhibitors of p38 Mapk, Smad 3 and Rac-1 during incubation with healthy human PCLS

During control incubation the gene expression of PDGF was increased after 24 and 48 hours and the gene expression of TGFβ was increased after 48 hours (fig. 5A). To evaluate if the fibrogenic pathways could be stimulated further in healthy human PCLS by these pro-fibrotic growth factors, PCLS were incubated in the presence of PDGF-BB and TGF-β1. Addition of 10 and 50 ng/ml PDGF-BB did not change the gene expression of the fibrosis markers and TGF-β1 increased only the PCOL1A1 gene expression at all concentrations (1-5 ng/ml) up to 2 fold but this increase was only significant at the lowest concentration of 1 ng/ml (fig. 5B, C). However, if both growth factors were added

together, the gene expression of HSP47 and PCOL1A1 was significantly increased 1.7 and 2.4 fold respectively (fig.5D). All concentrations of Sis3, SB203580 and NSC23766 incubated with healthy PCLS were non-toxic (data not shown). The p38 Mapk inhibitor, SB203580, decreased the gene expression of both HSP47 and PCOL1A1 at all concentrations, whereas Sis3 only slightly decreased the gene expression of HSP47, but only with the lowest concentration used, while NSC23766 only decreased the gene expression of HSP47 at the highest concentration of 25 µM (fig. 5E).

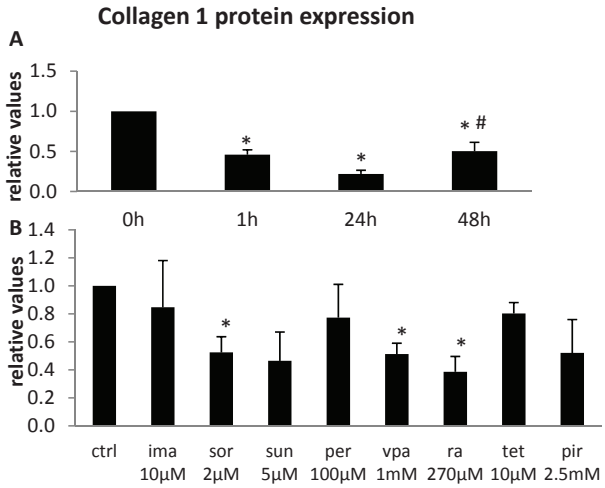

Fig. 4. Protein expression of collagen 1 (col1) in healthy control human PCLS incubated up to 48 hours in absence (A) and presence of 10 µM imatinib (ima), 2 µM sorafenib (sor), 5 µM sunitinib (sun), 100 µM perindopril (per), 1mM valproic acid (vpa),270 µM rosmarinic acid (ra), 10 µM tetrandrine (tet) and 2.5 mM pirfenidone (pir) (B). ctrl: control 48 hours. n=3. *p<0.05 vs 0h, #p<0.05 vs. 24h (A), *p<0.05 vs. ctrl (B).

Discussion

Previously, it was shown that incubation of rat PCLS for 48 hours resulted in an increased expression of fibrosis markers, which indicated that an early onset of liver fibrosis takes place in these PCLS (3,31). In addition, we showed that rat PCLS, prepared from healthy as well as fibrotic rat livers successfully reproduced the *in vivo* antifibrotic effects of drugs on the early onset and end-stage of liver fibrosis (2-4). Although several drugs have been shown to exert antifibrotic effects in animals studies, none of them reached the market due to lack of efficacy in man (7), reflecting the lack of translational potential of animal models. To close the gap between the preclinical efficacy studies of antifibrotic drugs in animal

experiments and the effect of these antifibrotic drugs in patients, we aimed in this study to investigate if human PCLS could be such a translational model for the early onset and end-stage of liver fibrosis.

Like in rat PCLS, the gene expression of HSP47 and PCOL1A1 was increased in healthy human PCLS after 48 hours of incubation, albeit to a lesser extend (3). Like in rat PCLS, αSMA gene expression was decreased after 24 and increased again after 48 hours in human PCLS, however the expression at 48

hours did not yet increase above the levels of not incubated PCLS. These results are in line with those of Van de Bovenkamp *et al.*, who also found an increase in PCOL1A1 gene expression and an initial decrease followed by an increase of αSMA gene expression in healthy human PCLS after 48 hours of incubation (6). They suggested that this may not solely point to a loss of expression in HSC, but also

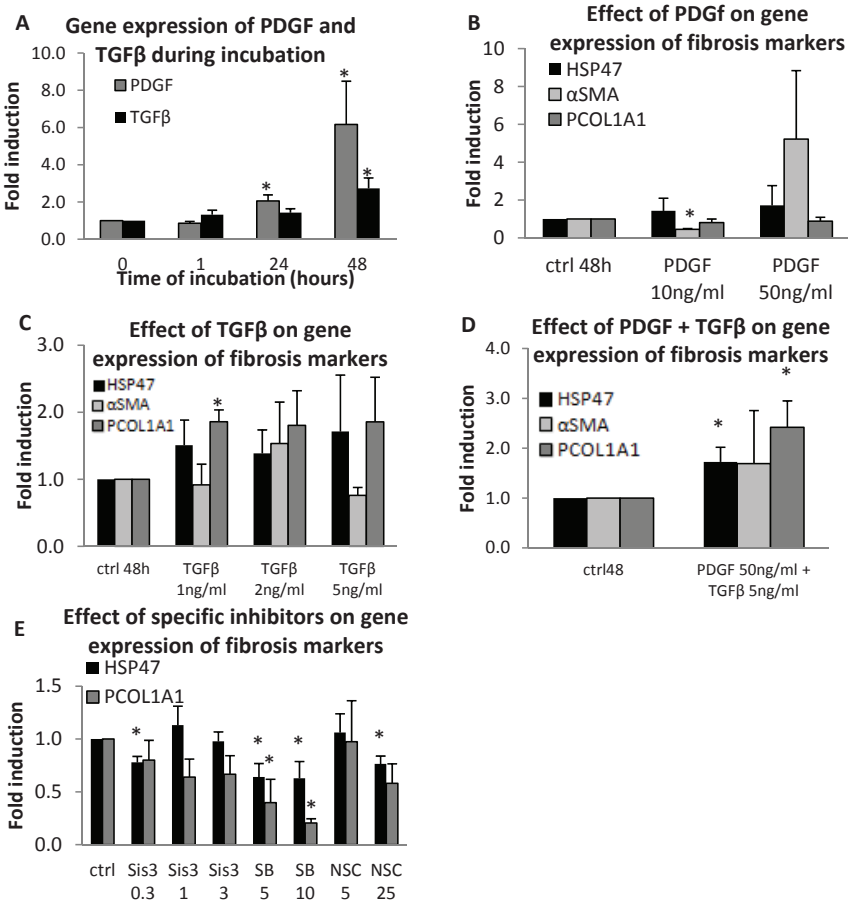

Fig.5 The gene expression of PDGF and TGFβ during incubation (n=5) (A) and gene-expression of HSP47, αSMA and PCOL1A1 of healthy human PCLS after addition of PDGF-BB (B), TGFβ-1 (C) and PDGF-BB + TGFβ-1 (D) for 48 hours. The effect of downstream inhibitors Sis3, SB203580 and NSC23766 on gene expression of HSP47 and PCOL1A1 (E). n= 4-5. *p<0.05 vs ctrl 48h. TGFβ: transforming growth factor β; PDGF: plateled derived growth factor; Sis3: specific inhibitor of smad 3 (μM); SB: SB203580 (μM); NSC: NSC23766 (μM).

reflects a loss of expression in (myo)fibroblast whereas synaptophysin, which is a specific marker for HSC, was not decreased (6).

In contrast to healthy human PCLS, culturing of PCLS from cirrhotic human livers did not increase the gene expression of HSP47 and even decreased PCOL1A1 and αSMA gene expression during culture.

These results are in line with a study of Guyot *et al.*, who showed a decrease in αSMA protein expression determined in immunohistochemical sections after culture of cirrhotic human PCLS for 1 week (32) and could indicate that the HSC re-acquire a quiescent phenotype or that myofibroblasts are eliminated (32). This is supported in the present study by the decrease of PCOL1A1 gene expression found in cirrhotic human livers.

However, in fibrotic rat PCLS, obtained from rats 3 weeks after bile duct ligation, Pcol1A1 gene expression was increased after 24 hours of culturing (4). This may be due to the different etiology of the fibrosis between rat and human or due to the difference in severity of the fibrotic disease, as the cirrhotic human livers are from patients with terminal liver disease. But it could also indicate a species difference in the effect of incubation of PCLS between rat and human. In addition, we cannot exclude that the gene expression of these markers will increase if the slices are incubated for 48 hours instead of 24 hours, as was observed in fibrotic rat PCLS. Experiments with longer incubation times are currently ongoing to elucidate this.

During the early onset of fibrosis in human PCLS, the TGFβ-inhibitors seemed more effective in decreasing the expression of the fibrosis markers than the PDGF-inhibitors. Among the PDGF-inhibitors only sunitinib had an antifibrotic effect, but most of the TGFβ-inhibitors, valproic acid, rosmarinic acid, tetrandrine and pirfenidone, decreased the PCOL1A1 gene expression. This is in contrast with the results previously found in the early onset of liver fibrosis in rat PCLS, where PDGF-inhibitors were more effective in inhibiting fibrosis markers than the TGFβ-inhibitors. This finding is in concordance with the finding that the TGF-β1 expression was not increased during incubation in rat PCLS (3) but increased in human PCLS (Fig 5A). Thus, as mentioned above, not only during control incubations of PCLS, but also during incubation of PCLS with antifibrotic compounds, species differences were observed. This might explain why a lot of potential antifibrotic compounds that showed effects in rats were not effective in patients during clinical trials.

In the cirrhotic human PCLS, the antifibrotic compounds were less effective than in the healthy human PCLS. Also here, the shorter incubation time of the cirrhotic PCLS or the severity of the disease might be an explanation for the difference in efficacy of antifibrotic compounds in human PCLS in end-stage fibrosis compared to the early onset of fibrosis.

In detail, although imatinib was the most potent inhibitor of the fibrosis markers in both normal and fibrotic rat PCLS, it only slightly decreased the HSP47 expression in healthy human PCLS, but had no significant effect on the αSMA and PCOL1A1 gene expression and on all 3 fibrosis markers in cirrhotic human PCLS. It is noteworthy that no clinical study for liver fibrosis has been reported with imatinib and in pulmonary fibrosis imatinib had no effect (7). However in LX2 cells (an immortalized human HSC line), imatinib attenuated the collagen 1A1 gene expression, while αSMA expression was not changed (33), therefore in the case of imatinib LX2 cells are not a good predictor of the antifibrotic effect in human fibrosis.

Similarly, the PDGF-inhibitor sorafenib had no effect on the early onset of gene expression of the fibrosis markers in human PCLS, although it was effective in reducing the fibrosis markers in normal and fibrotic rat PCLS (3,4). However sorafenib significantly reduced the protein expression of col1 protein. In addition, in cirrhotic human PCLS sorafenib seemed to have some antifibrotic effect as it decreased the HSP47 and PCOL1A1 gene expression. Also in LX2 cells sorafenib showed potential antifibrotic effects as it down-regulated the gene and protein expression of Collagen 1A (34).

Together these results suggest that sorafenib may be effective as antifibrotic compound for patients with established liver fibrosis.

Sunitinib was the only PDGF-inhibitor tested that decreased the gene expression of the fibrosis markers in the early onset of fibrosis in human PCLS, but it did not affect the col1 protein expression, which was comparable with the effects of sunitinib in rat PCLS (3). However, sunitinib had no effect on the fibrosis markers in human cirrhotic PCLS, while in fibrotic rat PCLS it down-regulated the fibrosis markers (4). This may indicate species differences in the efficacy of this PDGF-inhibitor mainly inhibiting the PDGF pathway, and also no positive antifibrotic clinical studies have been described for this compound. Sunitinib therefore could be successful in the early onset of fibrosis but seems to be ineffective in end-stage liver fibrosis.

The TGFβ-inhibitor perindopril did not have a significant effect on the gene expression of fibrosis markers and the COL1 protein expression in both healthy and cirrhotic human PCLS. This is in line with a clinical study by Yoshiji et al. where perindopril did not show an antifibrotic effect in patients after 48 months of treatment (35).

In healthy human PCLS valproic acid significantly reduced the onset of fibrosis as judged by the decreased gene expression of HSP47 and PCOL1A1 and the COL1 protein expression after 48 hours of incubation, but in cirrhotic human PCLS no antifibrotic effects were observed. In a model of the early onset of liver fibrosis, Watanabe *et al.* incubated human HSC (LI90 cell line) activated by TGFβ with 1mM valproic acid and showed a decrease in collagen 1A1 gene and protein expression and a decrease in the number of αSMA fibers (36). This may indicate that valproic acid is active in the early onset of human liver fibrosis. Future studies in PCLS with other promising HDAC inhibitors will reveal their use in liver fibrosis (37).

The TGFβ-inhibitor rosmarinic acid showed clear antifibrotic effects in both healthy and cirrhotic human PCLS, since it significantly decreased the Pcol1a1 gene expression. Also, col1 protein expression was decreased in healthy human PCLS. To the best of our knowledge, until now no studies on the antifibrotic effects of rosmarinic acid in human liver fibrosis have been published. In fibrotic rat PCLS, rosmarinic acid decreased the fibrosis markers, however in normal rat PCLS, rosmarinic acid had no antifibrotic effect (3,4). From our positive results in human PCLS we concluded that antifibrotic effects of rosmarinic acid in human liver fibrosis may be expected.

Like most TGFβ-inhibitors, tetrandrine and pirfenidone reduced the onset of liver fibrosis, as they decreased the gene expression of PCOL1A1 in healthy human PCLS after 48 hours of incubation. Both the non-toxic (0.5 mM) and toxic (1 and 2.5 mM) concentrations of pirfenidone were effective. In rat PCLS, tetrandrine also had this ameliorating effect on the early phase of fibrosis (3), in contrast to pirfenidone that did not change fibrosis markers during the onset of fibrosis. Both compounds showed no toxicity and had no effect in human cirrhotic PCLS, this in contrast to the studies in rat fibrotic PCLS, where they both reduced fibrosis. No studies with human liver cells or clinical studies with fibrotic patients were reported for tetandrine. Pirfenidone was tested in a study with patients with advanced liver fibrosis, where pirfenidone treatment (twelve months) decreased the gene- and protein expression of collagen 1a, TGFβ and TIMP-1, measured in liver biopsies (18). Pirfenidone tended to decrease the col1 protein content in human PCLS. In addition, *in vitro* in human in LX-2 cells, pirfenidone decreased αSMA and col1 gene expression (17). Our results of pirfenidone in the early onset model are in line with the antifibrotic effect in patients. However pirfenidone, like most

other inhibitors had no effect on fibrosis markers in cirrhotic human PCLS. It cannot be excluded that 24 hour treatment may not be long enough to establish an effect in these slices.

In addition to elucidating the effects of antifibrotic compounds in the human PCLS, we wanted to determine which downstream mechanisms of the pathways play an important role during fibrogenesis in healthy human PCLS. First, it was found that both PDGF and TGFβ expression were increased, indicating that both pathways may be activated during incubation. Subsequently we investigated whether the onset of fibrosis in healthy human PCLS can be further stimulated with either PDGF-BB or TGF-β1 or both growth factors together. Neither PDGF-BB nor TGF-β1 showed a clear effect on the fibrosis markers, while addition of both growth factors together resulted in a synergistic increase of the gene expression of fibrosis markers in PCLS. This in contrast with the results obtained in rat PCLS, where both growth factors alone increased the fibrosis markers considerably, but where TGFβ expression was not increased during incubation (3). This may be due to the fact that in human PCLS fibrosis pathways are already activated because of the (long) operation procedure, since in rats the liver is excised directly after the rat is anaesthetized, or due to an inherent species differences. The healthy human PCLS were however sensitive to further activation during culture, since their gene expression of PDGF-BB and TGF-β1 were increased after 48 hours of culture compared to 0 hour of incubation.

In addition, the effects of downstream inhibitors of p38-Mapk (SB203580), Smad 3 (Sis3), an enzyme in the TGFβ pathway (19) and Rac-1 (NSC23766), which activates NADPH oxidase that is necessary for PDGF to activate HSC (20), were investigated in healthy human PCLS to elucidate the specific mechanisms of the induced fibrosis in more detail.

P38-Mapk is involved in proliferation of HSC and can be activated by both PDGF and TGFβ as was previously found in rat HSC (22). Inhibition of p38-Mapk caused a marked decrease in HSP47 and PCOL1A1 gene expression in PCLS of healthy human livers (Fig. 5E). Inhibition of Smad3 by Sis3 and Rac-1 by NSC23766 had minimal effects, as was also shown before in rat PCLS (24). It seems that like in rat PCLS, the p38-Mapk pathway plays an important role in the early onset of liver fibrosis in human PCLS. Although it is known that P38-Mapk can be activated by ROS (38) and that the PCLS are cultured under high oxygen concentration, it is unlikely that the p38 Mapk pathway is activated by ROS because until now there are no other indications of ROS production, e.g. thiobarbituric acid reactants (TBAR) production, in liver slices (unpublished data). Together with the finding that the TGFβ pathway inhibitors attenuated the early onset of fibrosis in human PCLS, but that Smad3 inhibition did not decrease the fibrosis markers in PCLS, the inhibition of fibrosis markers by inhibition of p38 Mapk could indicate that in fibrogenesis in human PCLS the TGFβ pathway is non-Smad related, but p38 Mapk related. The results of Varela-Rey et al. support this, since they showed that the TGFβ-induced increase in col1a1 gene expression is prevented by SB203580 the inhibitor of p38 Mapk (39). Rac-1 may play a minor role in the PDGF pathway during fibrosis in PCLS, although it cannot be excluded that the concentration of both Sis3 and NSC23766, albeit effective at these concentrations *in vitro* in fibroblasts and HSC respectively, could have been too low to be effective, possibly due to metabolism of the compound by the liver slices. Therefore we are currently performing studies with higher concentrations of these downstream inhibitors. In addition, we are planning to determine Smad 3 phosphorylation to elucidate whether the Smad related TGFβ pathway is activated in PCLS.

In conclusion, both the early onset and end-stage of liver fibrosis, cirrhosis, can be reproduced in human PCLS by using healthy and cirrhotic human tissue respectively. The antifibrotic compounds acting on the TGFβ pathway are more effective in the early onset of fibrosis in human PCLS compared to the antifibrotic compounds acting predominantly on the PDGF pathway, indicating a more important role for the TGFβ pathway. This is in contrast to what was found in healthy rat PCLS, where the PDGF pathway plays a more prominent role and PDGF-inhibitors appeared more effective in the onset of fibrosis. This could indicate a species difference in the fibrosis pathways involved in the early onset of fibrosis in PCLS. However, as it is well known that species differences in drug metabolism, inhibition and induction are prominent (40), different pharmacokinetic properties in rat and man of the tested compounds may also contribute to the different results in rat and human PCLS.
Furthermore, in human PCLS the p38 Mapk pathway plays an important role during the onset of fibrosis. Finally, cirrhotic human PCLS are a promising model for end-stage liver fibrosis in humans. In cirrhotic human PCLS most of the antifibrotic compounds that show antifibrotic activity in animal studies had minimal effects, which may explain why these compounds have not reached the market as effective antifibrotic drugs. Therefore these cirrhotic human PCLS are a promising translational model to predict the efficacy of new antifibrotic compounds.

Acknowledgement
The authors would like to thank all the transplantation coordinators and surgeons at University Medical Centre Groningen for providing human liver samples. We also thank Marina de Jager, Miriam Langelaar-Makkinje, Marjolijn Merema, Sylvia Blomsma and Patricia Robbe for their help in generating human PCLS.

References

1. Westra I M, Pham B T, Groothuis G M, Olinga P. Evaluation of fibrosis in precision-cut tissue slices. Xenobiotica 2012; 43: 98-112.

2. van de Bovenkamp M, Groothuis G M M, Meijer D K F, Olinga P. Precision-cut fibrotic rat liver slices as a new model to test the effects of anti-fibrotic drugs in vitro. J Hepatol 2006; 45: 696-703.

3. Westra I M, Oosterhuis D, Groothuis G M M, Olinga P. Precision-cut liver slices as a model for the early onset of liver fibrosis to test anti-fibrotic drugs. Toxicol Appl Pharmacol 2014; 274: 328-38.

4. Westra I M, Oosterhuis D, Groothuis G M M, Olinga P. The effect of antifibrotic drugs in rat precision-cut fibrotic liver slices. PLoS One 2014; 9(4):e95462.

5. van de Bovenkamp M, Groothuis G M, Meijer D K, Slooff M J, Olinga P. Human liver slices as an in vitro model to study toxicity-induced hepatic stellate cell activation in a multicellular milieu. Chem Biol Interact 2006; 162: 62-9.

6. van de Bovenkamp M, Groothuis G M, Meijer D K, Olinga P. Liver slices as a model to study fibrogenesis and test the effects of anti-fibrotic drugs on fibrogenic cells in human liver. Toxicol In Vitro 2008; 22: 771-8.

7. Schuppan D, Kim Y O. Evolving therapies for liver fibrosis. J Clin Invest 2013; 123: 1887-901.

8. Yoshiji H, Noguchi R, Kuriyama S et al. Imatinib mesylate (STI-571) attenuates liver fibrosis development in rats. Am J Physiol Gastrointest Liver Physiol 2005; 288: G907-13.

9. Wang Y, Gao J, Zhang D, Zhang J, Ma J, Jiang H. New insights into the antifibrotic effects of sorafenib on hepatic stellate cells and liver fibrosis. J Hepatol 2010.

10. Tugues S, Fernandez-Varo G, Munoz-Luque J et al. Antiangiogenic treatment with sunitinib ameliorates inflammatory infiltrate, fibrosis, and portal pressure in cirrhotic rats. Hepatology 2007; 46: 1919-26.

11. Yoshiji H, Kuriyama S, Noguchi R et al. Combination of interferon-beta and angiotensin-converting enzyme inhibitor, perindopril, attenuates the murine liver fibrosis development. Liver International 2005; 25: 153-61.

12. Mannaerts I, Nuytten N R, Rogiers V, Vanderkerken K, van Grunsven L A, Geerts A. Chronic administration of valproic acid inhibits activation of mouse hepatic stellate cells in vitro and in vivo. Hepatology 2010; 51: 603-14.

13. Li G S, Jiang W L, Tian J W, Qu G W, Zhu H B, Fu F H. In vitro and in vivo antifibrotic effects of rosmarinic acid on experimental liver fibrosis. Phytomedicine 2010; 17: 282-8.

14. Di Sario A, Bendia E, Baroni G et al. Effect of pirfenidone on rat hepatic stellate cell proliferation and collagen production. J Hepatol 2002; 37: 584-91.

15. Garcia L, Hernandez I, Sandoval A et al. Pirfenidone effectively reverses experimental liver fibrosis. J Hepatol 2002; 37: 797-805.

16. Hsu Y, Chiu Y, Cheng C, Wu C, Lin Y, Huang Y. Antifibrotic effects of tetrandrine on hepatic stellate cells and rats with liver fibrosis. J Gastroen Hepatol 2007; 22: 99-111.

17. Zhao X Y, Zeng X, Li X M, Wang T L, Wang B E. Pirfenidone inhibits carbon tetrachloride- and albumin complex-induced liver fibrosis in rodents by preventing activation of hepatic stellate cells. Clin Exp Pharmacol Physiol 2009; 36: 963-8.

18. Armendariz-Borunda J, Islas-Carbajal M C, Meza-Garcia E et al. A pilot study in patients with established advanced liver fibrosis using pirfenidone. Gut 2006; 55: 1663-5.

19. Jinnin M, Ihn H, Tamaki K. Characterization of SIS3, a novel specific inhibitor of Smad3, and its effect on transforming growth factor-beta1-induced extracellular matrix expression. Mol Pharmacol 2006; 69: 597-607.

20. Choi S S, Sicklick J K, Ma Q et al. Sustained activation of Rac1 in hepatic stellate cells promotes liver injury and fibrosis in mice. Hepatology 2006; 44: 1267-77.

21. Gao Y, Dickerson J B, Guo F, Zheng J, Zheng Y. Rational design and characterization of a Rac GTPase-specific small molecule inhibitor. Proc Natl Acad Sci U S A 2004; 101: 7618-23.

22. Parsons C J, Takashima M, Rippe R A. Molecular mechanisms of hepatic fibrogenesis. J Gastroenterol Hepatol 2007; 22 Suppl 1: S79-84.

23. Cuenda A, Rouse J, Doza Y N et al. SB 203580 is a specific inhibitor of a MAP kinase homologue which is stimulated by cellular stresses and interleukin-1. FEBS Lett 1995; 364: 229-33.

24. Westra I M, Boersema M, Oosterhuis D, Groothuis G M M, Olinga P. The p38-Mapk pathway is involved in fibrogenesis in rat precision-cut liver slices. Manuscript in preparation 2013.

25. Elferink M G, Olinga P, van Leeuwen E M et al. Gene expression analysis of precision-cut human liver slices indicates stable expression of ADME-Tox related genes. Toxicol Appl Pharmacol 2011; 253: 57-69.

26. de Graaf I A, Olinga P, de Jager M H et al. Preparation and incubation of precision-cut liver and intestinal slices for application in drug metabolism and toxicity studies. Nat Protoc 2010; 5: 1540-51.

27. Tsukada S, Westwick J K, Ikejima K, Sato N, Rippe R A. SMAD and p38 MAPK signaling pathways independently regulate alpha1(I) collagen gene expression in unstimulated and transforming growth factor-beta-stimulated hepatic stellate cells. J Biol Chem 2005; 280: 10055-64.

28. Xu S W, Liu S, Eastwood M et al. Rac inhibition reverses the phenotype of fibrotic fibroblasts. PLoS One 2009; 4: e7438.

29. Lowry O H, Rosebrough N J, Farr A L, Randall R J. Protein measurement with the Folin phenol reagent. J Biol Chem 1951; 193: 265-75.

30. Hadi M, Westra I M, Starokozhko V, Dragovic S, Merema M T, Groothuis G M. Human precision-cut liver slices as an ex vivo model to study idiosyncratic drug-induced liver injury. Chem Res Toxicol 2013; 26: 710-20.

31. van de Bovenkamp M, Groothuis G M, Draaisma A L et al. Precision-cut liver slices as a new model to study toxicity-induced hepatic stellate cell activation in a physiologic milieu. Toxicol Sci 2005; 85: 632-8.

32. Guyot C, Lepreux S, Combe C et al. Fibrogenic cell phenotype modifications during remodelling of normal and pathological human liver in cultured slices. Liver Int 2010; 30: 1529-40.

33. Kim Y, Fiel M I, Albanis E et al. Anti-fibrotic activity and enhanced interleukin-6 production by hepatic stellate cells in response to imatinib mesylate. Liver Int 2012; 32: 1008-17.

34. Hong F, Chou H, Fiel M I, Friedman S L. Antifibrotic Activity of Sorafenib in Experimental Hepatic Fibrosis: Refinement of Inhibitory Targets, Dosing, and Window of Efficacy In Vivo. Dig Dis Sci 2012.

35. Yoshiji H, Noguchi R, Ikenaka Y et al. Combination of branched-chain amino acid and angiotensin-converting enzyme inhibitor improves liver fibrosis progression in patients with cirrhosis. Mol Med Report 2012; 5: 539-44.

36. Watanabe T, Tajima H, Hironori H et al. Sodium valproate blocks the transforming growth factor (TGF)-beta1 autocrine loop and attenuates the TGF-beta1-induced collagen synthesis in a human hepatic stellate cell line. Int J Mol Med 2011; 28: 919-25.

37. Van Beneden K, Mannaerts I, Pauwels M, Van den Branden C, van Grunsven L A. HDAC inhibitors in experimental liver and kidney fibrosis. Fibrogenesis Tissue Repair 2013; 6: 1,1536-6-1.

38. Adachi T, Togashi H, Suzuki A et al. NAD(P)H oxidase plays a crucial role in PDGF-induced proliferation of hepatic stellate cells. Hepatology 2005; 41: 1272-81.

39. Varela-Rey M, Montiel-Duarte C, Oses-Prieto J A et al. p38 MAPK mediates the regulation of alpha1(I) procollagen mRNA levels by TNF-alpha and TGF-beta in a cell line of rat hepatic stellate cells(1). FEBS Lett 2002; 528: 133-8.

40. Martignoni M, Groothuis G M, de Kanter R. Species differences between mouse, rat, dog, monkey and human CYP-mediated drug metabolism, inhibition and induction. Expert Opin Drug Metab Toxicol 2006; 2: 875-94

Chapter 7

General discussion and future perspectives

Liver fibrosis is a multicellular disease in which the deposition of extracellular matrix (ECM) proteins occurs after chronic liver injury. Two of the most important signaling pathways in liver fibrosis are the transforming growth factor β (TGFβ) pathway and the platelet derived growth factor (PDGF) pathway. Up till now no pharmacotherapeutic treatment is available for liver fibrosis, therefore it is imperative to develop antifibrotic medicines (1,2). Induction of liver fibrosis in animals is accompanied by an extended period of considerable discomfort caused by specific operations or the administration of toxic substances. In addition, species differences in fibrosis mechanisms and effects of antifibrotic compounds hamper the translation from animal to man. Therefore, liver fibrosis models to study liver fibrosis and antifibrotics, which contribute to the reduction, refinement and/or replacement of animal experiments are indispensable.

The aim of the research described in this thesis was to investigate if rat and human precision-cut liver slices (PCLS) can be used as an *ex vivo* model to study the early onset and end-stage of liver fibrosis. In addition, the efficacy of different antifibrotic compounds was investigated in PCLS in these different stages of fibrosis. Furthermore, it was elucidated which pathways are involved in liver fibrosis in PCLS. To reach that aim, the early onset of liver fibrosis was studied by prolonged culturing of PCLS of healthy rats and healthy human liver tissue, as well as the end-stage of liver fibrosis in liver slices from rats with liver fibrosis induced by bile duct ligation and from liver tissue of patients with liver cirrhosis using several markers for liver fibrosis. Compounds that showed antifibrotic effects in both *in vitro* and *in vivo* animal studies acting on different signaling pathways (table 1) were used to study the effects on fibrosis markers and pathways involved during various stages of liver fibrosis in human and rat PCLS.

Table 1: Compounds with antifibrotic effects determined mainly in in vitro (human and rodents) models and in rodents in vivo. Inhibitors mainly inhibiting the PDGF- and TGFβ pathway are used in chapter 3, 4 and 6. Colchicine is used in chapter 3 and 4. Downstream PDGF- and TGFβ pathway inhibitors are used in chapter 5 and 6.

PDGF-pathway inhibitors	**Mechanism**	**References**
Imatinib	Tyrosine kinase inhibitor	(3-7)
Sorafenib	Tyrosine kinase inhibitor	(8-12)
Sunitinib	Tyrosine kinase inhibitor	(13,14)
TGFβ-pathway inhibitors	**Mechanism**	**References**
Perindopril	ACE-inhibitor	(15-19)
Rosmarinic acid	Inhibitor of TGFβ expression	(20-22)
Valproic acid	Histone deacetylase inhibitor	(23-25)
Tetrandrine	Upregulation of Smad 7	(26-30)
Pirfenidone	Inhibitor of TGFβ expression	(31-35)
Direct effect on collagen	**Mechanism**	**References**
Colchicine	Effect on collagen disposition	(36-38)
Downstream inhibitors	**Mechanism**	**References**
Sis3	Smad 3 inhibitor	(39)
SB203580	P38 Mapk inhibitor	(40,41)
NSC23766	Rac-1 inhibitor	(42)

Markers for liver fibrosis in PCLS

Liver fibrosis is a multicellular process and is characterized by deposition of an excessive amount of ECM, among others collagen, in which the hepatic stellate cell (HSC) plays a very important role. Activation of HSC leads to proliferation and transdifferentiation into myofibroblasts that express increased levels of alpha smooth muscle actin (αSMA) and heat shock protein 47 (HSP47) and start to increase the production of collagen (43,44). For this reason, the gene expression of HSP47, αSMA and pro-collagen 1A1 (PCOL1A1) and protein expression of collagen were used as fibrosis markers in this thesis. Previously, it was already shown that in liver slices these markers are up-regulated during prolonged (48 hour) culture and are therefore markers to study the mechanism of fibrosis in the PCLS and the effects of antifibrotic compounds on these markers (45).

The early onset of liver fibrosis in PCLS

During the initiation phase, HSC differentiate into myofibroblast-like cells, membrane receptors are up-regulated and therefore the cells are more responsive to cytokines, which can induce proliferation and fibrogenesis (46). In addition, apoptotic hepatocytes and Kupffer cells as well as inflammatory cells play a role in fibrogenesis by releasing reactive oxygen species (ROS) and producing profibrogenic cytokines (47). We established that the early onset of liver fibrosis can be studied in both rat and human liver slices (chapter 3 and 6). In rat liver slices *Hsp47*, *αSma* and *Pcol1A1* gene expression was spontaneously up-regulated during 48 hours of incubation, however in human PCLS only HSP47 and PCOl1A1 expression was up-regulated but αSMA gene expression was decreased during incubation compared to non incubated slices. However, expression increased again between 24 and 48 hours. While this decrease of αSMA was shown before in human slices (48), the cause is still unknown. Van de Bovenkamp *et al.* suggested that the (myo)fibroblasts and not the HSCs are mainly responsible for the decrease of αSMA gene expression since synaptophysin, which is a specific marker for HSC, was not decreased (48). Carpino et al. showed that in human liver biopsies αSMA is a reliable marker of HSC activation (49). Also, in rat slices an initial decrease of *αSma* at 24 hours was shown and after 48 hours this initial decrease was changed into an up-regulation of *αSma*. Perhaps, in human liver slices the increase of αSMA after the initial decrease occurs later or at a lower rate than in rat liver slices.

During the onset of liver fibrosis in rat liver slices, the PDGF signaling pathway plays an important role since antifibrotic compounds mainly acting on the PDGF-pathway (the PDGF-inhibitors, table 1) are very effective in inhibiting the increase of the gene expression of fibrosis markers, though collagen 1 protein expression was decreased by imatinib only. In addition, compounds that mainly inhibit the TGFβ pathway (TGFβ-inhibitors, table 1) only showed minor effects on the gene expression of *Hsp47*, *αSma* and *Pcol1A1* but the collagen 1 protein expression was attenuated by perindopril, tetrandrine and pirfenidone.

The opposite was shown in human liver slices during the onset of fibrosis (chapter 6). In human PCLS only the PDGF-inhibitor sunitinib showed clear antifibrotic effects on the gene expression and only sorafenib on the protein expression of collagen 1, while of the TGFβ-inhibitors rosmarinic acid, valproic acid, tetrandrine and pirfenidone were effective in inhibiting the increase in gene expression of the fibrosis markers. In addition, valproic acid and rosmarinic acid also decreased the collagen 1

protein expression. This indicates the existence of species differences in the relative contribution of the pathways involved in the onset of liver fibrosis in liver slices and thus possibly also *in vivo*. This might be a reason why a lot of compounds with promising antifibrotic effects either *in vitro* or *in vivo* in rats fail to show an effect in patients. The finding that not all compounds that inhibited the PCOL1A1 gene expression in human healthy PCLS showed an effect on the protein expression of collagen 1 might be explained by the fact that it takes longer before an effect on the protein level is found. Therefore, in the early onset of liver fibrosis in PCLS, gene expression of fibrosis markers seemed a better marker for liver fibrosis than protein expression of collagen 1.

Additionally, specific intracellular pathways involved in liver fibrosis were investigated in rat PCLS during different stages of liver fibrosis by inhibiting p38-Mapk, Smad 3 and Rac-1, key enzymes in these pathways. In both rat and human PCLS, the p38-Mapk pathway appeared to be important in the early onset of fibrosis, since inhibition of p38-Mapk by SB203580 resulted in a decrease in the gene expression of genes encoding for collagen synthesis and breakdown and also the three fibrosis markers used throughout this thesis. P38-Mapk can be activated by both PDGF and TGFβ (50). Also ROS derived from NADPH-oxidase can activate P38-Mapk, but since inhibition of Rac-1, which activates NADPH-oxidase, did not show an effect in PCLS, it is more likely that P38 Mapk in PCLS is activated by either PDGF or TGFβ or both. Also, Smad 3 inhibition by Sis3 only slightly decreased *Pcol1A1* gene expression and lysyl oxidase like gene expression in the onset of liver fibrosis. It can be concluded that the effect of TGFβ on collagen expression in rat PCLS is mediated via the p38 Mapk and not via the Smad signaling pathway.

The PDGF- as well as the TGFβ-pathway may be activated during incubation since the gene expressions of both PDGF-β and TGF-β1 were up-regulated during incubation in healthy human PCLS. Furthermore, stimulation of these slices with PDGF-BB and TGF-β1 together resulted in an increased gene expression of fibrosis markers, however, when PCLS were stimulated with either PDGF-BB or TGF-β1 alone, no clear effect was observed. This in contrast with normal rat PCLS where the *TGF-β1* gene expression was not increased during incubation, while addition of PDGF-BB or TGF-β1 caused a significant increase in the gene expression of fibrosis markers. This might be explained by the fact that in human liver slices the fibrosis pathways are already activated due to the long operation procedure, while in rats the liver is directly excised after anesthesia. During the early onset of fibrosis in human PCLS most likely TGFβ plays a dominant role, while in rat PCLS it is primarily PDGF. The LDA study showed that during the prolonged incubation of healthy rat PCLS, the gene expression of *Timp1* and *Havcr1* (kidney injury molecule 1 (*Kim1*)) were increased. *In vivo*, during the early onset of fibrosis, *Timp1* was also up-regulated (51) and *Kim1* was increased in the kidney by ischemia and toxic injury (52). In future studies, *Timp1* and *Kim1* might be used as early markers for fibrogenesis in PCLS. Furthermore, the gene expression of catalase was down-regulated during prolonged incubation in the rat PCLS. Catalase expression can be reduced by ROS (53). Future experiments should investigate whether ROS are produced during prolonged culture in PCLS.

End-stage liver fibrosis in PCLS

In addition to the early onset of fibrosis, also end-stage liver fibrosis, or cirrhosis, was studied in this thesis in both rat and human PCLS. Liver slices from fibrotic livers from rats subjected to 3 weeks bile duct ligation (BDL) were used to study end-stage liver fibrosis and the effect of antifibrotics on the

resolution of fibrosis by investigating the effects of these compounds on different fibrosis markers. BDL results in biliary fibrosis and cirrhosis (54). In this thesis it was shown that in fibrotic PCLS, in contrast to the early onset of liver fibrosis in healthy rat PCLS, where only PDGF-inhibitors seemed effective, both the PDGF- and TGFβ-inhibitors were effective in inhibiting the increase of the gene expression of fibrosis markers during culture (chapter 4). Furthermore, also the protein expression of collagen 1 was inhibited by both PDGF- and TGFβ-inhibitors. Based on these findings together with the finding that PCLS from healthy rat liver could respond to PDGF-BB and TGF-β1, it can be concluded that the TGFβ-pathway plays a more important role in the end-stage of liver fibrosis than during the early stage of liver fibrosis in rat PCLS, but that the PDGF pathway is involved during both stages of the disease.

To elucidate the mechanisms of end-stage fibrosis in rat PCLS, it was shown (chapter 5) that inhibition of p38 Mapk resulted in inhibition of gene expression of genes involved in collagen synthesis and breakdown. In addition, it seems that the TGFβ pathway in rat PCLS is not Smad-related since inhibition of Smad 3 did not result in effects on genes coding for collagen synthesis and breakdown or on the gene expression of the fibrosis markers.

Future experiments could focus on testing the efficacy of combination therapies of PDGF and TGFβ inhibitors in PCLS. In literature it was already shown that a combination of imatinib and perindopril ameliorated liver fibrogenesis in CCl_4-induced fibrosis in rats (55).

Furthermore, human liver slices from cirrhotic liver tissue from patients with end-stage liver disease who underwent a liver transplantation, were cultured for 24 hours and used for the research of established human liver fibrosis, cirrhosis (chapter 6). The slices were cultured for 24 hours instead of 48 hours, since the amount of RNA that could be isolated, was already low after 24 hours compared to cirrhotic human PCLS at the start of the incubation period. In these cirrhotic human PCLS most of the antifibrotic compounds that show antifibrotic activity in animal studies had minimal effects. This result may explain why these compounds have not reached the market as effective antifibrotic drugs. Only for pirfenidone studies in patients are described where pirfenidone treatment (twelve months) decreased the gene- and protein expression of collagen 1a, TGFβ and TIMP-1, measured in liver biopsies (31). In this light, the *ex vivo* cirrhotic human liver model is a promising translational model to test the efficacy of new antifibrotic compounds. Future research on cirrhotic human PCLS should focus on extension of the culture period of these PCLS, since 24 hours is a short period to establish effects of antifibrotic compounds, hence, in liver tissue from patients with liver cirrhosis, the deposition of collagen and other ECM components is extensive and resolution of fibrosis may consequently take longer. Moreover, the ECM plays a major role in the liver, not only in liver architecture, but also signaling function between liver cells and since in fibrosis the ECM is 3-5 fold increased, this change will lead to altered cell signaling in the liver (56). Therefore, fPCLS seem more promising in testing the efficacy of antifibrotic compounds than healthy PCLS, also because antifibrotic drugs will be mainly used by patients with end-stage liver fibrosis.

Conclusion

The research described in this thesis showed that rat and human PCLS can be successfully used to study the mechanism of liver fibrosis and the efficacy of antifibrotic drugs both in the early- and end-stage of liver fibrosis. During the onset of fibrosis in rat PCLS the PDGF-pathway plays a more

important role than the TGFβ-pathway, while in end-stage liver fibrosis in the rat both pathways are activated. In addition, p38-Mapk is involved in both the early onset and end-stage of liver fibrosis in rat PCLS, while Smad3 and Rac-1 seemed to be of less importance. In human PCLS, the TGFβ pathway plays a more dominant role than the PDGF pathway during the onset of fibrosis. We started with the culture of cirrhotic human PCLS and showed that antifibrotic compounds can be tested during 24 hours of culture. With these studies we prevalidated the use of PCLS for liver fibrosis and for testing of antifibrotic compounds.

In this thesis, species differences became apparent indicating again the importance of translational research using human tissue. Therefore, the application of the models described in this thesis in preclinical studies will lead to a considerable reduction of the use of animal experiments in testing of antifibrotic compounds and lead to better translatable results. Moreover, this *ex vivo* model for fibrosis could be used in the search for new biomarkers and can also be translated to other organs.

References

1. Schuppan D, Kim Y O. Evolving therapies for liver fibrosis. J Clin Invest 2013; 123: 1887-901.

2. Friedman S L, Sheppard D, Duffield J S, Violette S. Therapy for fibrotic diseases: nearing the starting line. Sci Transl Med 2013; 5: 167sr1.

3. Kim Y, Fiel M I, Albanis E et al. Anti-fibrotic activity and enhanced interleukin-6 production by hepatic stellate cells in response to imatinib mesylate. Liver Int 2012; 32: 1008-17.

4. Kinnman N, Goria O, Wendum D et al. Hepatic stellate cell proliferation is an early platelet-derived growth factor-mediated cellular event in rat cholestatic liver injury. Lab Invest 2001; 81: 1709-16.

5. Kuo W L, Yu M C, Lee J F, Tsai C N, Chen T C, Chen M F. Imatinib mesylate improves liver regeneration and attenuates liver fibrogenesis in CCL4-treated mice. J Gastrointest Surg 2012; 16: 361-9.

6. Neef M, Ledermann M, Saegesser H et al. Oral imatinib treatment reduces early fibrogenesis but does not prevent progression in the long term. J Hepatol 2006; 44: 167-75.

7. Yoshiji H, Noguchi R, Kuriyama S et al. Imatinib mesylate (STI-571) attenuates liver fibrosis development in rats. Am J Physiol Gastrointest Liver Physiol 2005; 288: G907-13.

8. Friedman S L. Antifibrotic activity of sorafenib in experimental hepatic fibrosis - refinement of targets, dosing and window of efficacy in vivo. Hepatology 2011; 54: 360A-1455A.

9. Hennenberg M, Trebicka J, Kohistani Z et al. Hepatic and HSC-specific sorafenib effects in rats with established secondary biliary cirrhosis. Lab Invest 2010.

10. Hennenberg M, Trebicka J, Stark C, Kohistani A Z, Heller J, Sauerbruch T. Sorafenib targets dysregulated Rho kinase expression and portal hypertension in rats with secondary biliary cirrhosis. Br J Pharmacol 2009; 157: 258-70.

11. Mejias M, Garcia-Pras E, Tiani C, Miquel R, Bosch J, Fernandez M. Beneficial effects of sorafenib on splanchnic, intrahepatic, and portocollateral circulations in portal hypertensive and cirrhotic rats. Hepatology 2009; 49: 1245-56.

12. Wang Y, Gao J, Zhang D, Zhang J, Ma J, Jiang H. New insights into the antifibrotic effects of sorafenib on hepatic stellate cells and liver fibrosis. J Hepatol 2010.

13. Tugues S, Fernandez-Varo G, Munoz-Luque J et al. Antiangiogenic treatment with sunitinib

ameliorates inflammatory infiltrate, fibrosis, and portal pressure in cirrhotic rats. Hepatology 2007; 46: 1919-26.

14. Majumder S, Piguet A C, Dufour J F, Chatterjee S. Study of the cellular mechanism of Sunitinib mediated inactivation of activated hepatic stellate cells and its implications in angiogenesis. Eur J Pharmacol 2013; 705: 86-95.

15. Ni S, Li Y, Huang S, Luo W, Li C, Li X. Perindopril and losartan attenuate intrahepatic Toll-like receptor 4 protein expression in rats with bile duct ligation-induced hepatic fibrosis. Nan Fang Yi Ke Da Xue Xue Bao 2012; 32: 211-4.

16. Xu W, Song S, Huang Y, Gong Z. Effects of perindopril and valsartan on expression of transforming growth factor-beta-Smads in experimental hepatic fibrosis in rats. J Gastroenterol Hepatol 2006; 21: 1250-6.

17. Yeki M, Koda M, Matono T, Sugihara T, Maeda K, Murawaki Y. Preventative and therapeutic effects of perindopril on hepatic fibrosis induced by bile duct ligation in rats. Mol Med Report 2009; 2: 857-64.

18. Yoshiji H, Kuriyama S, Noguchi R et al. Combination of interferon-beta and angiotensin-converting enzyme inhibitor, perindopril, attenuates the murine liver fibrosis development. Liver International 2005; 25: 153-61.

19. Yoshiji H, Noguchi R, Fukui H. Combined effect of an ACE inhibitor, perindopril, and interferon on liver fibrosis markers in patients with chronic hepatitis C. J Gastroenterol 2005; 40: 215-6.

20. Domitrovic R, Skoda M, Marchesi V V, Cvijanovic O, Pugel E P, Stefan M B. Rosmarinic acid ameliorates acute liver damage and fibrogenesis in carbon tetrachloride-intoxicated mice. Food Chem Toxicol 2012.

21. Li G S, Jiang W L, Tian J W, Qu G W, Zhu H B, Fu F H. In vitro and in vivo antifibrotic effects of rosmarinic acid on experimental liver fibrosis. Phytomedicine 2010; 17: 282-8.

22. Zhang J J, Wang Y L, Feng X B, Song X D, Liu W B. Rosmarinic acid inhibits proliferation and induces apoptosis of hepatic stellate cells. Biol Pharm Bull 2011; 34: 343-8.

23. Mannaerts I, Nuytten N R, Rogiers V, Vanderkerken K, van Grunsven L A, Geerts A. Chronic administration of valproic acid inhibits activation of mouse hepatic stellate cells in vitro and in vivo. Hepatology 2010; 51: 603-14.

24. Watanabe T, Tajima H, Hironori H et al. Sodium valproate blocks the transforming growth factor (TGF)-beta1 autocrine loop and attenuates the TGF-beta1-induced collagen synthesis in a human hepatic stellate cell line. Int J Mol Med 2011; 28: 919-25.

25. Ikura Y, Iwasa Y, Ueda M. Valproic acid administration for hepatic fibrosis: a balance between antifibrotic efficacy and hepatotoxicity. Hepatology 2010; 51: 2227,8; author reply 2228.

26. Chen Y, Li D, Wu J, Chen Y, Lu H. Tetrandrine inhibits activation of rat hepatic stellate cells stimulated by transforming growth factor-beta in vitro via up-regulation of Smad 7. J Ethnopharmacol 2005; 100: 299-305.

27. Hsu Y, Chiu Y, Cheng C, Wu C, Lin Y, Huang Y. Antifibrotic effects of tetrandrine on hepatic stellate cells and rats with liver fibrosis. J Gastroen Hepatol 2007; 22: 99-111.

28. Hsu Y, Chiu Y, Lee C, Wu C, Huang Y. Anti-fibrotic effects of tetrandrine on bile-duct ligated rats. Can J Physiol Pharm 2006; 84: 967-76.

29. Park P H, Nan J X, Park E J et al. Effect of tetrandrine on experimental hepatic fibrosis induced by bile duct ligation and scission in rats. Pharmacol Toxicol 2000; 87: 261-8.

30. Yin M, Lian L, Piao D, Nan J. Tetrandrine stimulates the apoptosis of hepatic stellate cells and ameliorates development of fibrosis in a thioacetamide rat model. WORLD JOURNAL OF GASTROENTEROLOGY 2007; 13: 1214-20.

31. Armendariz-Borunda J, Islas-Carbajal M C, Meza-Garcia E et al. A pilot study in patients with established advanced liver fibrosis using pirfenidone. Gut 2006; 55: 1663-5.

32. Di Sario A, Bendia E, Baroni G et al. Effect of pirfenidone on rat hepatic stellate cell proliferation and collagen production. J Hepatol 2002; 37: 584-91.

33. Di Sario A, Bendia E, Macarri G et al. The anti-fibrotic effect of pirfenidone in rat liver fibrosis is mediated by downregulation of procollagen alpha 1(I), TIMP-1 and MMP-2. Digest Liver Dis 2004; 36: 744-51.

34. Garcia L, Hernandez I, Sandoval A et al. Pirfenidone effectively reverses experimental liver fibrosis. J Hepatol 2002; 37: 797-805.

35. Schaefer C J, Ruhrmund D W, Pan L, Seiwert S D, Kossen K. Antifibrotic activities of pirfenidone in animal models. Eur Respir Rev 2011; 20: 85-97.

36. Nikolaidis N, Kountouras J, Giouleme O et al. Colchicine treatment of liver fibrosis. Hepatogastroenterology 2006; 53: 281-5.

37. Poo J L, Feldmann G, Moreau A, Gaudin C, Lebrec D. Early colchicine administration reduces hepatic fibrosis and portal hypertension in rats with bile duct ligation. J Hepatol 1993; 19: 90-4.

38. Rambaldi A, Gluud C. Colchicine for alcoholic and non-alcoholic liver fibrosis and cirrhosis. Cochrane Database Syst Rev 2005; (2): CD002148.

39. Jinnin M, Ihn H, Tamaki K. Characterization of SIS3, a novel specific inhibitor of Smad3, and its effect on transforming growth factor-beta1-induced extracellular matrix expression. Mol Pharmacol 2006; 69: 597-607.

40. Cuenda A, Rouse J, Doza Y N et al. SB 203580 is a specific inhibitor of a MAP kinase homologue which is stimulated by cellular stresses and interleukin-1. FEBS Lett 1995; 364: 229-33.

41. Tsukada S, Westwick J K, Ikejima K, Sato N, Rippe R A. SMAD and p38 MAPK signaling pathways independently regulate alpha1(I) collagen gene expression in unstimulated and transforming growth factor-beta-stimulated hepatic stellate cells. J Biol Chem 2005; 280: 10055-64.

42. Gao Y, Dickerson J B, Guo F, Zheng J, Zheng Y. Rational design and characterization of a Rac GTPase-specific small molecule inhibitor. Proc Natl Acad Sci U S A 2004; 101: 7618-23.

43. Hernandez-Gea V, Friedman S L. Pathogenesis of liver fibrosis. Annu Rev Pathol 2011; 6: 425-56.

44. Schuppan D, Afdhal N H. Liver cirrhosis. Lancet 2008; 371: 838-51.

45. van de Bovenkamp M, Groothuis G M, Draaisma A L et al. Precision-cut liver slices as a new model to study toxicity-induced hepatic stellate cell activation in a physiologic milieu. Toxicol Sci 2005; 85: 632-8.

46. Moreira R K. Hepatic stellate cells and liver fibrosis. Arch Pathol Lab Med 2007; 131: 1728-34.

47. Kisseleva T, Brenner D A. Hepatic stellate cells and the reversal of fibrosis. J Gastroenterol Hepatol 2006; 21 Suppl 3: S84-7.

48. van de Bovenkamp M, Groothuis G M, Meijer D K, Olinga P. Liver slices as a model to study fibrogenesis and test the effects of anti-fibrotic drugs on fibrogenic cells in human liver. Toxicol In Vitro 2008; 22: 771-8.

49. Carpino G, Morini S, Ginanni Corradini S et al. Alpha-SMA expression in hepatic stellate cells and quantitative analysis of hepatic fibrosis in cirrhosis and in recurrent chronic hepatitis after liver transplantation. Dig Liver Dis 2005; 37: 349-56.

50. Parsons C J, Takashima M, Rippe R A. Molecular mechanisms of hepatic fibrogenesis. J Gastroenterol Hepatol 2007; 22 Suppl 1: S79-84.

51. Wang H, Lafdil F, Wang L, Yin S, Feng D, Gao B. Tissue inhibitor of metalloproteinase 1 (TIMP-1) deficiency exacerbates carbon tetrachloride-induced liver injury and fibrosis in mice: involvement of hepatocyte STAT3 in TIMP-1 production. Cell Biosci 2011; 1: 14,3701-1-14.

52. Ichimura T, Bonventre J V, Bailly V et al. Kidney injury molecule-1 (KIM-1), a putative epithelial cell adhesion molecule containing a novel

immunoglobulin domain, is up-regulated in renal cells after injury. J Biol Chem 1998; 273: 4135-42.

53. Dong Y, Qu Y, Xu M, Wang X, Lu L. Catalase ameliorates hepatic fi brosis by inhibition of hepatic stellate cells activation. Front Biosci (Landmark Ed) 2014; 19: 535-41.

54. Hayashi H, Sakai T. Animal models for the study of liver fibrosis: new insights from knockout mouse models. Am J Physiol Gastrointest Liver Physiol 2011; 300: G729-38.

55. Yoshiji H, Kuriyama S, Noguchi R et al. Amelioration of liver fibrogenesis by dual inhibition of PDGF and TGF-beta with a combination of imatinib mesylate and ACE inhibitor in rats. Int J Mol Med 2006; 17: 899-904.

56. Bedossa P, Paradis V. Liver extracellular matrix in health and disease. J Pathol 2003; 200: 504-15.

Appendices

Summary

Nederlandse samenvatting

Dankwoord

Curriculum vitae

Summary

Fibrosis is characterized by excessive deposition of extracellular matrix proteins and is considered a serious complication associated with chronic injury and ultimately results in organ deterioration. Liver fibrosis is a common disease, however successful antifibrotic pharmacotherapies are currently not available, and patients with end-stage liver fibrosis, cirrhosis, can only be treated by liver transplantation. The mechanism of liver fibrosis is complex and different cell types are involved. The hepatic stellate cells (HSC) are, in activated state, the major contributor of collagen deposition in the liver, but also Kupffer cells, fibroblasts, endothelial cells and hepatocytes are engaged in the process of fibrogenesis. Two of the most important signaling pathways in liver fibrosis are the transforming growth factor β (TGFβ) pathway and the platelet derived growth factor (PDGF) pathway. Therefore compounds that inhibit these pathways were developed as potential antifibrotic drug. Animal models of chronic injury are widely utilized to study liver fibrosis and to develop antifibrotic drugs. The initiation and progression of liver fibrosis in animals is accompanied by an extended period of considerable discomfort caused by specific surgical operations or the chronic administration of toxic substances. To study the process of liver fibrosis and to test anti-fibrotic drugs in a physiologic milieu, it is important to use an *ex vivo* system that can close the gap between *in vitro* and *in vivo* models. In precision-cut liver slices (PCLS), an *ex vivo* model, all cell types of the liver are present in their original context and remain viable up to 48 hours. From one rat liver, approximately 250 liver slices can be prepared, therefore this model could substantially contribute to the reduction of animal experiments when it will be used for fibrosis research. The use of PCLS from human liver would favor a direct translation to man and even further reduce the use of experimental animals.
The aim of this thesis was to study human and rat precision-cut liver slices as model for liver fibrosis and for testing of anti-fibrotic drugs (**chapter 2**).

First the current literature on the use of precision-cut tissue slices in research on fibrosis in liver, lung, intestine and kidney was reviewed as is described in **chapter 1**.

In **chapter 3** the PCLS model was used to investigate the early onset of liver fibrosis in rats. Prolonged incubation up to 48 hours of rat PCLS from healthy rat liver tissue was used to induce the onset of liver fibrosis. After verification that slice viability was not changed during incubation the gene expression of fibrosis markers heat shock protein 47 (*Hsp47*), α smooth muscle actin (*αSma*), pro-collagen 1A1 (*Pcol1A1*), *PDGF-β* and *TGF-β1* and the protein expression of collagen 1 were determined. Furthermore, the effects of anti-fibrotic drugs predominantly inhibiting the PDGF pathway (PDGF-inhibitors, imatinib, sorafenib and sunitinib), drugs inhibiting mainly the TGFβ signaling pathway (TGFβ-inhibitors, valproic acid, rosmarinic acid, tetrandrine and pirfenidone) and colchicine, a drug with a direct effect on collagen content, were determined. Culturing of PCLS for 48 hours indeed induced the early onset of fibrosis while maintaining slice viability. The fibrosis process could be further stimulated by adding PDGF-BB or TGF-β1 to the PCLS incubation. The fibrosis markers were down-regulated by the antifibrotic compounds that act on the PDGF pathway and also colchicine slightly reduced the fibrosis markers. However, compounds acting on the TGFβ pathway had only a limited effect, indicating the predominance of the PDGF pathway in the early onset of

fibrosis in rat liver slices. This was confirmed by the findings that expression of *TGF-β1* was not influenced while *PDGF-β* expression was increased during the early onset of fibrosis in PCLS. Rat PCLS appeared to be a useful model for research of the early onset of fibrosis and for testing of antifibrotic drugs inhibiting the PDGF-pathway.

Chapter 4 describes the study on end-stage liver fibrosis in liver slices from fibrotic rat liver tissue. In this study, we investigated established liver fibrosis by using PCLS from bile duct ligated (BDL) rats and tested the PDGF-inhibitors and TGFβ-inhibitors that were also used in chapter 3. The fibrosis markers in the fibrotic liver slices were already elevated at the start of the culture period compared with liver slices from healthy rat liver tissue. After 48 hours of incubation the gene expression of the fibrosis markers, the total collagen, the fibrillar collagens and the collagen 1 protein expression were further increased in these fibrotic liver slices, which is an indication that the fibrosis process continues during incubation. Most PDGF-inhibitors and TGFβ-inhibitors significantly inhibited the gene expression of *Hsp47*, *αSma* and *Pcol1A1*. Protein expression of collagen 1 was significantly reduced by all PDGF-inhibitors and TGFβ-inhibitors, while total collagen expression and fibrillar collagens were not changed. Here a difference was shown in end-stage and onset of liver fibrosis in rat liver slices, since TGFβ-inhibitors were effective in inhibiting fibrosis markers in the end-stage of liver fibrosis, but not in the onset of liver fibrosis, which suggests that the TGFβ pathway plays a minor role in the early onset of liver fibrosis in PCLS and a larger role in end-stage liver fibrosis in fibrotic PCLS. In conclusion, PCLS from fibrotic livers from 3 weeks BDL rats can be used as a functional *ex vivo* model of established liver fibrosis and the antifibrotic effects of compounds inhibiting the PDGF- and TGFβ signaling pathway can be investigated.

In addition to these two studies, we wanted to take a closer look at the mechanisms involved in liver fibrosis in these rat PCLS. Therefore, in **chapter 5** the role of three different downstream inhibitors of components in the pathways involved in fibrogenesis (p38 Mapk, Smad 3 and Rac-1) in rat liver slices were investigated. The downstream inhibitors of these three components were incubated for 48 hours with healthy rat PCLS and fibrotic rat PCLS. The effects on the gene expression of genes encoding for collagen synthesis and breakdown were studied using a custom made low density array (LDA) and compared with the effects on the fibrosis markers that were also used in the studies described in chapter 3 and 4. Inhibition of p38-Mapk resulted in a decrease in the gene expression of several genes involved in collagen synthesis and breakdown in both the early onset and end-stage of liver fibrosis in rat PCLS. This was confirmed by the decrease in the gene expression of *Hsp47*, *αSma* and *Pcol1A1*. Inhibition of Smad3 and Rac-1 had only minor effects on the pathways involved in fibrosis in the liver slices. The p38-Mapk pathway plays an important role in the increase of the fibrosis markers during culture. Either PDGF, TGFβ or ROS, or all together could be responsible for the activation of p38 Mapk. However, since inhibition of Rac-1 leads to less production of ROS and we showed that Rac-1 plays a minor role in fibrogenesis in PCLS, it is more likely that p38 Mapk is activated by PDGF and TGFβ in the PCLS. Also, Smad 3 seemed to be of minor importance during fibrogenesis in PCLS, this will be further investigated by future experiments focusing on the phosphorylation of Smad 3 in PCLS.

These three studies on liver fibrosis in liver slices were performed with rat liver tissue. To close the gap between animal experiments and outcome in patients, in **chapter 6**, we aimed to investigate if the early onset and late stage of liver fibrosis can be studied in human PCLS. Studies were performed with liver slices from healthy and cirrhotic human liver tissue. The PCLS from healthy livers were cultured for 48 hours but the cirrhotic human liver slices were cultured for 24 hours instead of 48 hours, since the amount of RNA that could be isolated was already low after 24 hours compared to cirrhotic human PCLS at the start of the incubation period. The effects of PDGF-inhibitors and TGFβ-inhibitors were investigated in both models. In healthy human liver slices, HSP47 and PCOL1A1, but not αSMA gene expression was increased during 48 hour of incubation. In contrast to the early onset of liver fibrosis in rat liver slices, during the initial phase of fibrosis in human liver slices the TGFβ-inhibitors were more effective than the PDGF-inhibitors in inhibiting the increased gene expression of HSP47 and PCOL1A1 after 48 hours of incubation. However, both PDGF and TGFβ1 gene expressions were increased in PCLS during culture. The different results in human and rat could indicate a species difference in the fibrosis pathways involved in PCLS. In cirrhotic human PCLS antifibrotic compounds had minimal effects, but as the incubation period was short, future research should focus on extension of the culture period of cirrhotic human PCLS.

In conclusion, the research described in this thesis showed that rat and human PCLS can be successfully used to study the mechanism of liver fibrosis and the efficacy of anti-fibrotic drugs in the early- and end-stage of liver fibrosis. In addition, species differences became apparent indicating again the importance of translational research using human tissue. Our results will lead to a considerable reduction of the use of animal experiments in testing antifibrotic compounds when included in fibrosis research and preclinical drug studies and hopefully to a more reliable prediction of the effects of drugs in humans.

Nederlandse samenvatting

Fibrose is een ernstige ziekte waarbij buitensporig veel extracellulaire matrix (ECM) eiwitten worden geproduceerd, vaak ontstaan door chronische schade en uiteindelijk leidt fibrose tot een verslechtering van de functie van de aangetaste organen. Fibrose in de lever is een wereldwijd veel voorkomende ziekte waar op dit moment nog geen anti-fibrotische geneesmiddelen voor verkrijgbaar zijn. Daardoor kunnen patiënten met het eindstadium van leverfibrose, cirrose, alleen behandeld worden met een levertransplantatie. Het mechanisme van het ontstaan van de ziekte is complex, waarbij verschillende soorten levercellen betrokken zijn. Twee van de belangrijkste signaalroutes die een rol spelen bij fibrose zijn de "transforming growth factor β" (TGFβ) signaalroute en de "platelet derived growth factor" (PDGF) signaalroute. Proefdiermodellen met chronische leverschade worden wereldwijd gebruikt om leverfibrose te onderzoeken en geneesmiddelen te ontwikkelen. Het verloop van leverfibrose in deze dieren gaat gepaard met een lange periode van aanzienlijk ongerief dat veroorzaakt wordt door ingrijpende operaties of het toedienen van stoffen die giftig zijn voor de lever. Om het proces van leverfibrose te onderzoeken in een *in vitro* (buiten het lichaam) model in een fysiologische omgeving en om potentiële anti-fibrotische geneesmiddelen te testen is het belangrijk om een *in vitro* systeem te gebruiken dat zoveel mogelijk overeenkomt met de *in vivo* (in het complete levende lichaam) situatie. In dit proefschrift wordt gebruik gemaakt van "precies gesneden leverslices" (precision-cut liver slices (PCLS)), een model waarin alle celtypes van de lever aanwezig zijn in hun originele context en deze leverslices blijven gedurende 48 uur levensvatbaar. Omdat dit model de leverstructuur intact laat noemen we dit model een *ex vivo* model, die een brug kan vormen tussen de *in vitro* modellen en de *in vivo* situatie. Uit een rattenlever kunnen tot 250 leverslices gemaakt worden, waarmee dit model enorm zou kunnen bijdragen aan de reductie van het aantal dierexperimenten als het gebruikt zou kunnen worden bij leverfibrose onderzoek. Het doel van dit proefschrift was om humane en ratten PCLS te onderzoeken als model voor leverfibrose en voor het testen van anti-fibrotische geneesmiddelen (**hoofdstuk 2**).

Allereerst is de huidige literatuur over het gebruik van precies gesneden weefsel slices in het onderzoek naar fibrose in de lever, long, darm en nier besproken in **hoofdstuk 1**.

In **hoofdstuk 3** werd het PCLS model gebruikt om de beginfase van leverfibrose in ratten te onderzoeken. De beginfase van leverfibrose werd geïnduceerd door rattenleverslices van gezond leverweefsel van ratten 48 uur te incuberen. De leverslices werden 48 uur lang gekweekt en nadat werd vastgesteld dat de PCLS nog levensvatbaar waren, werd de genexpressie van de fibrose markers "heat shock protein 47" (Hsp47), "α smooth muscle actin" (αSma) en "pro-collagen 1A1" (Pcol1A1) en de eiwitexpressie van collageen 1 (het meest voorkomende extracellulaire matrix eiwit in fibrose) bepaald. Bovendien werden de effecten van anti-fibrotische middelen die met name de PDGF-signaalroute (PDGF-remmers) en geneesmiddelen die met name de TGFβ-signaalroute (TGFβ-remmers) remmen bepaald. Door het 48 uur lang kweken van PCLS werd er inderdaad leverfibrose geïnduceerd in deze PCLS terwijl ze nog steeds levensvatbaar waren. Dit fibroseproces kon verder gestimuleerd worden door het toevoegen van PDGF of TGFβ. De expressie van de fibrose markers

was verlaagd als er PDGF-remmers toegevoegd waren bij de slices, terwijl de TGFβ-remmers maar heel weinig effect hadden op de genexpressie van de fibrose markers. Dit duidt op een overheersing van de PDGF-signaalroute in de beginfase van leverfibrose in rattenleverslices. Ratten PCLS lijken een bruikbaar model voor het onderzoek naar de beginfase van leverfibrose en voor het testen van anti-fibrotische geneesmiddelen die via de PDGF-signaalroute werkzaam zijn.

Hoofdstuk 4 beschrijft de studie naar het eindstadium van leverfibrose in leverslices van fibrotisch rattenleverweefsel. In dit onderzoek hebben we gebruik gemaakt van PCLS van ratten waarbij de galgang gedurende 3 weken was afgesloten (BDL ratten), waardoor fibrose in de lever is ontstaan. De anti-fibrotische geneesmiddelen die ook in hoofdstuk 3 zijn gebruikt werden getest op deze fibrotische leverslices. Voordat de PCLS gekweekt werden was, zoals verwacht, de genexpressie van fibrose markers al veel hoger dan in de gezonde rattenleverslices. Na 48 uur incubatie was de genexpressie van de fibrose markers verder verhoogd in de fibrotische rattenleverslices, net als het totale collageen, het fibrillaire collageen en de collageen 1 eiwitexpressie, wat erop duidt dat het fibrose proces gewoon doorgaat tijdens incubatie. Veruit de meeste PDGF- en TGFβ-remmers remden de genexpressie van Hsp47, αSma en Pcol1A1 significant, maar de totale collageen expressie en de fibrillaire collageen expressie was niet veranderd na toevoeging van deze remmers. Er is dus een verschil tussen het begin- en eindstadium van leverfibrose in ratten PCLS, aangezien de TGFβ-remmers effect hadden op de fibrose markers in het eindstadium van fibrose, maar niet in het beginstadium van fibrose. Dit suggereert dat de TGFβ-signaalroute een minder belangrijke rol speelt in het beginstadium van leverfibrose in leverslices en een grotere rol in het eindstadium van leverfibrose in leverslices van fibrotische levers van ratten. Concluderend kunnen we zeggen dat PCLS van fibrotische levers van BDL ratten gebruikt kunnen worden als een functioneel *ex vivo* model voor het eindstadium van fibrose en de anti-fibrotische effecten van geneesmiddelen die de PDGF- en TGFβ-signaalroute remmen kunnen worden onderzocht in dit model.

Na deze twee studies wilden we diepgaander kijken naar de signaalroutes die een rol spelen in leverfibrose in deze ratten PCLS. Daarom hebben we in **hoofdstuk 5** de rol van drie verschillende signaalroutes (de p38 Mapk, Smad 3 en Rac-1 signaalroute) gedurende het fibrose proces in rattenleverslices onderzocht. Specifieke remmers van sleutelenzymen binnen die drie signaalroutes werden gedurende 48 uur geïncubeerd met gezonde en fibrotische ratten PCLS. De effecten op de genexpressie van genen die coderen voor collageensynthese en -afbraak werden bestudeerd met behulp van een “low density array” (LDA) en vergeleken met de effecten op de fibrosemarkers die ook gebruikt werden in hoofdstuk 3 en 4. Remming van p38 Mapk had een verlaging van de genexpressie van meerdere genen die betrokken zijn bij collageen synthese en afbraak in zowel het begin- als eindstadium van leverfibrose in ratten PCLS tot gevolg. Dit effect op fibrose werd bevestigd door de verlaging in de genexpressie van Hsp47, αSma en Pcol1A1. Remming van Smad 3 en Rac-1 had weinig tot geen effect op de fibrose in de leverslices. Uit deze resultaten concluderen we dat de p38-Mapk signaalroute de belangrijkste intracellulaire route is bij het ontstaan en handhaven van leverfibrose in PCLS.

Deze drie onderzoeken over leverfibrose in leverslices werden uitgevoerd met leverweefsel van ratten. Om de kloof te dichten tussen dierexperimenten en uitkomsten in patiënten werd er in **hoofdstuk 6** onderzocht of het begin- en eindstadium van leverfibrose onderzocht kan worden in PCLS van humaan leverweefsel. Studies werden uitgevoerd met PCLS van gezond en cirrotisch (cirrose is het eindstadium van fibrose) humaan leverweefsel. De effecten van de PDGF- en TGFβ-remmers werden onderzocht in beide modellen. In gezonde humane leverslices, was de genexpressie van HSP47 en PCOL1A1, maar niet de genexpressie van αSMA, verhoogd ten opzichte van slices die niet geïncubeerd waren. In tegenstelling tot de beginfase van leverfibrose in ratten PCLS, waren in humane PCLS gedurende de beginfase van fibrose de TGFβ-remmers effectiever dan de PDGF-remmers in het remmen van de verhoogde genexpressie van HSP47 en PCOL1A1 na 48 uur incubatie. Echter, de genexpressie van zowel PDGF als TGFβ waren verhoogd na incubatie. De cirrotische humane PCLS werden in plaats van 48 uur maar 24 uur geïncubeerd, aangezien de hoeveelheden RNA die geïsoleerd konden worden al sterk waren afgenomen na 24 uur ten opzichte van cirrotische humane PCLS aan het begin van de incubatieperiode. In de cirrotische humane leverslices hadden de anti-fibrotische middelen slechts minimale effecten. Aangezien de incubatietijd van deze cirrotische humane leverslices kort was, zou vervolgonderzoek zich moeten richten op het verlengen van de incubatieperiode van deze slices.

Uit het onderzoek dat in dit proefschrift is beschreven, kunnen we concluderen dat het ratten en humane PCLS model succesvol gebruikt kan worden om het mechanisme van leverfibrose en de werkzaamheid van anti-fibrotische middelen in het begin- en eindstadium van leverfibrose te bestuderen. Bovendien kwamen er soortverschillen (tussen rat en mens) aan het licht die opnieuw wijzen op het belang van translationeel onderzoek dat gebruik maakt van humaan weefsel. Als dit model opgenomen wordt in onderzoek naar fibrose en in preklinische studies van nieuw te ontwikkelen anti-fibrotische middelen zal dat kunnen leiden tot een aanzienlijke reductie in het gebruik van dierexperimenten bij het testen van anti-fibrotische middelen en hopelijk ook tot een meer betrouwbare voorspelling van de effecten van die geneesmiddelen bij de mens.

Dankwoord

Graag wil ik iedereen bedanken die mij op vele manieren heeft geholpen bij mijn traject als aio.

Allereerst wil ik graag Peter Olinga bedanken. Je was gedurende vier jaar mijn directe begeleider. Bedankt voor het vertrouwen dat je in me had toen je vroeg of ik zou willen promoveren op het project. Ik heb erg veel van je mogen leren en daar prijs ik mezelf gelukkig mee. Vakinhoudelijk over leverfibrose en leverslices, maar ook over het interpreteren van resultaten, het bekijken van problemen vanuit een ander perspectief en het ontwikkelen van eigen ideeën en inzichten over het onderzoek. Verder was het erg leuk en leerzaam om samen naar congressen te gaan.

Daarnaast natuurlijk Geny Groothuis , mijn promotor gedurende de afgelopen vier jaar. Geny, ook jou wil ik bedanken voor het vertrouwen dat je in me had om als aio op het project te gaan werken. Jouw overzicht en tegelijk ook oog voor detail hebben me vaak anders naar mijn resultaten laten kijken.

Furthermore, I would like to thank the members of the reading committee, Prof. Dr. Dr. Schuppan, Prof. Dr. Bank and Prof. Dr. Porte for reading and evaluating my thesis.

Het is een fijne gedachte dat mijn paranimfen, Dorenda Oosterhuis en Marijke Westra, straks naast mij staan tijdens de promotie. Dorenda, bedankt voor je tomeloze inzet voor het project. Na anderhalf jaar kwam je op het project werken en wat was ik blij met jou hulp bij de BDL'en, bij het slicen, bij de ATP enz. enz. Daarnaast was het erg gezellig met jou op het lab en was het fijn dat ik zowel mijn positieve als minder positieve momenten van het aio-schap altijd met je kon delen. Heel erg bedankt! Marijke, jij ging mij een aantal jaar geleden voor en toen mocht ik naast jou staan als paranimf. Nu is het andersom en ben ik blij dat je er bij bent. Jij wist wat het was om aio te zijn en mijn overwinningen en frustraties begreep je dan ook als geen ander. Bedankt voor je luisterend oor en je suggesties.

Al het humane werk zou niet mogelijk geweest zijn zonder de hulp van alle analisten van de humane groep. Miriam Langelaar, Marina de Jager en Marjolijn Merema, en in de beginjaren Patricia Robbe en Sylvia Blomsma, ik wil jullie bedanken voor jullie hulp met de humane experimenten die veelal 's avonds en in het weekend plaatsvonden. Ik was erg blij met jullie bereidheid om daar aan mee te werken! Daarnaast was het natuurlijk ontzettend gezellig om jullie als collega's en in het geval van Marjolijn en Miriam als kamergenootjes te hebben.

BT, I really had a nice time with you as fellow PhD student in Peter's group. Your attitude to be as direct as Dutch people was sometimes very funny and other times very confronting, but always with the best intentions. Thank you for the nice time we had and good luck with finishing your project!

Mackenzie Hadi en Xiaoyu Niu, you were both my roommates for three years and I was very lucky to share not only a room but also thoughts about research and more broader about life with both of you. Nice to see how different cultures can find each other and learn and change views about so

many important and also very unimportant ;-) things in life. Thank you for the nice time I had with you. Xiaoyu good luck with finishing your thesis!

Graag wil ik Klaas Poelstra, Inge de Graaf, Leonie Beljaars, Barbro Melgert en Angela Casini bedanken voor hun advies en bijdrage in de discussie over mijn onderzoek tijdens de research meetings.

Erik Frijlink, bedankt dat je het mogelijk hebt gemaakt dat ik mijn onderzoek kon voortzetten het laatste jaar van mijn project.

Gillian Nieuwenhuis-Dempsey, bedankt voor je hulp bij alle algemene zaken. Jan Visser, Eduard Post en Catharina Reker-Smit bedankt voor alle hulp op het lab.

I would also like to thank all my (former) colleagues of the Pharmacokinetics, Toxicology and Targeting department and of the Pharmaceutical Technology and Biopharmacy department. Thanks for the help and support during my four years as PhD student.

Naast collega's zou ik ook graag mijn vrienden en familie willen bedanken. Bedankt voor jullie interesse, support en vriendschap. Graag wil ik enkelen hier specifiek noemen. Coby, onze wekelijkse lunches waarbij we elkaar in en weer uit de "aio put" praatten waren voor mij erg waardevol. Doordat we in relatief dezelfde situatie zitten is het erg makkelijk om elkaar te begrijpen en te helpen. Daarnaast was het vooral natuurlijk erg gezellig! Bedankt, en heel veel succes met de laatste loodjes van je proefschrift! Roos, ik kon altijd met mijn verhalen bij je terecht en je kijk op mijn aio-schap was op vele manieren verfrissend ;-). De biomeiden: Leonie, Suzette, Mariska en Kitty, met jullie ben ik het hele biologen avontuur begonnen. Erg leuk dat we elkaar nog steeds zien en bedankt voor jullie interesse, hulp en bovenal vriendschap. Leonie, het duurt niet lang meer en dan gaat het voor jou ook gebeuren, succes!

Tot slot, Eelco, Nelly, Erika en Marijke, bedankt voor jullie steun en vertrouwen en dat jullie er voor me zijn.

Curriculum vitae

Inge Westra werd geboren op 31 december 1982 te Heerenveen. In juni 2001 behaalde zij haar VWO diploma aan scholengemeenschap 'OSG Sevenwolden' in Heerenveen. In september 2001 werd begonnen met de studie Biologie aan de Rijksuniversiteit Groningen. Het doctoraal examen van deze studie met als afstudeerrichting Medische Biologie werd in augustus 2006 behaald aan de Rijksuniversiteit Groningen. Tijdens deze opleiding werden drie onderzoeksstages gedaan. De eerste stage vond plaats bij de afdeling Pathologie van het Universitair Medisch Centrum Groningen (UMCG) getiteld 'Partly prevention of allergic asthma by intra-uterine T-cell tolerance induction in the Mouse'. De tweede stage was getiteld 'Analysis of biomarkers for cervical cancer' en werd uitgevoerd bij de basiseenheid Analytische Biochemie van de afdeling Farmacie aan de Rijksuniversiteit Groningen. De titel van de laatste stage was 'The effect of plasma from non-pregnant, pregnant and pre-eclamptic women on single and cocultures of monocytes and endothelial cells' en vond plaats op de afdeling Medische Biologie van het UMCG. Van oktober 2006 tot september 2009 werkte zij als research analist bij Waterlaboratorium Noord te Glimmen en deed onderzoek naar de ontwikkeling van moleculaire methoden voor het detecteren van bacteriën in water. Van september 2009 tot september 2013 werkte zij als promovendus bij de basiseenheid Farmacokinetiek, Toxicologie en Targeting en de basiseenheid Farmaceutische Technologie en Biofarmacie van de afdeling Farmacie van de Rijksuniversiteit Groningen. Hier werd het onderzoek beschreven in dit proefschrift, gesubsidieerd door ZonMw (project Dierproeven Begrensd II, 114000098), uitgevoerd onder begeleiding van Dr. P. Olinga en Prof. Dr. G.M.M. Groothuis. Van november 2013 tot en met mei 2014 werkte ze als regulatory affairs officer bij Astellas Pharma Europe b.v. te Meppel. In juni 2014 zal zij beginnen als researcher advanced therapies bij het Leids Universitair Medisch Centrum te Leiden.